HYDRODYNAMIC MODELLING OF LAKE ONTARIO

by

ERIN HALL

A thesis submitted to the
Department of Civil Engineering
in conformity with the requirements for
the degree of Masters of Science (Engineering)

Queen's University
Kingston, Ontario, Canada
October 2008

Abstract

The 2006 Clean Water Act requires each municipality to come up with science-based plans to protect the quality and quantity of their drinking water. A literature review concerning applicable processes in Lake Ontario along with previous modelling of the lake is presented.

The three dimensional Estuary, Lake and Coastal Oceans Model (ELCOM) is used to model Lake Ontario on a 2 $\times$ 2 km grid scale. The model is forced using meteorological data from the 2006 summer season, inflows and outflows. The lake-wide model is evaluated using field data from thermistor chains and ADCPs as well as historical water level data. Simulated and observed temperature profiles compared well. However, modelled temperature profiles were slightly cooler than observed. Current results were more variable than temperature profile results but compared better to observed data in the offshore regions. Simulating Lake Ontario water levels proved to be problematic because an accurate water balance is difficult to force with a large drainage basin.

A 300 $\times$ 300 m nearshore model of the eastern portion of Lake Ontario and the upper St. Lawrence River is also presented. The open boundary is forced using temperature data which is (A) varied with depth, (B) constant with depth and (C) spatially varied over the length of the open boundary and varied with depth. Both spatially varied and non-varied water level data forcing the open boundary is also compared. Spatially varied temperature and water level data is computed from the coarse grid lake-wide model. Lake-wide coarse grid model error appears to propagate through the open boundary negatively affecting nearshore modelled current when coupling the models. It was concluded that lake-wide model results should not be used to force the open boundary for the nearshore model. Nearshore model results using constant temperature with depth forcing files and non-spatially varied water level data agree well with observed temperature profiles, but further analysis is required for better confidence in the model's ability to properly reproduce currents at a 300×300 m grid scale.

Acknowledgments

Thanks first of all to my parents, sisters, grandparents and aunts for their unconditional love and support throughout my entire education at Queen's. A special thanks goes to officemates Jonathan my voice of calming reason, Imran and Whitney as well as all my 4th floor and other Ellis friends. Thank you to my housemates Anne, Morgan, Jarrett, Pico and Alex who have listened to my boring, nerdy grad student stories and rants as well as provided me with much needed distractions.

Thank you to Leon for providing me with this opportunity and to Kevin for guiding me through this process that is called a Masters as well as giving me the chance to practice some very important life skills not normally exercised in the realm of a Masters through APSC 190. Thanks also go to the lovable and very helpful civil office ladies and to Bob Rosswell and the captain of his little tin ship at NWRI for getting me out of my little office and on the water for a day!

Thanks to all my friends who have made my time at Queens so memorable, in particular Sarah, Valerie, Alisa and my soccer ladies. Thank you to my fellow servers at Tango and the lovable kitchen staff who I've very much enjoyed working with over the last year of my Masters.

Finally a great big thanks to Paul for pulling me through these very difficult last few months even from the other side of the world and giving me the best "almost

submitted” present ever!

This thesis is dedicated to Lyn, who taught me how to find the value in all of life's experiences.

Table of Contents

List of Tables

List of Figures

Chapter 1

Introduction

1.1 The Relationship Between the Great Lakes and Society

The Great Lakes serve many functions including providing source drinking water and a sink for pollutants and runoff [1] as well as a source of recreation for many urban areas surrounding them. Circulation in the Great Lakes has been of interest since the late 19th century for a variety of applications such as transportation, fishing, agriculture, waste disposal and now source water. Most recently, due to the Clean Water Act passed in October 2006 by the Ontario government, the responsibility of drinking water protection has been placed in the hands of each municipality.

Considerable interest has now evolved in determining new alternatives for providing safe drinking water to communities [1]. These new alternatives include, identification of potential sources of contamination and the creation and implementation of a plan to protect the quality and quantity of drinking water. The coastal zones of large lakes are the areas of most immediate concern to the general public because circulation and mixing in the nearshore region is very important for the loading, pathways and fate of pollutants in lakes and for locating water intakes and waste water treatment plants [2]. These zones are areas of intense biological, chemical and geological processing of materials arriving from both on and offshore zones [3] and the currents associated with the nearshore are especially important for understanding the dispersal of pollutants and waste heat in the lakes as well as recreational usage [4].

Modelling of lake hydrodynamics also plays a large role in tracking and better understanding algal blooms which affects water quality [5, 6]. The proper representation of temperature stratification is of particular significance in regulating vertical transport of nutrients, plankton and oxygen, enabling a better understanding of the occurrence of of hypolimnetic anoxia [7].

1.2 The Need for Hydrodynamic Modelling for Water Quality

Increasing concern with source water quality has stimulated interest in the study of numerical models as a tool for understanding the relevant processes in a source water body with the purpose of predicting the effect of changing conditions and to simulate the input and dispersion of contaminants [6]. It is important to understand the physical processes and mean circulation patterns in the Great Lakes for ecological management issues as they provides an indication of transport pathways of nutrients and contaminants [8, 9].

For many environmental problems in the Great Lakes, it is necessary to know the time-dependent, three-dimensional temperature distribution and circulation which is frequently dominated by wind-induced upwellings and coastally trapped waves [10]. Being able to capture the physics of internal waves is also considered valuable as internal waves break along sloping boundaries and distribute their momentum and energy which impacts mixing across the pycnocline, sediment resuspension, and the distribution of both phytoplankton and nutrients in the water column which influences the biogeochemical systems in a lake [11, 12]. Therefore, hydrodynamic modelling is the appropriate transport foundation for an accurate lake mass balance model because it offers a basis for simulating transport in response to meteorological forcing functions and its results can be scaled to the desired spatial and temporal resolution [6]. The air/water interface and its processes such as wind and waves, are important phenomena to understand because this is where the exchange of the physical quantities such as heat, kinetic energy, momentum, and matter (gases, vapor, aerosols, etc.) occurs [13]. Accurate forcing data is essential for these models. However, basin-scale internal waves provide the driving forces for vertical and horizontal fluxes in a stratified lake below the mixed layer therefore modelling the basin-scale internal wave behaviour is a priori requirement to modelling and quantifying the flux paths of nutrients in a stratified lake [14].

Studies have shown that there is significant value in performing comprehensive three-dimensional simulations to evaluate possible pollutant concentration levels to protect source water [1]. The flow patterns in hundreds of lakes and reservoirs around the world have been modelled with the goal of protecting source water, some of these include Lake Kinneret in Isreal [14], Lake Biwa in Japan [15] and the Great Lakes in North America [1, 6, 16].

1.3 Other Benefits of Lake Modelling for Scientific Advancement

Large enclosed and rotating basins like the Great Lakes are subjected to many of the same forcings as coastal oceans and can serve as examples for understanding the more complicated coastal ocean dynamics [3]. Lakes are easier to study than coastal ocean zones because they are not subjected to salinity effects or tides and open boundary conditions are not required [10]. The size of the Great Lakes also makes them of interest to hydrodynamic modellers because the effects of the Earth's rotation are important to their dynamics but they are not large enough for the curvature effects of the Earth's surface to be of significance. Furthermore, variations of the Coriolis parameter are negligible but lateral boundaries cannot be ignored [9]. These boundaries can, however, emphasize wave-induced complexities for lakes, reservoirs, and estuarine waters compared to in the open ocean [13]. A better understanding of these processes will provide a better prediction in both the lake and ocean environments [10].

1.4 Study Objectives and Outline

The objective of the Intake Protection Zone (IPZ) study initiated by the CRCA is to first delineate drinking water intake protection zones and then produce an inventory and map of all threats and issues in those zones. The first stage in water quality tracking is understanding circulation which in this case necessitates the construction of an accurate flow model. Three dimensional hydrodynamic modelling is an appropriate tool for understanding the relevant processes in a source water body to simulate the changing conditions which may affect the quality of drinking water [6]. The objectives of this thesis project are to first test a course 2×2 km model of Lake Ontario and evaluate its performance in the near and offshore regions by comparing its results to observed temperature, current and water level data. Secondly, the Kingston basin and the upper portion of the St. Lawrence river are modelled on a finer 300×300 m grid scale with an open boundary with the goal of evaluating the sensitivity of the open boundary and how well the model performs at this grid scale in the nearshore areas in terms of temperature and currents.

Chapter 2 presents a literature review which discusses physical processes applicable to circulation of large lakes and introduces the three dimensional hydrodynamics model used to simulate the circulation in Lake Ontario in Chapters 3 and 4. Modelling limitations are also discussed and two examples of the model's previous use are detailed.

Chapter 3 presents a coarse grid lake-wide three dimensional hydrodynamic model of Lake Ontario. The model is evaluated using thermistor chain, historical water levels and ADCP data. Lake-wide circulation results are also compared to Lake Ontario circulation patterns from literature. The goal is to evaluate the model's ability to reproduce general circulation patterns in the near and offshore regions.

Chapter 4 provides a description of a nearshore fine grid model of the Kingston basin and the upper portion of the St. Lawrence River. Three simulations using an open boundary forced by temperature and water level data are compared. Resulting temperature profiles and currents are compared to thermistor chain, ADCP and current meter data with the goal of evaluating how well general circulation patterns are reproduced by the model on a fine grid scale in the nearshore areas.

Lastly, Chapter 5 summarizes the findings from the lake-wide and nearshore models presented in Chapters 3 and 4.

Chapter 2

Literature Review

2.1 Review of Physical Processes in Large Lakes

2.1.1 Introduction

Circulation in the Great Lakes is driven primarily by wind stress and surface heat fluxes. The combination of these two factors coupled with the lake's unique bathymetry makes circulation patterns in large lakes rather complex [8, 9]. Density currents also play a part in forming the driving energy fluxes in a large stratified lake [14].

The energy flux from the wind is of particular interest because of its dominant role in setting the thermocline in motion, which, in the absence of inflows and outflows, is the primary energy store for transport and mixing below the wind-mixed layer [14, 17]. Many other physical processes are either initiated by or associated with wind and must be considered to properly understand the physical processes which drive water movement in large lakes. Wind stress induces seiches, different types of internal waves such as Poincaré waves, Kelvin waves, coastal jets and more. Temperature is the other main contribution to circulation. The Great Lakes are considered dimictic lakes and therefore have a period of thermal stratification and a period of almost uniform water temperature throughout the lake's water column. Temperature stratification plays a large role in the development of circulation in large lakes at mid latitudes like the Great Lakes.

2.1.2 Thermal Stratification

In Lake Ontario, summer circulation is characterized by thermal stratification [17]. Thermal stratification usually occurs in late May or early June and lasts through October [4, 8]. During stratification, the lake is characterized by an upper layer of more or less uniformly warm, circulating and sometimes turbulent water called the epilimnion. The thermocline separates the upper warm waters from the colder and denser bottom layer of the lake, the hypolimnion, and is the plane of maximum rate of decrease of temperature with respect to depth [18]. If it is a windy spring, the thermocline will setup lower and gradually rise as further heating occurs. If there are light winds at the time of thermocline onset, stratification will setup higher and progressively descend as wind-induced mixing establishes the epilimnion. After setup, the depth of the thermocline will deepen as the upper layer gains small amounts of heat throughout the period of stratification [18]. During the summer, when the daily heat input exceeds the nighttime loss, the thermocline will strengthen and deepen. In the fall, nighttime cooling exceeds daytime heating and the stratification is eroded.

At the onset of stratification, a thermal bar occurs. There is an inclined thermocline separating warmer water in the nearshore band from the still barotropic cooler waters in the middle of the lake. As time progresses, the volume of warm water increases and the thermocline becomes stronger and moves further out from shore [4] and eventually establishes thermal stratification throughout the entire lake.

Although the greatest source of heat to lakes is solar radiation, the direct absorption of solar radiation accounts for only about 10% of the observed distribution of heat. Most of the heat distribution profile results from circulation caused by wind stress [18]. Significant motion is confined to the warmer layers above the thermocline [4]. The transport of heat by turbulence decreases as the stability of stratification increases throughout the summer months and the heat flux in the hypolimnion varies minimally with increasing depth [18]. The stable and rapid change in water density at the thermocline acts as a semi-permeable barrier which can dissipate basin-scale energy from basin-scale waves via turbulent mixing through shear instabilities as would a lake boundary such as the lake floor in the absence of thermal stratification [19]. This type of internal turbulence accounts for approximately 10% of the decay of internal wave energy whereas internal wave energy dissipation at the lake perimeter accounts for about 90%. Thermoclines can also support internal gravity waves generated by atmospheric pressure fluctuations, wind, buoyancy flux, interaction of basin-scale motion with bottom topography, instabilities in the mean currents and non-linear wave-wave interaction [15].

A difference of only a few degrees is sufficient to prevent circulation of water between the hypolimnion and the epilimnion [18]. Because of the density barrier created by the steep temperature gradient of the thermocline, the hypolimnion can move in a different direction from the epilimnion. In the deeper offshore regions, the pressure gradient (caused by the surface water level gradient) can generate transport opposite to the wind direction [8]. This was also seen in studies conducted by Bennett [20].

Wind-induced transport of heat is usually of greater importance than direct solar heating in most lakes, especially where light is rapidly attenuated with increasing depth as it is in Lake Ontario [18]. Wind stress applied to a stratified lake forms a turbulent surface mixing layer. Turbulence distributes wind momentum and heat through the depth of the water layer, therefore the epilimnion moves downwind [19]. Continued application of wind stress to a stratified water body will gradually deepen the mixed layer because of an excess of turbulent kinetic energy (TKE) caused by breaking waves or coupling of pressure fluctuations between wind and water, velocity shear in drift currents and Langmuir cells as well as convective penetration. These processes allow warmer surface water in the spring or cooler surface water in the fall to overcome the density barrier caused by the thermocline and be mixed in the hypolimnion [21]. In the fall, this progressive erosion of the metalimnion is called entrainment and results in a rising thermocline depth [22]. This progression leads to the erosion of the thermocline, the fall overturn and eventually barotropic lake conditions [18]. Winter water temperatures vary only slightly between 0°C and 4°C [23].

2.1.3 Surface Currents and General Circulation Patterns

The surface waters of large lakes like Lake Ontario tend to circulate in large swirls typically called gyres. Gyres are strongly influenced by large, long waves and shifts in duration of strong prevailing winds. These inertial motions occur at all depths and all seasons, even under ice cover [18]. Because of its rather simple bathymetry, a horizontally uniform wind generates a two-gyre circulation pattern in Lake Ontario [8]. In this long and narrowish lake with wind blowing along its axis, such as the southwest summer prevailing wind, a cyclonic vorticity (a counterclockwise motion) will form to the right of the wind, and anticyclonic vorticity (a clockwise motion) to the left of the wind. The cyclonic gyre is reinforced at the downwind end of the lake and anticyclonic vorticity is generated at the upwind end of the lake. The net result is the counterclockwise rotational gyre pattern with a small clockwise gyre in the northwest portion of the lake for summer circulation because of the prevailing southwest winds [17] which is generally what is considered summer circulation in Lake Ontario.

Generally, the velocity of wind-driven currents is about 2% of the wind speed driving them and is independent of surface wave height [18]. Storm-induced currents in the Great Lakes can be quite strong (up to several tens of cm/s), but the average currents are rather weak throughout most seasons of the year (on the order of only a few cm/s) [8].

Under stratified conditions there is also a tendency for colder, denser water to collect on the left side of the current leaving less dense, warmer waters on the right side of the current [18]. It is common knowledge that the shore to the right of the prevailing southwesterly winds in the summer, which is the southern shore of Lake Ontario, is considered the warm shore, the north shore of the lake is colder due to frequent upwellings [17]. The Ekman Spiral is usually responsible for these upwellings as the wind drift current is caused to deflect 45° from the direction of the wind [18, 10].

2.1.4 Seasonal Circulation

On a large scale, the lake's circulation can be divided into two seasons: summer circulation which is considered baroclinic or thermally stratified and winter circulation which is entirely barotropic as the entire depth of the water column is the same temperature and density depends only on pressure variations in depth [8].

Seasonal interannual circulation variability may occur as a one-gyre pattern was observed during the 1982-83 winter season and strong eastward currents of up to 8 to 10 cm/s were observed near the south shore of Lake Ontario during both the 1972-73 winter and the 1982-83 winter [8, 23, 24]. There is further evidence of significant year-to-year variability in the Great Lakes Coastal Forecasting System (GLCFS) results which reinforces the idea that general circulation patterns deduced from only one or two experiments are likely to have high uncertainty [5]. However, interannual variability has not been systematically studied in any of the Great Lakes probably because of the lack of long-term observations. Some features of summer circulation appear to be very stable, such as the cyclonic circulation in central Lake Ontario and the eastward current near the south shore of Lake Ontario. These were observed in several studies [8].

Summer circulation in lake Ontario was predominantly cyclonic because of the density-driven cyclonic currents with the larger, more stable cyclonic gyre in the main part of the lake and a smaller anicyclonic gyre in the north-western section of the lake. Summer circulation is more complex than winter circulation because of the presence of baroclinic effects, whereas winter circulation is entirely wind-driven [8].

Surface Waves

Wind over water creates a frictional movement of water at the surface producing traveling surface waves. If these waves are large enough to break, their energy flux and dispersion is transferred to the water. Traveling surface waves are confined to the surface and cause little displacement to deeper water layers. Short surface waves cause water particles to move in a circular path. Water is displaced vertically and gravity returns the water particle to equilibrium state. Surface waves with wavelengths less then $2/\Pi$ cm are referred to as gravity waves. Waves of lesser wavelengths involve surface tension effects and are called ripples or capillary waves. When the angle of the wave exceeds a wave height to wavelength ratio of 1:10, the wave tip collapses and whitecaps are formed. In lakes of large surface areas such as Lake Ontario, wave height and length increases with water depth in contrast to surface waves in small lakes where wave height appears to be nearly independent of water depth. For large lakes, the highest wave heights are proportional to the square root of the fetch (the distance over water that wind blows uninterrupted by land) [18].

Deep Water Waves

In deep water, the wavelength (λ) of surface waves is less then the depth (d) of the water ($\lambda < d$) and they travel at speeds proportional to $\sqrt{\lambda}$. Vertical transfer of energy is of greater interest and the height (h) of vertical oscillation is quickly attenuated with depth. This decrease in vertical motion corresponds to halving the cycloid diameter every depth increase of $\lambda/9$. The amplitude or height of the surface waves is not directly proportional to wavelength, however a common average of $h : \lambda$ is about 1:20 [18].

Shallow Water Waves

When the wavelength of a wave becomes more then 20 times the water depth, the wave has transformed into a shallow water or long wave and the circular motion of a water particle of that wave becomes elliptical and extends all the way to the bottom of the water column and forms a to-and-fro sloshing motion. As deep water waves transform to shallow water waves, their velocity decreases as the square root of depth decreases. There is also a coinciding reduction in wavelength. The wave height first decreases slightly, then increases dramatically to the point where it becomes unstable and a breaker results [18].

Langmuir Circulation

Langmuir circulation is a prominent and complex feature of the surface boundary layer (SBL) of lakes [13]. The dispersion of wave energy can lead to sporadic turbulence in the epilimnion under stratified conditions. Langmuir cells occur under certain circumstances when the motions associated with turbulent transport are organized into vertical helical currents in the upper layers of the lake oriented in the wind direction [13, 18]. A series of clockwise and counterclockwise rotations results in linear convergence and divergence of water which cause streaks of particles (bubbles, leaves or other particulate matter) at the surface of the water body

(Figure 2.1) [18]. These vortices are slightly asymmetric with higher downwelling than upwelling velocities [13]. Langmuir circulation can occur with winds speeds between 2-7m/s. At higher wind speeds surface turbulence is great enough to form particle streaks [18]. In addition to their rotation, cells also propagate downwind with horizontal velocities comparable to the downwelling velocities [13]. In the presence of Langmuir circulation, wind energy is not only converted into a helical structured circulation but also into waves, random turbulence, and mean shear flow. However, this energy is often not substantial enough to break through the barrier formed by density gradients and this type of turbulence remains in the epilimnion [13, 18].

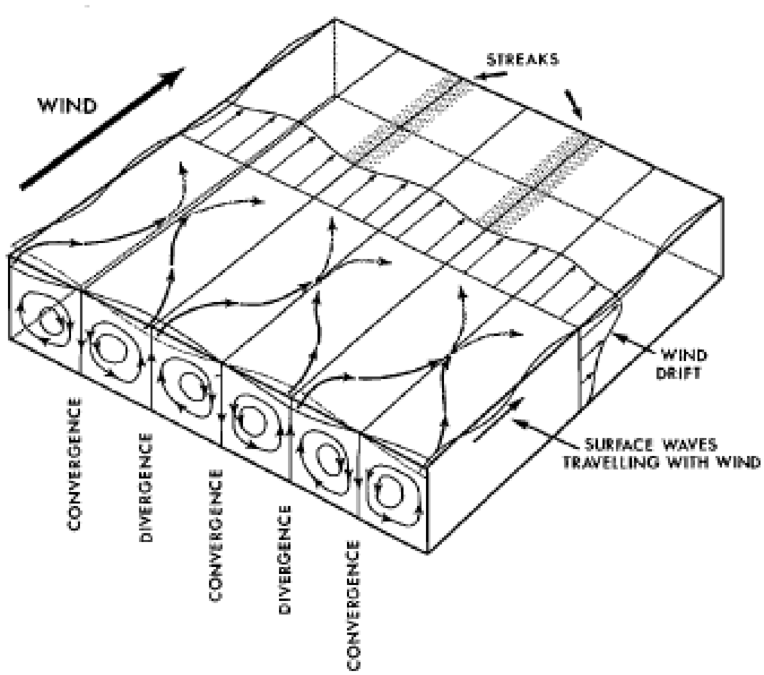

Figure 2.1: Langmuir circulation [18]

Surface Seiches

Seiche motions are produced by surface-level changes. These water level changes are most noticeable in deep water because surface-level variations in shallow waters are overwhelmed by the local effects of wind stress [17]. During the stratified season, large wind events will cause upwelling and downwelling of the thermocline along the shore [3]. These events are significant because they facilitate the exchange of water from nutrient-rich subsurface waters to surface levels as there may be a significant mass of inshore water exchanged with offshore water [2].

The most common cause of seiches is the wind induced tilting of the thermocline or the surface water. The accumulated water mass is gradually pulled down by gravity creating a to-and-fro sloshing motion about one or more nodal points until equilibrium is reached again [18]. Surface seiches occur very much like seiches on the thermocline but are much smaller in magnitude and can occur under barotropic conditions [18]. Once in motion, oscillation of the surface seiche is dampened by gravity as the water mass returns to equilibrium. The magnitude of dampening depends on the complexity of the basin shape. Deep lakes with uncomplicated shapes have low dampening effects and the seiche oscillations can persist well after the storm has passed. The calculated period of a surface seiche in Lake Ontario is 304 min. Uninodal seiches are common in very large lakes but if pressure is periodically exerted and released multinodal surface seiches can be observed [18].

2.1.5 Internal Waves

Internal water circulation is closely tied to thermal stratification [22] because baroclinic lake conditions are necessary for internal wave motions to occur. Internal waves are an important component of the circulation in any stratified lake [6]. They carry momentum and energy over large distances and can redistribute these quantities over different time and length scales [15]. There is ample evidence showing that basin-scale motions of the thermocline provide the driving forces for vertical and horizontal fluxes in a stratified lake beneath the surface layer [14].

The subject of internal wave dynamics has proven to be complex and the understanding of this phenomenon still requires significant improvements. However, it has been shown that most of the momentum and energy that passes through the epilimnion and enters the interior is transferred to basin-scale internal wave motions. Typically about 10% of the total wind energy input to the lake, is transformed to small-scale turbulence and utilized for mixing. Energy is dissipated in major part by bottom shear from seiche currents and periodic breaking of internal waves on the slopping lake bed. The minor part of the energy is dissipated by shear instabilities of breaking of internal waves on the thermocline[13].

Basin-scale wind-induced motions such as internal waves are driven by temporal variations in wind stress, residual circulation dependent on bathymetry, density distribution of the water column and the earth's rotation [19]. These waves have periods ranging from a few hours to several days. They are sinusoidal in shape in the direction of propagation and their nodes correspond to lines of zero isotherm surface displacement when effects of the earth's rotation are not considered [15]. Internal progressive waves and the turbulence associated with them are similar to surface wave motions but are much larger and are very influential in the transport of heat and other properties through the metalimnion [14].

It is generally assumed that internal waves dissipate energy by overturning or shear instability. Viscous attenuation, distortion and wave-wave interaction are other important mechanisms of internal wave dissipation. Besides these dissipation mechanisms, the interaction of internal waves on bottom topography, such as slopping boundaries, and the existence of a turbulent benthic boundary layer have also been shown to contribute to the vertical transportation of mass [15]. Since large internal waves break on the sides of the basin their effects coupled with the vertical movement of the internal seiche on which they move are particularly important [18].

Internal Seiches

One of the main effects of the wind forcing in a stratified lake is the generation of basin-scale, internal seiches [15]. The uninodal seiche of the thermocline is the most common internal wave in stratified lakes. Horizontal flow is largest at the node or equilibrium point and at a minimum at the points of maximum vertical deflection. In a basin where rotation is ignored the points of maximum vertical deflection are at the upwind and downwind ends of the lake and the node would then be situated in the center of the lake. The increased horizontal water velocity at the node of a seiche leads to increased transport of heat and other dissolved substances in lakes. In large lakes like Lake Ontario, multinodal seiches form the dominant type of resonance in the lake because of wind forcing, dampening and other short period disturbances [18].

Sustained winds impart both momentum and TKE to the water in the surface layer. The TKE distributes momentum vertically in the water column, initiating downwind transport in the surface layer, which results in metalimnion depression at the downwind end and upwelling at the upwind end [14]. The accumulated water mass is gradually pulled down by gravity and when it encounters the denser water of the metalimnion it flows back in the opposite direction to the prevailing wind resulting in a tilted thermocline and creating basin-wide isotherms in a fan-shape which varies the density profile across the lake [18]. After the winds have subsided, the layers slide back over each other and the tilted thermocline sloshes back and forth until equilibrium is reestablished. This displacement of water masses leads to rhythmic oscillations in the entire lake. These long waves or seiches have wavelengths of the same order of magnitude as the basin dimensions. Seiches are reflected at the lake boundaries and combine into standing wave patterns on the thermocline [18].

2.1.6 Effects of the Earth's Rotation

The Coriolis force due to the Earth's rotation is evident in lakes the size of Lake Ontario. In the northern hemisphere, surface waters are deflected to the right of the wind direction and once the water is set in motion it follows a circular track. The Coriolis force is dependent on latitude and the speed of the current. For a given current speed, the deflection is greater at the poles and zero at the equator. If the basin is thermally stratified, this motion could be associated with internal waves [18].

The Rossby Radius is the horizontal scale at which rotational effects become as important as buoyancy effects [25]. When basin dimensions exceed 15 km, at latitudes of the Great Lakes, the geostrophic effects of the Earth's rotation come into effect for long surface and internal waves. The Rossby Radius is a function of latitude and water velocity. The Coriolis force will cause water to move in a circle [18]. The radius of this circle for the Great Lakes is usually on the order of 3-5 km [3].

The balance of forces in the region of upwelling is between the wind stress, Coriolis force, and internal pressure gradient. When the wind subsides, a new balance of forces must be established. If the bottom is flat, this results in two types of free internal waves: the Kelvin wave and the Poincaré wave [18].

In the case of large lakes like Lake Ontario, where the Earth's rotation influences the internal wave field significantly, as the width of the lake is larger than its Rossby Radius, large, low frequency internal waves can be classified as either Kelvin or Poincaré waves [13, 15]. These waves are important components of transport below the wind-mixed layer [14].

Kelvin Waves

The Coriolis force causes the lake's surface layer to move to the right of the wind and initiates a wave induced thermocline propagating around the lake in the form of a Kelvin wave [2]. The Kelvin wave is a long gravity wave formed in response to a large wind event and subject to the Coriolis force [3, 13, 14]. This type of wave is confined to a narrow strip of the coast propagating along the righthand shoreline or counterclockwise in the northern hemisphere and can be compared to a spinning coin just before it falls [2, 3, 13, 14]. Kelvin waves have a sinusoidal shape and propagate along the shore of the lake [15]. Bounded only on one side by the shoreline and defined by the Rossby Radius of deformation, gravity causes these waves to exponentially decay as the distance from the shore increases [3, 12, 18]. Therefore, the wave's largest amplitudes are found at the boundaries [13]. What makes the Kelvin wave unique to other open lake circulation is that the momentum imparted by the wind stress is balanced by bottom friction inshore and by the Coriolis force offshore [3]. This progression of the wave along a lake basin induces currents along the shores which are parallel to the direction of the wave propagation and the shoreline [18].

The number of Kelvin waves supported in a circular basin is a function of basin size and latitude [14]. An analysis of fixed-point current-meter records in Lake Ontario has shown that a Kelvin wave traveling a full cycle, back and forth along the lake has a period of the order of 14 days. For large lakes such as Lake Ontario, progress of the Kelvin wave is often interrupted by a new wind event or storm because its period is so long. In lakes of this size, the Poincaré model will dominate. However, in smaller lakes the Kelvin model will be more prominent [17].

Poincaré Waves

Also a geostrophic wave but compared to the Kelvin wave, the Poincaré wave, has a more complex structure and may be visualized as a combination of two sinusoidal waves with equal amplitude, wavelength, and frequency traveling in directions that form equal angles with the main axis of the basin [15]. Poincaré waves are a basin-wide response with oscillations in the thermocline across the entire lake and an anticyclonic phase propagation (in the Northern Hemisphere)

[3, 26]. Poincaré wave amplitudes do not decrease exponentially away from the shoreline as do Kelvin wave amplitudes. Therefore, Poincaré waves occur in the open waters of large lakes and their reflection at the shoreline generates Kelvin waves. Poincaré waves circulate in a standing wave pattern resulting in a cellular pattern of rising and falling hills and valleys with a corresponding cellular pattern of wave-associated currents [18]. A simple vertical cross-section showing the surface displacement of a Poincaré wave in 2D is generally indistinguishable from a linear seiche, but in the horizontal plane, the wave-induced velocity is a rotation of velocity vectors in a clockwise sweep (in the Northern Hemisphere) that results in horizontal orbital transport as opposed to the linear back-and-forth motion of a seiche [14].

Larger-amplitude Poincaré waves occur mainly following storms, after which they decay with a half-life on the order of several internal periods. Most effective in exciting a given Poincaré wave mode is a wind-stress episode lasting for half a wave period. In large lakes the lowest modes have periods close to 17 hours, which should be best excited by wind-stress impulses of about 8 hours in durations. Coincidentally, this is the typical lifetime of a strong wind-stress episode at mid-latitudes. During summer stratification, thermocline oscillations of a period close to the inertial (but somewhat less) are certainly prominent, and can be labelled Poincaré waves. However, some complications have been observed such as internal-wave fronts progressing across the lake [17].

The important differences between the Kelvin and Poincaré waves is that the Poincaré wave extends with undiminished amplitude across the whole lake whereas the Kelvin wave decreases in amplitude away from the shore and is therefore considered trapped along the shore creating a band of about 20 km for most large lakes. The Kelvin and Poincaré wave models are oversimplified and are not valid for natural lakes because of their varied bathymetry, however, they provide a useful interpretation of what is observed in large lakes [18]. It has been demonstrated that the Pointcaré wave has many of the characteristics of thermocline oscillations observed in Lake Ontario [17].

Coastal Currents

At the onset of stratification, shallow, nearshore water can heat up more rapidly causing a density gradient called a thermal bar separating the newly stratified water from the isothermal water in the center of the lake. Currents along the shoreline are often trapped by this density barrier. The Earth's rotation can induce a counterclockwise coastal current inside the thermal bar and little mixing occurs between the inshore and offshore waters temporarily isolating the inshore water from the offshore cooler water. The thermal bar moves progressively offshore as the heat influx warms the open water mass until stratification of the whole basin sets in. This transition may take weeks in lakes the size of Lake Ontario [18].

During the stratified summer and fall in Lake Ontario, there can be a well-defined coastal boundary layer about 10 km in width which is characterized by relatively persistent currents called a coastal jet [27]. The velocity of these layers above the thermocline is considerably higher than any current-bands in the cold water. This circulation phenomenon is important in dictating the transport and pathways of materials entering the coastal environment [4, 17]. There is usually an accompanying thermocline elevation on the left side of the wind or a depression to the right of the wind. The amplitudes of which are often large enough to bring the thermocline to the surface or depress it to a depth of the order of twice the equilibrium depth or more [17]. Uptilts occur most often on the north shore of Lake Ontario and are associated with eastward surface flows. Downtilts or downwellings are associated with westward flows. The westward coastal jet on the north shore is more often observed probably because the eastward flows tend to drift southward due to the Coriolis force making them harder to track [4, 27].

2.2 ELCOM

The Estuary Lake and Coastal Ocean Model (ELCOM) was developed at the University of Western Australia. It is a three-dimensional hydrodynamics model used to predict the velocity, temperature and salinity distribution in natural water bodies subjected to external environmental forcing, such as wind stress, surface heating or cooling as well as inflows and outflows using the hydrostatic assumption of pressure. ELCOM solves the unsteady, Navier-Stokes equations for incompressible flow using the hydrostatic assumption for pressure as well as the Boussinesq approximation and Reynolds averaged transport equations [28]. Modelled and simulated processes include baroclinic and barotropic responses, rotational effects, tidal forcing, wind stresses, surface thermal forcing, inflows, outflows and transport of salt, heat and passive scalars [29]. The hydrodynamic equations can be found in Appendix D.

ELCOM applies a separate one-dimensional mixed-layer model to each water column to provide vertical turbulent transport, whereas three-dimensional transport of TKE is used to provide the dynamic effect of three-dimensional motions on the TKE available for vertical mixing [14].

ELCOM uses an Arakawa C-grid in which velocities are defined on cell faces with free-surface heights and scalar concentrations defined on cell centers [19]. Sidewall and bottom boundary conditions are non-slip and the free surface height in each column of grid cells moves vertically through grid layers as required [14]. Z-coordinates are used to spatially resolve the vertical grid scale.

The energy transfer across the free surface is separated into non-penetrative components of long-wave radiation, sensible heat transfer, and evaporative heat loss, complemented by penetrative shortwave radiation. Non-penetrative effects are introduced as sources of temperature in the surface mixed layer, whereas penetrative effects are introduced as source terms in one or more grid layers on the basis of an exponential decay and an extinction coefficient [14].

Correct modelling of mixing requires correct modelling of basin-scale internal waves. A successful model must accurately capture the forced and free internal waves in the metalimnium setup by downwind transport in the surface wind-mixed layer [14]. ELCOM reproduces internal waves extremely well and properly captures all other fundamental basin-scale motions of a stratified lake especially when the spatial variability of the wind field is taken into consideration [6].

Long-term preservation of lake stratification is ensured using a potential energy conserving filtering technique to counteract the accumulation of numerical error. ELCOM's success at modelling internal wave fields is due to its use of a mixing layer model combined with a conservative flux-limiting scalar advection scheme which improve the estimation of stratification in a highly stratified lake [6]. Numerical diffusion and damping are also critical problems in ELCOM [14]. Laval *et al*. noticed that the accumulation of numerical error caused by strong internal wave motions leads to numerical diffusion resulting in the smearing of the pycnocline. However, many practical engineering models are conducted at relatively coarse grid scales where numerical diffusion is unavoidable [28]. Some smearing of the thermocline and reduced vertical stratification can be accounted for by the model's failure to properly simulate high-frequency waves (wavelengths 10 - 100 m) that can transfer energy to the boundaries of the lake because of the coarse grid scales which cannot capture this scale of waves [7].

2.2.1 Modelling Limitations

Observations and mapping of the Great Lakes has been of interest for over 100 years however, inter-annual variability of summer circulation has not been investigated because of the lack of long-term observations. Scientific studies have taken place intermittently, therefore there is insufficient data lengths to determine any long term trends [8]. The lack of observational data is also a problem for numerical model evaluation [10].

Another problem facing three-dimensional computer models of lakes is computational requirements. To avoid unmanageable computation times, grid scale resolutions are coarse as in the case of the study by Hurdowar-Castro *et al*. who modelled the nearshore along the Toronto waterfront on a 500 m grid scale in order to evaluate the optimum position for a new drinking water intake. This resolution was too coarse so a smaller model with a 100m grid scale was also evaluated to improve study results [1].

It is also necessary to have a high enough grid resolution to resolve the dynamics of nearshore barotropic and baroclinic processes [20]. To model baroclinic coastal jets, the numerical grid resolution should be at least comparable to the baroclinic Rossby Radius of deformation [10].

Hydrodynamic models have often neglected the inflow and outflow of tributaries. Models were run with closed boundaries and they usually only considered idealized wind forcing. The impact of inflows and outflows on lake circulation has not been addressed specifically in past studies [5].

2.2.2 Previous ELCOM Modelling

ELCOM has been shown to accurately simulate the hydrodynamics in several other lakes such as Lake Kinneret in Israel and Lake Erie in North America.

Lake Kinneret

Lake Kinneret has been widely modelled and several analytical methods have been used [7, 12, 14, 19, 28, 30]. It is approximately 22 km by 15 km with a maximum depth of 42 m [7] and surface area of 167 km^2 [12]. It has been the subject of extensive research because of its role in providing drinking water for Israel [14].

Several analytical methods have been used and compared to observed data [12, 14, 19, 28, 30]. ELCOM results for Lake Kinneret are compared with field data under summer stratification conditions to identify and illustrate the spatial structure of the lowest-mode basin-scale Kelvin and Poincaré waves which account for the two largest peaks in the lake's internal wave energy spectra [14]. On another occasion, the influence of spatial and temporal variations in wind forcing on the circulation in Lake Kinneret was studied using ELCOM. Model results were evaluated with observed data from six thermistor chain moorings equipped with wind speed and direction sensors spread out over the lake. From field data, the 24 hour Kelvin and the 12 hour Poincaré waves were evident [19]. Overall, the model adequately represents the metalimnion setup caused by the daily sea breeze and subsequent internal-wave motions are well modelled using a uniform wind field provided that this wind field represents the horizontally averaged wind stress. However, a spatially varied wind field is required to simulate the surface-layer circulation because mean surface circulation is directly forced by the combined wind stress moment [19].

Lake Erie

Lake Erie's central basin has exhibited the greatest amount of primary production of the entire lake in the 1990s. Gyre-like circulation is probably a key mechanism for retaining externally supplied nutrients causing this problem. Variations in the circulation patterns in the lake likely contribute to variability of primary production and its spatial distribution in the central basin. Both the clockwise and anticlockwise gyres in the eastern basin were consistent with previously mapped, computed and observed hydrodynamics for summer conditions [6].

ELCOM simulations for the whole of Lake Erie were conducted based on 1994, 2001, 2002 and 2003 field and meteorological data. A spatially variable wind field was expected to be critical in simulating mean surface circulation[6] especially seeing that Lake Erie's surface area measures 25745 km^2 [31] which is 155 times larger than Lake Kinneret. Modelled output for all simulations generally showed very good agreement. As predicted, the results also showed the predominant along-shore average circulation in the coastal zone of both central and east basins [6].

Chapter 3

Lake Ontario Basin Scale Hydrodynamics Model

3.1 Introduction

The Great Lakes are among the most important resources in the world. They contain 18% of the freshwater on earth and 95% of the freshwater in North America. Over 36 million people live in the Great Lakes basin [31] and these lakes play an important role in society, be it through many industrial uses, waste disposal systems, recreation and source drinking water.

Serious water quality problems have been identified within the Great Lakes basin as a result of increased urbanization and industrial activity which is generally the cause of environmental degradation of many nearshore areas due to municipal and industrial discharge [32]. Although substantial advances have been made in the regulation of outfall location and permissible effluent quality, the ever increasing total volumes of wastewater heightens the need to understand coastal physical processes in greater detail [2].

In 2006, the provincial government transferred the responsibility of ensuring clean drinking water onto individual communities. Each community is responsible for identifying potential sources of contaminants and creating a plan to protect its drinking water. The Ontario Clean Water Act is intended to ensure communities take the appropriate steps in protecting their drinking water supply through developing locally driven, science-based protection plans [33].

The study of hydrodynamics in the Great Lakes has been of interest for over 100 years beginning with the tracking of drift bottles to map general circulation patterns. The first truly whole-basin Eularian current measurement program in Lake Ontario was conducted during the International Field Year for the Great Lakes (IFYGL) in 1972 [8]. This program encompassed year-round operation of some 20 buoys distributed evenly over the lake, weekly quasi-synoptic ship cruises, and various smaller projects [34] with the goal of documenting mean temperature and current patterns throughout the lakes [35].

Data collected from the IFYGL has been used in many studies of circulation in Lake Ontario. Simons developed and tested a three-dimensional barotropic and baroclinic numerical model designed to compute water levels, currents, temperature and the transport of dissolved or suspended materials [34, 36]. Previous to this, Rao and Murty modelled the barotropic circulation in Lake Ontario, for the first time using actual bathymetry (excluding islands), uniform and spatially varied winds as well as inflow and outflow from the Niagara and the St. Lawrence Rivers [9]. Bennett later found, through his modelling of Lake Ontario, that it is easier to improve results by resolving the coastal zone and lowering friction than by varying the turbulence formulation or the atmospheric forcing [20].

Primitive three-dimensional models have been in use for quite some time. The success of these studies and future ones initiated the rapid progress in conceptual and numerical models for lake physics [8]. In 1995, IDOR, a three-dimensional hydrodynamic/water quality model successfully used a nested approach where a coarse grid model (2 km^2 grid) was used to provide the necessary boundary conditions for a fine grid model (500 m^2 gird) of the Toronto waterfront [32]. Hayashida *et al.* (1999) modelled all of Lake Ontario with a two-dimensional FEM model with grid sizes varying between 80 m and 5 km using idealized meteorological forcing data with constant Niagara flows of 5000 m^3/s and 7000 m^3/s [37]. Prakash *et al.* (2007) used a three-dimensional particle tracking model (PTM) to evaluate mean seasonal circulation in Lake Ontario. The results were compared with previous lake measurements but also with the Great Lakes Coastal Forecasting System (GLCFS) to evaluate reasonableness and compensate for the lack of comprehensive data sets [5]. Lastly, IDOR was used to model the Toronto area waterfront in order to evaluate potential locations of drinking water intakes [1].

The goal the Intake Protection Zone (IPZ) study initiated by the Cataraqui Region Conservation Authority (CRCA) is to first delineate drinking water IPZs and then produce an inventory and map of all threats and issues in those zones. Because the first stage in water quality tracking is understanding circulation, construction of an accurate flow model is necessary. Three dimensional hydrodynamic modelling is an appropriate tool for understanding the relevant processes in a source water body to simulate the changing conditions which may affect the quality of drinking water [6]. The objectives of this project is to test a course 2×2

km model of Lake Ontario and evaluate its performance in the near and offshore regions by comparing its results to observed temperature, current and water level data.

3.2 Methods and Materials

3.2.1 Model Description

Long-term circulation in the Great Lakes is primarily driven by wind stress and surface heat fluxes. The combination of these two factors coupled with the lake's unique bathymetry make circulation patterns in large lakes rather complex [8]. With this in mind, the Estuary Lake and Coastal Ocean Model (ELCOM) is used as a tool for understanding the relevant hydrodynamic processes in Lake Ontario. The primary objective (1) is to test the model's ability to properly simulate offshore hydrodynamics in Lake Ontario and a second objective (2) is to test its ability to reproduce nearshore hydrodynamics with a coarse grid. A validated lakewide model can provide the open boundary conditions for a fine grid model of the Kingston basin and the Upper St. Lawrence River in order to delineate IPZs to protect source water within computational limits.

ELCOM is a three-dimensional hydrodynamics computational model used to predict the velocity, temperature and salinity distributions in lakes and coastal regions [6]. It solves the unsteady Navier-Stokes equations for incompressible flow using the hydrostatic assumption for pressure. Modelled and simulated processes account for barotropic and baroclinic responses, rotational effects, tidal forcing, wind stresses, surface thermal forcing, inflows and outflows, and transport of heat, salt and passive scalars [29]. ELCOM's computational limits are determined by the grid resolution and available computational resources. The model's requirements for simulation are environmental forcing data which includes wind speed, direction, air temperature, relative humidity, short- and long-wave radiation, atmospheric pressure and rain data. ELCOM uses z-coordinates to spatially resolve the vertical grid scale.

ELCOM has been demonstrated to capture the correct thermocline forcing with a three-dimensional, mixed-layer model for surface dynamics results in a good representation of general circulation and low-frequency internal wave dynamics for several lakes and reservoirs [38].

3.2.2 Data Sources

ELCOM is driven by meteorological files comprised of wind speed (m/s), wind direction (degrees clockwise from north), air temperature (°C), relative humidity, measured shortwave radiation (W/m^2), incoming long-wave radiation (W/m^2) and atmospheric pressure (Pa) (Figures 3.1 and 3.2) obtained from three moored surface buoys equipped with weather stations at locations throughout the lake (Figure 3.4) provided by the National Water Research Institute (NWRI). The shortwave and incoming long-wave radiation were scaled by 0.9 and 1.15 respectively (Appendix A) in all four simulations in order to compensate for ELCOM's tendency to underestimate temperatures [28]. Rainfall data (m/day) [1] is also included in the meteorological forcing files. The daily rainfall values were computed using

[1] Rainfall data was provided by Tim Hunter at NOAA

a Thiessen polygon method which weights the observed data at every station according to its representative area (Figure 3.3) [39]. All meteorological data, including rain were input into ELCOM at 10 min intervals. Inconsistencies and gaps in any of the three data sets were filled with data from the nearest station. Realistic wind forcing has been shown to have a significant effect on resulting circulation patterns [16]. Because of the size of the lake and the possibility of significant cross-lake meteorological variability [6, 40], spatially varied wind forcing was determined to be the most realistic way to force the model. The lake was divided into 3 sections corresponding to the 3 weather stations moored in the lake, stations 1263, 586 and 403 shown in Figure 3.4 (Table 3.1).

One of the limiting factors in lake-wide modelling is computational resources and both horizontal and vertical grid dimensions play an integral role in this. Gridded bathymetric data (2×2 km in the horizontal) was obtained from the National Oceanic and Atmospheric Administration (NOAA) - Great Lakes Environmental Research Laboratory (GLERL) [41]. ELCOM allows for a vertical grid spacing with layers (dz) of various thickness. In order for simulations with dz of different sizes to yield results with the greatest accuracy, the size of dz should vary slowly because abrupt changes in grid sizes will provide less accurate results [42]. The sizes of dz were chosen based on the dz values used for the ELCOM model of Lake Erie. In order not to exceed computational limitation, the vertical layers start with a thickness of dz=0.1 m at the surface and gradually increase to dz=1 m at a depth of 30 m to accurately capture the change in temperature with depth due to stratification. The layers then increase in dz to a maximum of dz=16 m to a maximum depth of 249 m and a total of 77 layers.

The impact of inflows and outflows on lake circulation has not been addressed specifically in past studies [5]. Major monitored Lake Ontario inflows occur at the Niagara River and the Welland Canal. The inflow data is calculated from information reported by the St. Lawrence Seaway Management Corporation, Ontario Power Generation, the New York Power Authority and the New York State Canal System[2]. Lake Ontario flows out by way of the St. Lawrence River. As the model ends at Kingston, the flow measured at Cornwall was split with 45% and 55% flowing to the north and to the south of Wolfe Island out to the St. Lawrence River respectively [43]. Most minor tributaries discharging into Lake Ontario are monitored. However, at the time of writing only modelled monthly tributary flow data was available for the 2006 summer season from NOAA[3] (Table B.1) to account for the 14% of the lake's total inflow which is associated with the minor tributaries around the lake [44]. Monthly tributary values are modelled and have not yet been varified with field data. These values were converted to daily values by scaling the monthly data to correspond to the daily rainfall values (Figure 3.3). Inputting tributary flows as rain assumes the temperature of the water to be the same as the ambient air temperature as opposed to having to define a temperature for a point source inflow [42]. Lake Ontario is the smallest of the Great Lakes with a surface area of 18,960km^2, but it has the highest ratio of watershed to lake surface area [44]. Most models do not account for overland flow as point sources are found to have significantly more impact to the system [1].

[2]Inflow and outflow data was obtained Len Falkiner at Environment Canada's Great Lakes St. Lawrence Regulation Office

[3]Modelled tributary flow data was provided by Tim Hunter at NOAA

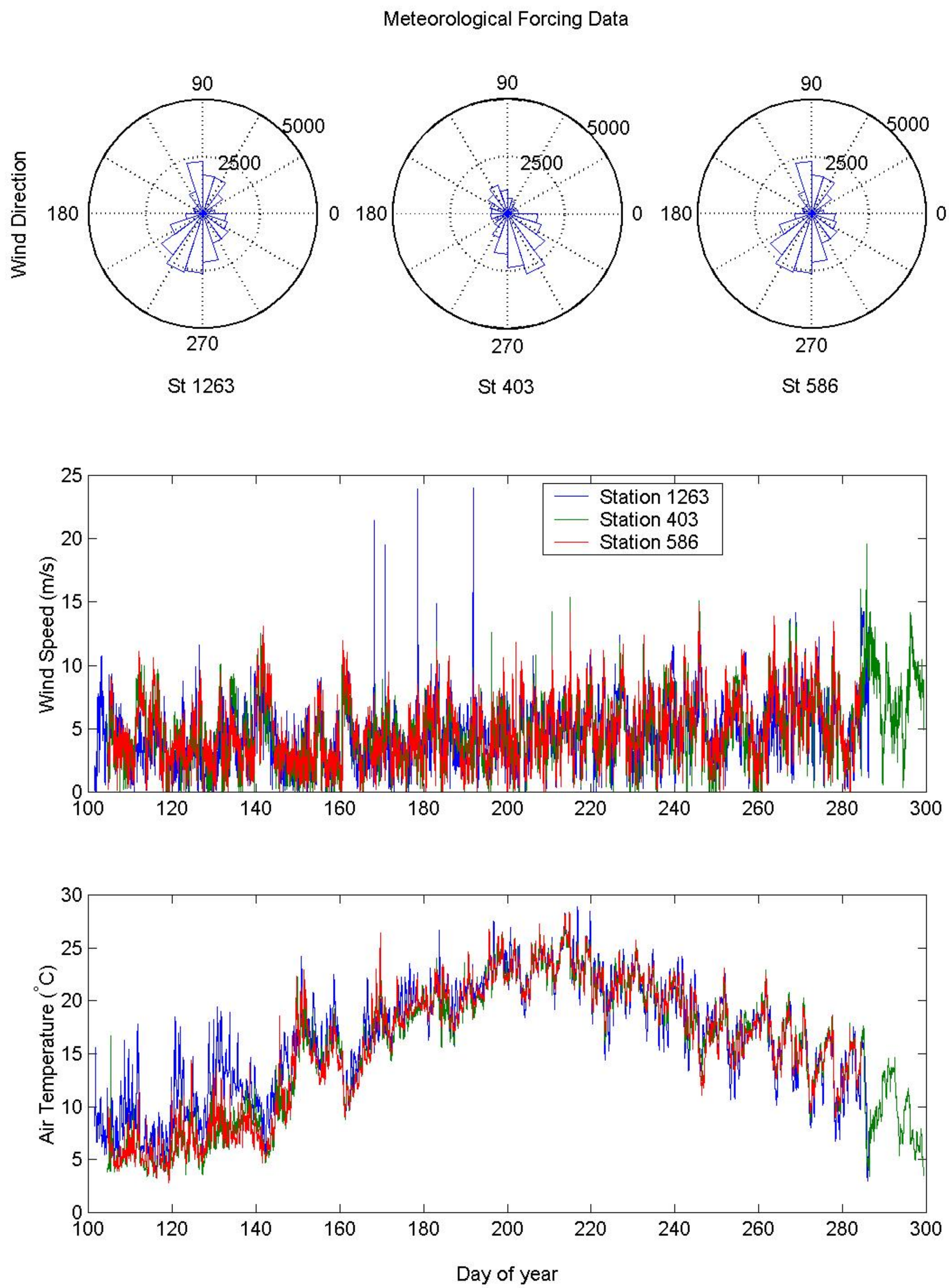

Figure 3.1: Meteorological forcing data used for simulations - occurrence of wind direction (top) in 18° bins, wind speed (middle) in m/s and air temperature (bottom) in °C at 10 min intervals.

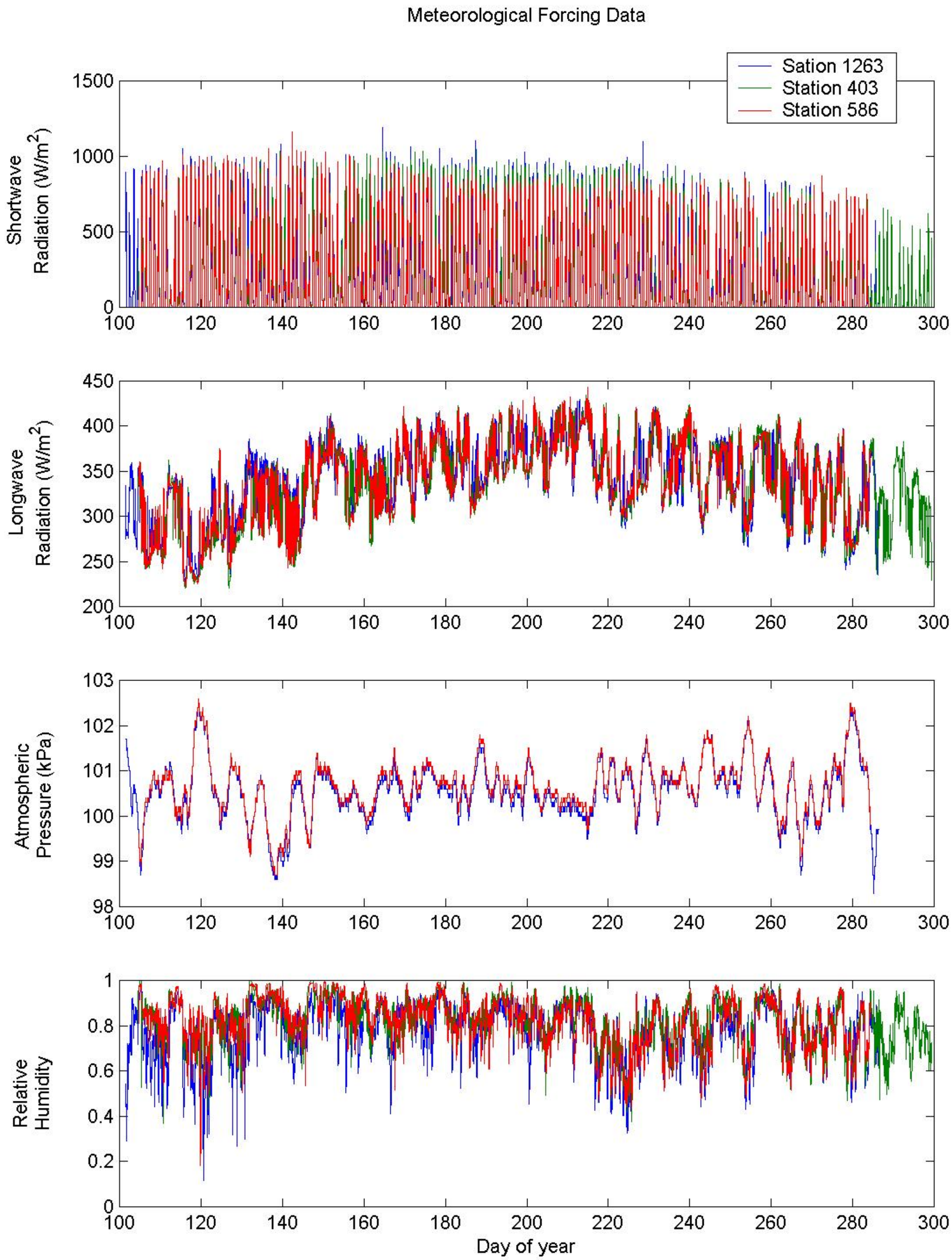

Figure 3.2: Meteorological forcing data used for simulations - short (top) and long-wave (middle-top) in W/m^2, atmospheric pressure (middle-bottom) in kPa and relative humidity (bottom) at 10 min intervals.

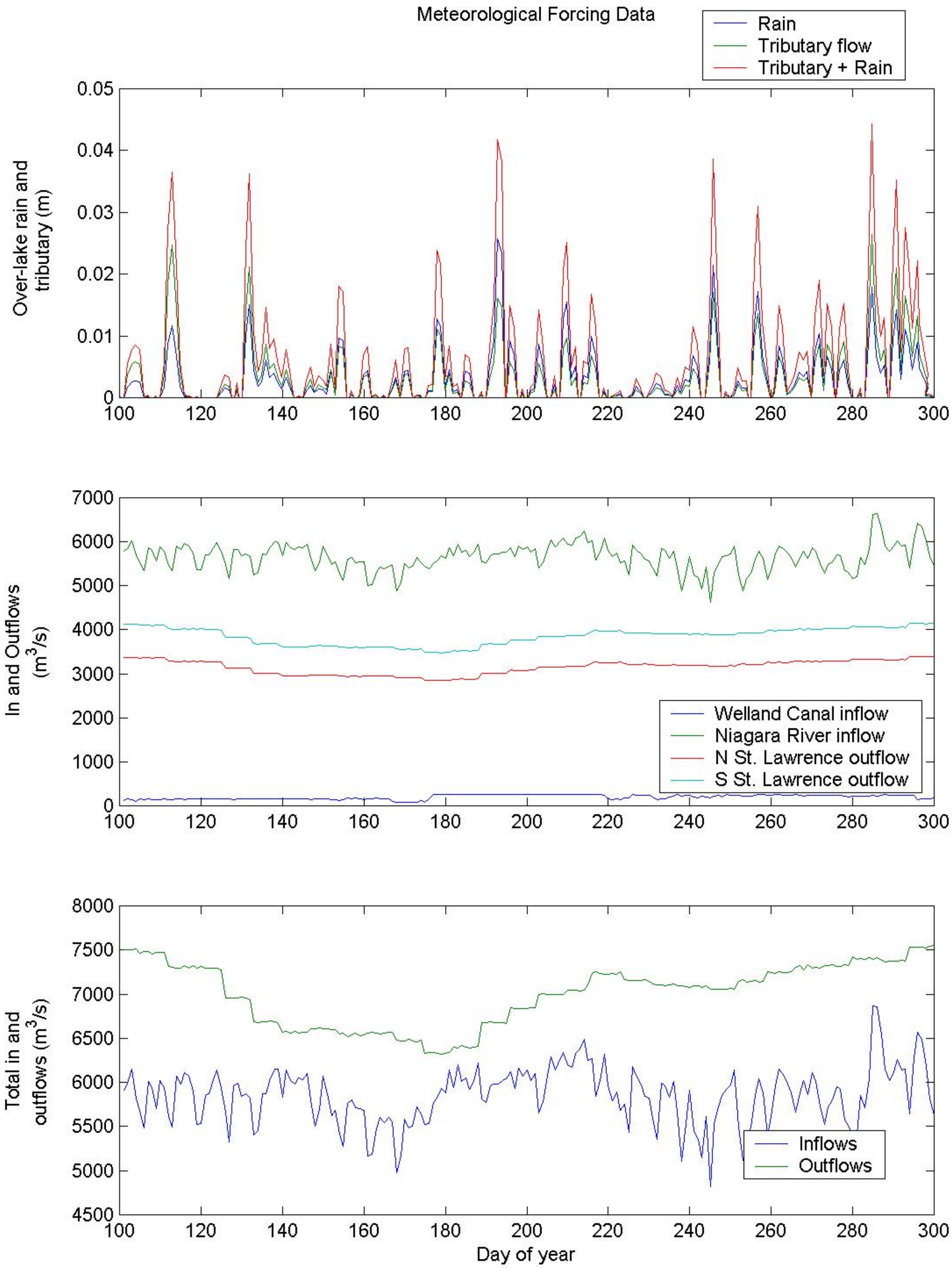

Figure 3.3: Rain and tributary flow (top) in m over the lake surface, Welland Canal and Niagara River inflows with north and south St. Lawrence River outflows (middle) in m^3/s and total major inflows and outflows (bottom) in m^3/s.

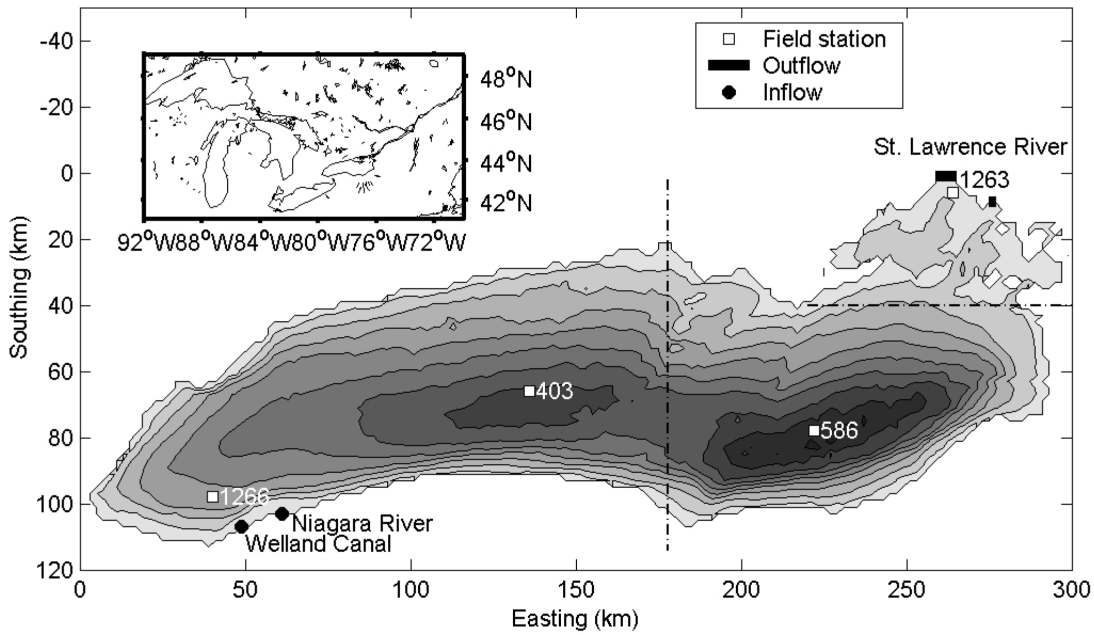

Figure 3.4: Gridded 2 × 2 km Lake Ontario bathymetry showing the location of all data forcing and evaluation stations and in- and outflows. Meteorological forcing sections are separated by dashed lines. Isobaths are shown at every 25 m.

Table 3.1: Moored surface buoy locations and data associated with each.

Station	Location	Data
403	Western-central	Meteorological Thermistor chain
586	Eastern-central	Meteorological Thermistor chain
1263	Kingston basin	Meteorological Thermistor chain ADCP
1266	Western	Thermistor chain ADCP

3.2.3 Simulations

The summer season is of interest in this study because of the lake's baroclinic nature and the complex thermally driven circulation associated with it. There is ample evidence showing that basin-scale internal waves on the thermocline provide the driving forces for vertical and horizontal fluxes in a stratified lake beneath the surface layer [14]. However, the purpose of this study is to model the first order properties of Lake Ontario's circulation, the setup and decay of stratification and the mean currents in the offshore and nearshore reagions. With the lake's internal Rossby Radius of the order of 5 km, Kelvin waves cannot be resolved with a grid size of 2 $\times$ 2 km. Internal wave motions as simulated in ELCOM are described by Hodges *et al.* [14].

ELCOM simulations lasted approximately 2.5 days starting on day 101 of 2006 (April 11) well before the onset of temperature stratification which allows for a uniform initial temperature of 3.4°C in the lake. The initial water temperature of the lake was calculated from the available thermistor chain data from stations 403, 586 and 1266[4]. This start date also permits capturing the entire onset of stratification. The simulation time-step is 5 min, as used in a similar model of Lake Erie by León *et al.*, as it was shown to give the best results at an acceptable computational efficiency [6]. ELCOM can interpolate for a smaller time-step when its forcing data time-step is larger [29] as it is 10 min for this model. Simulations end on day 299 (October 26, 2006) giving a large enough window into the baroclinic hydrodynamics of the lake allowing for the visualization of the onset of stratification as well as the beginning of its deterioration and the lake's return to barotropic conditions

[4]Observed water temperature and current profile data was provided by C. H. Marvin, R. Yerubandi and B. Schertzer at NWRI

(Figure 3.5).

For effective model evaluation, simulated temperature profiles, currents and water levels were compared to observed data. ELCOM simulations were compared with thermistor chain data and ADCP data from 2006 provided by the National Water Research Institute (NWRI)[5] as well as historic water level data obtained from a variety of different gauges around the lake [45]. Thermistor chain data was collected with Tidbit data loggers with 12-bit resolution and a precision sensor with 0.2°C accuracy over a temperature range between -20 and 30°C [46]. ADCP data was measured at every meter throughout the water column with a velocity resolution of 0.125 to 0.25 cm/s and an accuracy of 0.5 cm/s [47].

3.3 Results

3.3.1 Temperature Profiles

Observed temperature data recorded every 10 min from the four moorings were were compared to modelled output at 10 min intervals. The modelled temperature data was plotted using values from the same depths as the observed data recorded from thermistor chains. Figures 3.5, 3.6, 3.7 and 3.8 show the measured and simulated temperature profiles of the entire water column at each of the four stations throughout the lake where thermistor chains were located. Maximum rate of temperature change portraying the thermocline occurs between temperatures of about 13 to 20°C once stratification has set in for temperature profiles at stations 403, 586 and 1266. Water depth at station 1263 is too shallow for the occurrence of

[5]Observed water temperature current data was provided by C. H. Marvin, R. Yerubandi and B. Schertzer at NWRI

temperature stratification, therefore the entire water column is uniformly warmed with depth.

With the effect of scaling the shortwave radiation by 0.9 and the long-wave radiation by 1.15, ELCOM satisfactorily simulates temperature at all stations in the lake both in the nearshore regions and the offshore regions. Small differences in modelled to observed temperature profiles should be expected because of the use of such a coarse grid scale. As there are a total of four thermistor chains spread out over the entire lake with which observed data was collected to evaluate simulations, it can be inferred that ELCOM properly replicates the temperature stratification in the entire lake.

Both modelled and observed temperature profiles show that the water at station 1263 warms almost consistently throughout the depth of the water column although the top of the water column warms faster with respect to the bottom then is observed in the field data. Cooling is shown to be constant with depth for the observed data in the fall at station 1263 but the bottom is cooler throughout the simulation in the model. ELCOM's tendency to underestimate temperature is exemplified in the modelled profile at this station because of the shallow depth of the water column compared to the greater depth of the three other locations. The model portrays an infusion of cooler water around day 230 but warmer water is observed at that time. It is difficult to compare the success of nearshore temperature profiles to that of offshore temperature profiles because of the great difference in their depth.

The deepest temperature profile comparison is at station 586 where warming of surface water looks to be slightly premature compared to the observed data.

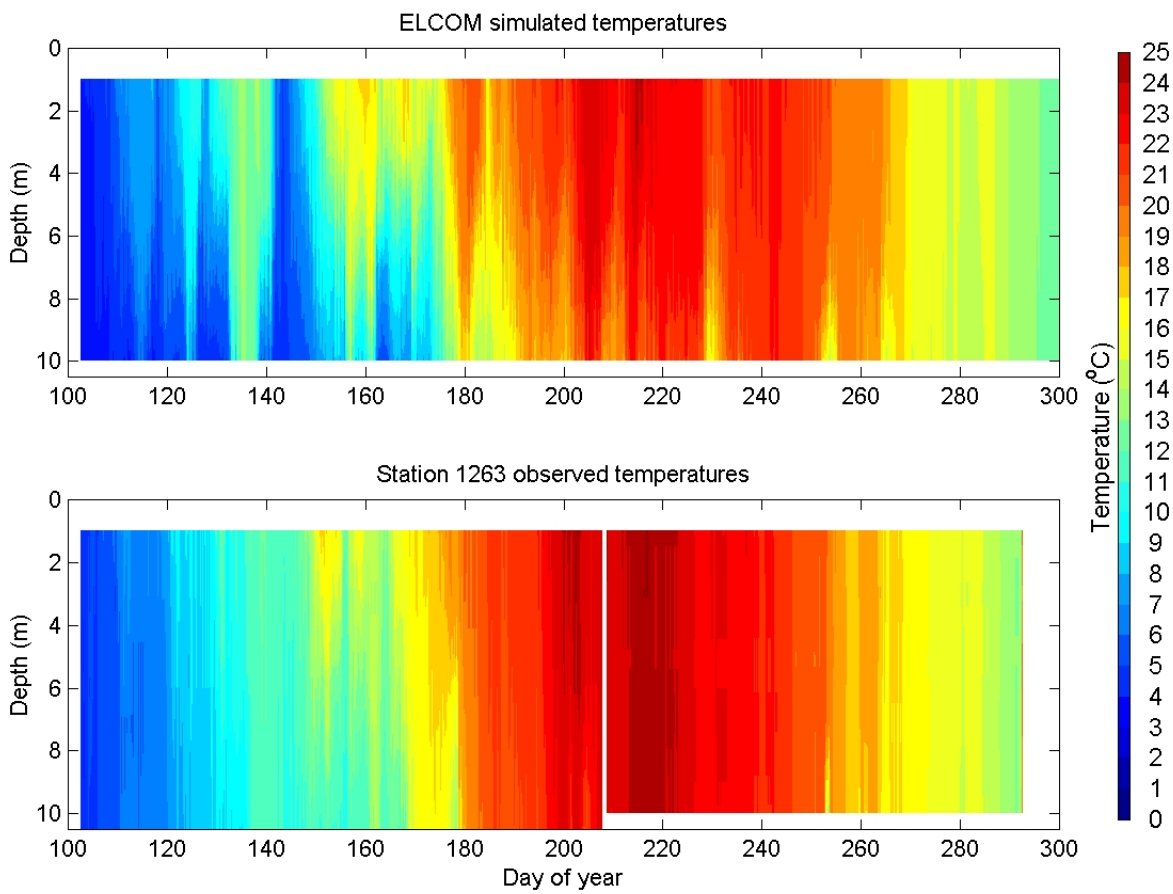

Figure 3.5: Modelled (top) and observed (bottom) temperature profiles at station 1263 at 10 min intervals. Modelled temperature output was interpolated at 1, 3, 5, 7 and 10 m depths to match observed data.

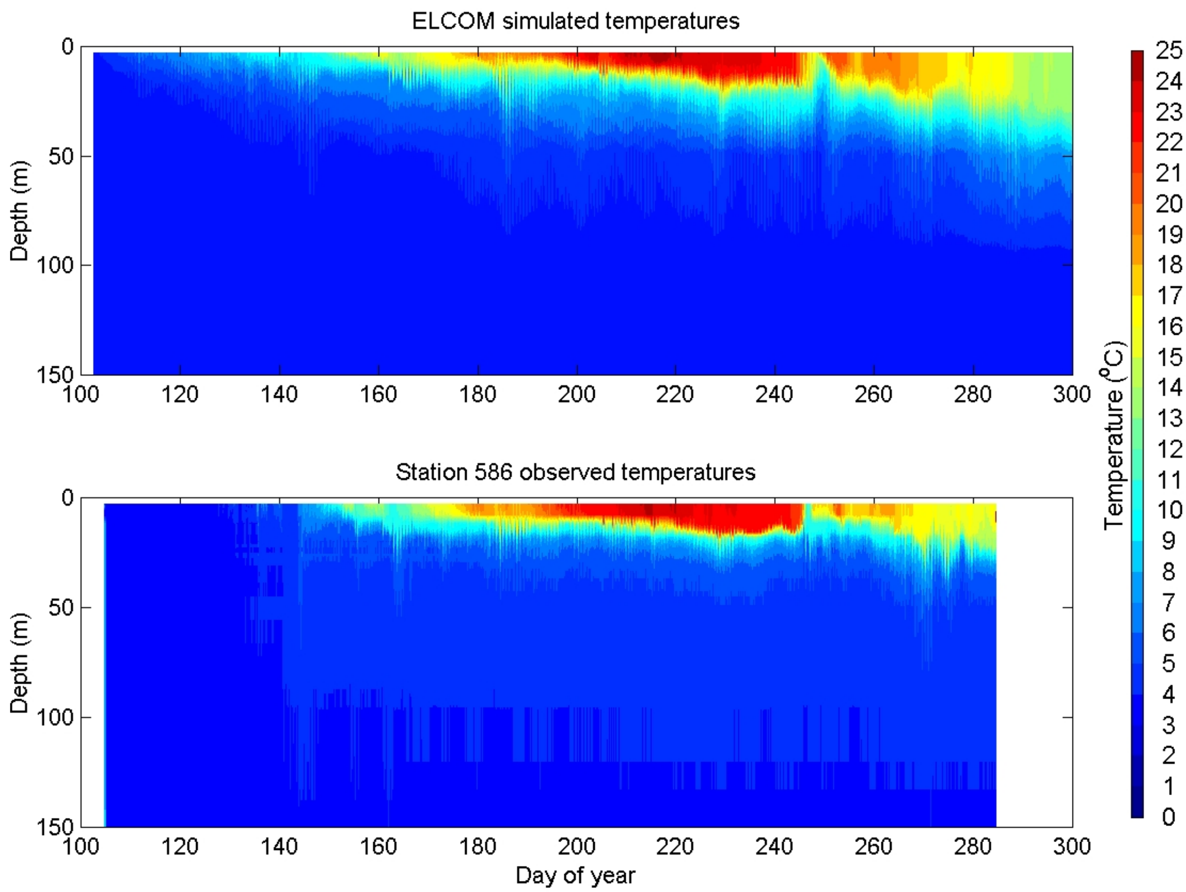

Figure 3.6: Modelled (top) and observed (bottom) temperature profiles at station 586 at 10 min intervals. Modelled temperature output was interpolated at 2.7, 4, 6, 8, 12, 14, 16, 18, 20, 22, 24, 26, 30, 35, 40, 50, 100 and 150 m depths to match observed data.

Smearing of the pycnocline is slightly exaggerated by in the modelled results as well. The cool water observed around day 250 is properly captured by the model but the modelled thermocline reestablishes too low and modelled water in the epilimnion is therefore warmer than observed. The thermocline depth at this station looks to compare well but because of the depth of the water column in this area of the lake, small differences in thermocline depth between modelled and observed profiles are difficult to distinguish. Another example of ELCOM's tendency to underestimate temperatures occurs between days 175 and 200 at this station as the modelled thermocline depth is higher in the modelled profile compared to observations.

In the modelled temperature profile at station 403, the gradual warming of the water with depth starts immediately whereas, warming in the observed profile starts suddenly at a depth of 30 m around day 130. The thermocline is observed to establish itself at a depth of about 25 m around day 190 and the modelled profile shows it establishing at the same time but at a depth well above 20 m. The modelled thermocline does not look as sharp as it does in the observed profile. The modelled temperature profile does not capture the extent of the cooling event from day 145 to 155. However, the start date of stratification deterioration is well captured by the model.

The modelled temperature profile at station 1266 reproduces the small warming event before the onset of stratification at day 115. The observed depth of the thermocline is slightly greater than the modelled results. This is opposite to the comparison at station 403. The observed vertical transport of heat in the hypolimnion is not efficiently captured by the model. A small cooling event just prior

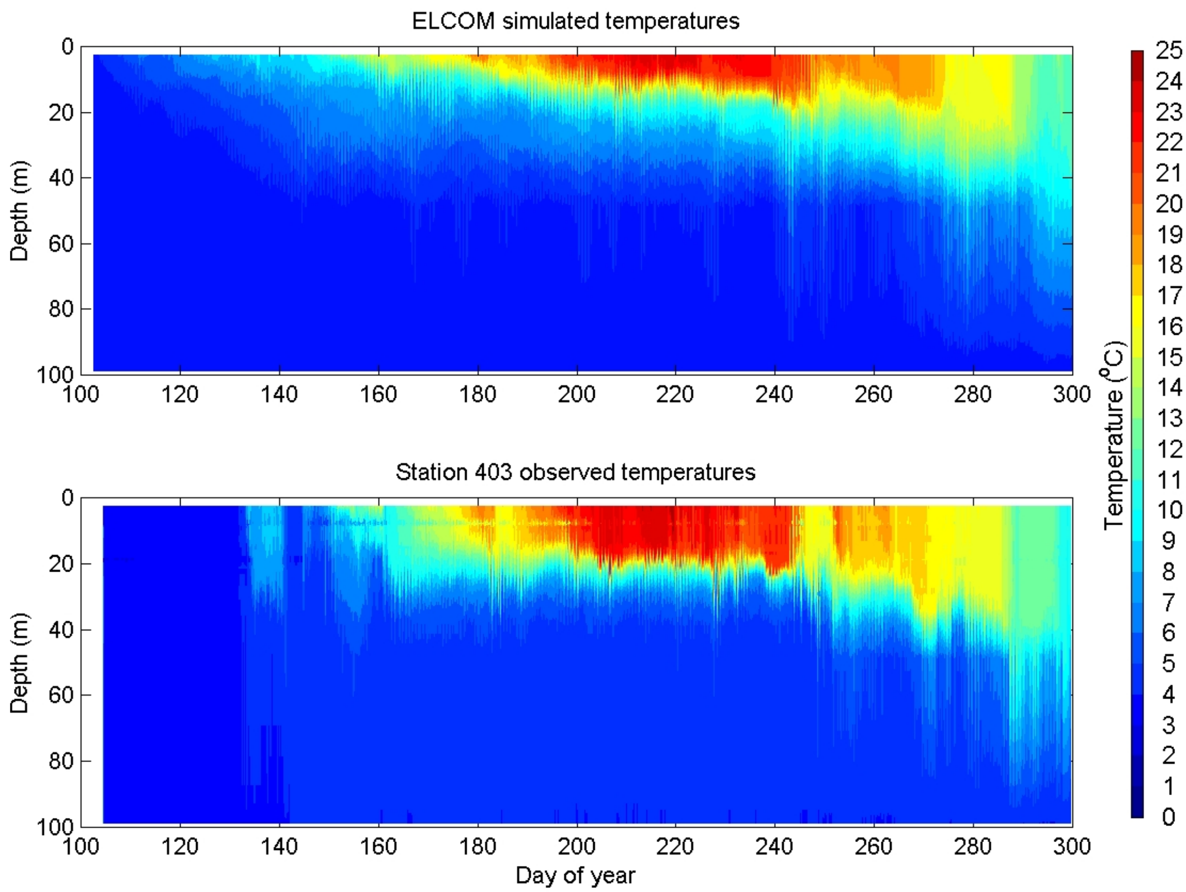

Figure 3.7: Modelled (top) and observed (bottom) temperature profiles at station 403 at 10 min intervals. Modelled temperature output was interpolated at 2.7, 4, 6, 8, 9, 13, 15, 17, 19, 21, 23, 25, 29, 34, 39, 49 and 99 m depths to match observed data.

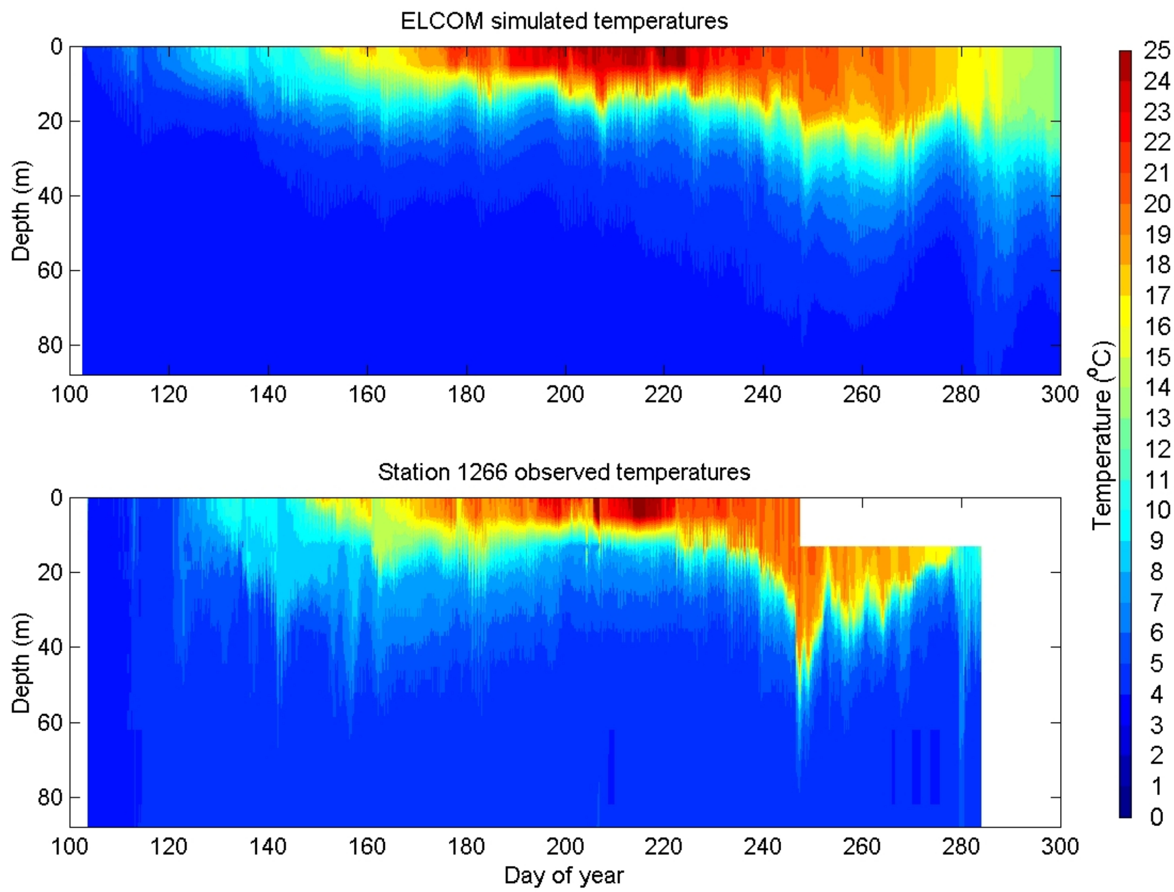

Figure 3.8: Modelled (top) and observed (bottom) temperature profiles at station 1266 at 10 min intervals. Modelled temperature output was interpolated at 0.3, 5, 13, 14.5, 17, 19.5, 22, 27, 32, 37, 42, 47, 52, 57, 62, 72, 82, 87 and 88 m depths to match observed data.

to day 180 is not shown in modelled results. When stratification is strongest, between days 190 and 230, there is less vertical transport of heat in the hypolimnion in both the observed and modelled profiles. Lastly, modelled results do not capture the extent of the depth of the event just before day 250.

3.3.2 Water Levels

A literature search for previous work reporting on ELCOM water level simulations was performed with no success. Verifying ELCOM water levels as well as temperature results with field data are of particular importance to this study. The modelled water level and temperature profiles can be used to force an open boundary for simulating the hydrodynamics of a fine-grid model of the nearshore area in the Kingston basin and the upper St. Lawrence River. This could provide more precise hydrodynamic results in the nearshore area.

The model was initially forced including only outflow at the St. Lawrence River, rain and inflows from the Niagara River and the Welland Canal. Figure 3.9 shows the water level comparisons at Kingston when only major inflows, outflows and rain are modelled. The water levels are plotted hourly to show surface level fluctuation as well as daily mean values giving a clearer view of the seasonal rise and fall of the lake surface.

Figure 3.9 shows steadily declining water levels with a difference of 0.41 m at peak water levels with respect to the observed. The modelled water level continues to diverge from observed water levels and near the end of the simulation there is a difference of 0.55 m. Therefore, including only major inflows, outflows and rain in ELCOM simulations does not account for all the components in the lake's

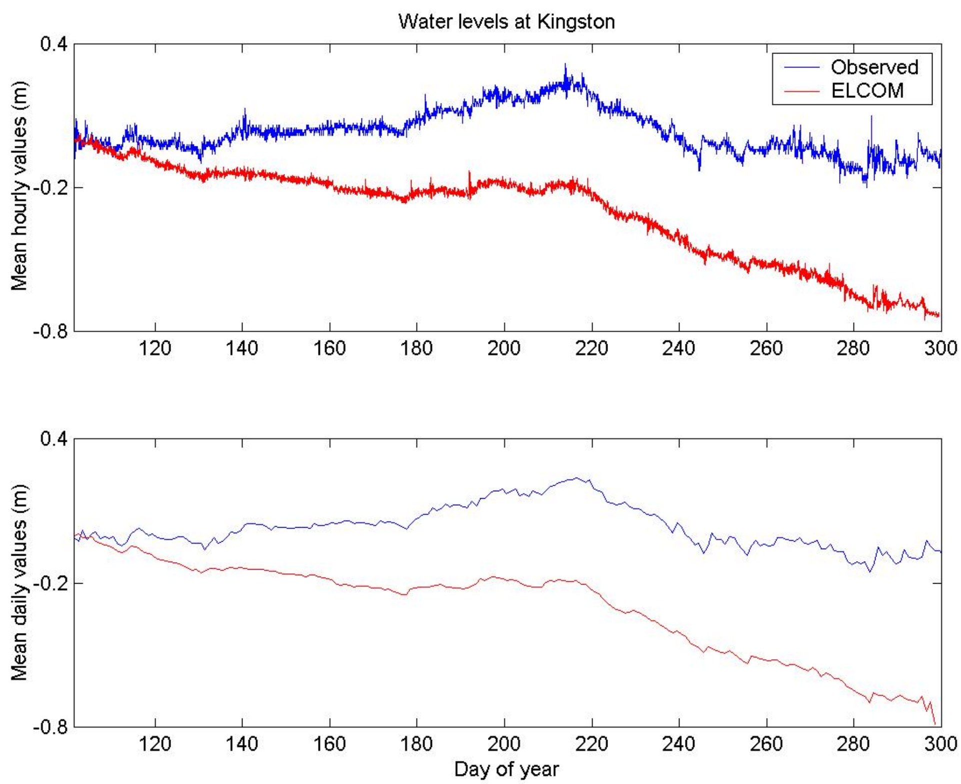

Figure 3.9: Modelled and observed hourly (top) and daily (bottom) water level fluctuations at station 1263. Simulation includes major inflows, outflows and precipitation.

water balance. In most lakes tributary and overland flow is considered negligible. Because of the size of Lake Ontario and its drainage basin, tributary and overland flow accounts for about 14% of all Lake Ontario inflow [44]. The modelled monthly tributary data was provided in metres over the lake surface. These values were divided into daily totals and scaled to correspond to the amount of daily precipitation associated with each day. Scaled tributary values were then added to the precipitation values uniformly over the lake surface as shown in Figure 3.3. Modelled results including tributary flows are shown in Figure 3.10.

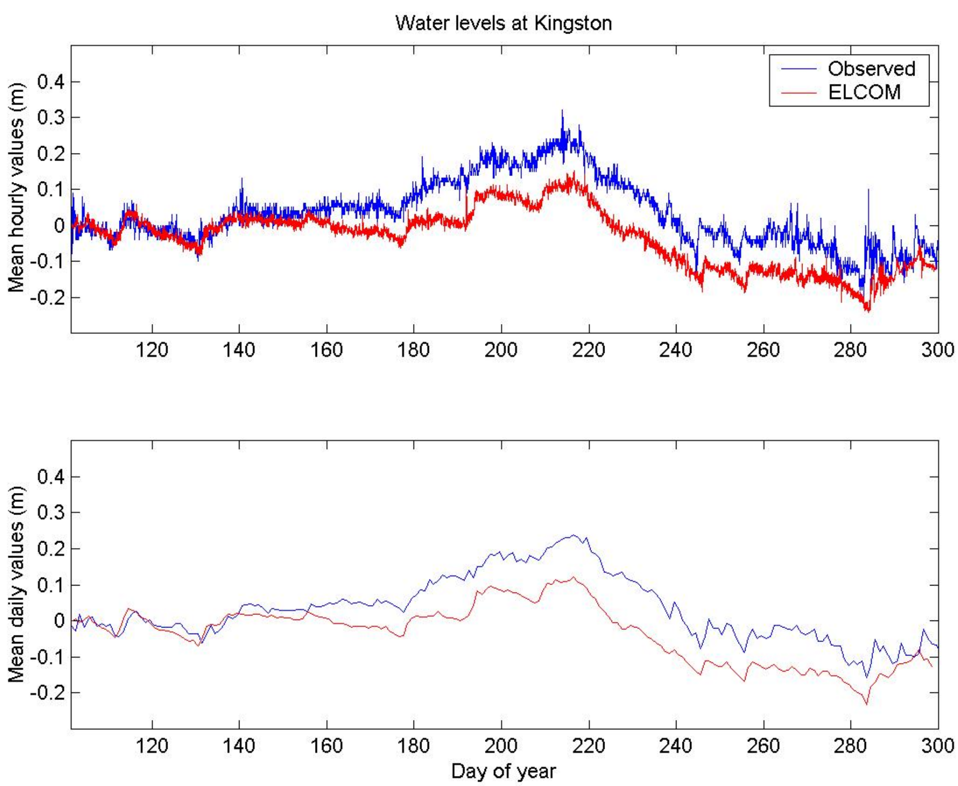

Figure 3.10: Modelled and observed hourly (top) and daily (bottom) water level fluctuations at station 1263. Simulation includes modelled tributary flow, precipitation and major inflows and outflow.

With the added modelled tributary data, the simulated water levels compare well for the first 40 days of the simulation and then the simulated and observed water levels start to diverge and the ELCOM water levels end up about 0.12 m lower then the peak observed water levels. Modelled water levels at various locations around the lake were compared to historical data in nearby locations to verify that the model is performing equally well all around the lake. As water level results were all satisfactory and the Kingston basin area is of interest as well as for brevity, the results are not shown for these simulations.

3.3.3 Currents

The goals of this study are to test the ELCOM's ability to represent offshore and nearshore water movement. Therefore, it is necessary not only to look at how well ELCOM simulates temperature fluctuations in the water column and water level fluctuations but to look at how modelled currents compare with observed data. Current observations were available for the second half of the simulation at station 1266 and for the first half of the simulation at station 1263.

Currents at station 1266 (Figure 3.11) in the hypolimnion range between 5 and -5 cm/s. The water above the thermocline reaches speeds much higher then in the hypolimnion. However, events of increased east or west velocities are observed throughout the water column but are not reproduced at depth in the ELCOM simulation. The event seen in the observed temperature profile for station 1266 around day 250 is also portrayed in the observed east component of velocity profile with a smaller representation in the observed north component profile. Like in the temperature profile comparisons, ELCOM current profiles do not capture the extent

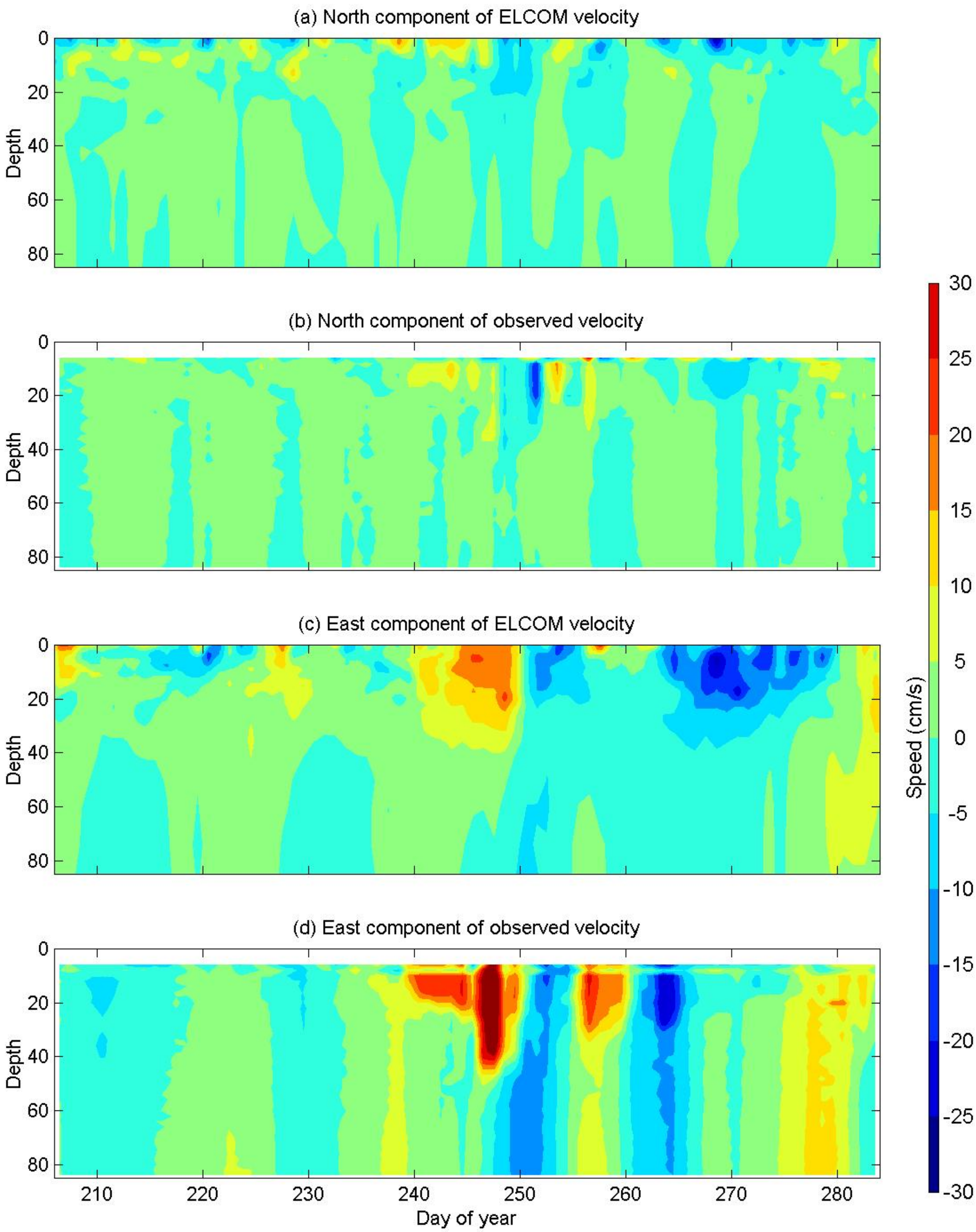

Figure 3.11: Modelled north (a) and east (c) components of velocity compared to north (b) and east (d) components of observed velocity at station 1266 at daily intervals. Observed velocity was measured at 2 m intervals throughout the water column.

of this event. Increases in the north component of observed velocity previous and after this event are weakly reproduced in ELCOM. Generally ELCOM does not reproduce currents to the entire depth at which they are observed. ELCOM shows an increased westward water movement in the modelled epilimnion which is not evident in the observed data. Observed temperature data for this period is unavailable making interpretation of this portion of the current profiles very difficult.

The observed north component of velocity at station 1263 (Figure 3.12) varies only between 5 and -5 cm/s before day 160 which coincides with the date that water at this location starts to significantly warm. Increased water velocities and mixing in this shallow area facilitates the warming of the entire water column. ELCOM simulated north component of velocity in the top 5 m of the water column is too high in magnitude compared to observed data previous to day 160. After day 160, ELCOM does a good job of reproducing the currents in the top 5 m of the water column. However, the mid portion of the simulated water column portrays a north velocity slightly higher than what is observed. Very little water movement is observed in the east-west direction. ELCOM greatly over estimates this for the entire simulated time period shown. ELCOM also portrays much more west moving water in the bottom portion of the water column than is observed between day 160 and 210. Once the water in the entire depth of the water column has warmed (after day 160), ELCOM shows a consistent north-westerly water current direction for the bulk of the water column below a 5 m depth. However, it is however observed that the flow direction switched back and forth fairly consistently between north-west and south-east directions.

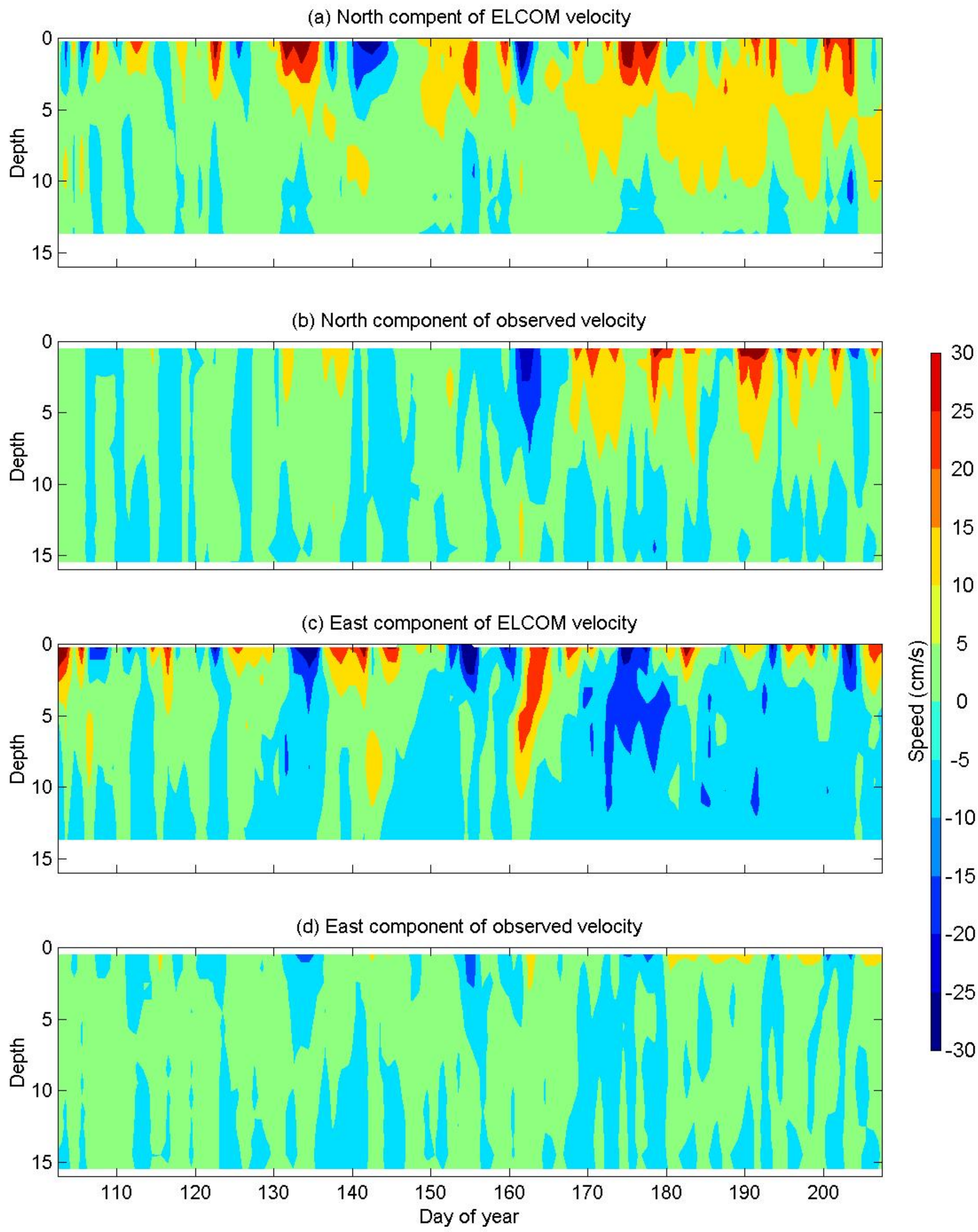

Figure 3.12: Modelled north (a) and east (c) components of velocity compared to north (b) and east (d) components of observed velocity at station 1263 at daily intervals. Observed velocity was measured at 1 m intervals throughout the water column.

Although current profiles give a good idea of how well the model is performing, only simulated temperature profiles and water levels are needed to force an open boundary in ELCOM. Grid size plays a significant role in how accurate the results are especially in the nearshore region as bathymetry plays a larger role in determining water movement because of the shallower water depth. In the offshore region, ELCOM currents compare well to measured data (Figure 3.11). However, in the nearshore region, results are less accurate (Figure 3.12). The difference between modelled and observed velocity was plotted and is shown in Appendix **??**.

3.4 Discussion

3.4.1 Temperature Evaluation

Temperature profiles are an excellent means of visualizing basin-scale waves [4, 10, 12, 20, 27] and have been a main component of numerical model evaluations as seen in literature [6, 14, 19, 30]. For confidence that the model is adequately reproducing the hydrodynamics in the entire lake, it is important that there be good agreement between observed and simulated temperature profiles throughout the lake.

Long and shortwave radiation as well as air temperature are the components of meteorological forcing that most prominently effect the lake's simulated temperatures. It was found that using the method of scaling seen in Laval *et al.* gave the best agreement between ELCOM simulated results and observed data. However, even with these scaling factors, ELCOM is shown to underestimate modelled temperature at station 1263. Scaling factors of 1.15 and 0.9 for long- and shortwave radiation were used for Lake Kinneret simulations [28]. Lake Kinneret is a much smaller lake requiring less energy to heat. Further simulations would be required to obtain scaling coefficients for long and shortwave radiation unique to Lake Ontario.

The simulation length is of importance because results portray the setup and deterioration of stratification. The variation in depths of the station locations, from the shallow waters of station 1263 in the Kingston basin to the deepest portion of the lake at station 586, allows for the visualization of the temperature variations in areas of different depths. However, because of the large variance in depth of the nearshore and offshore temperature profiles, it is difficult to determine if ELCOM better reproduces temperature stratification in the offshore or nearshore profiles.

The observed temperature profile at station 1266 (Figure 3.8) shows evidence of a storm event that was not captured to the same depth in the model. This could be attributed to the great distance between station 1266 and the closest moored weather station (Figure 3.4) and therefore the intensity of this storm was not accurately captured by these results. Therefore spatially varied meteorological forcing is essential when modelling large lakes and this model of Lake Ontario may benefit from more varied meteorological forcing files. Evidence of this event is also apparent in the temperature profiles at stations 586 and 403 (Figure 3.6 and 3.7) where during this time period the simulated temperature is warmer then the observed data. This is opposite to the rest of the simulation period and could be associated with the event recorded on the observed profile at station 1266. Therefore, it is possible that other localized storm events not captured by the meteorological forcing files could be the cause of variance between observed and simulated temperature profiles.

3.4.2 Water Level Evaluation

It has been previously found that the Niagara and the St. Lawrence Rivers have little impact on the overall modelled circulation of the lake and that any impact is mostly confined to a region in the order of 10 km from each respective river [5]. However, all inflows and outflows to and from the lake are important for modelling water level fluctuations. Evaluation of modelled water level fluctuations is a method of assuring that the model accurately represents all the hydrodynamic processes in the lake. (See Appendix B for more information on the importance of water level evaluation.) Previous to this, the literature has not covered ELCOM's performance with predicting water levels. Evaluating the water levels is of particular importance for this study as the water levels produced by this model can be used to force an open boundary to a finer grid model.

Modelling the water balance of Lake Ontario has many flaws. Its large drainage basin, many minor tributaries and overland flow are variables which are difficult to accurately monitor. Both rain and tributary flow data is accounted for in metres over the surface of the lake. Therefore the surface area of the modelled lake directly influences the volume of water input into the the model through these variables. Because of the coarse 2×2 km grid, the modelled surface area of the lake may not match the surface area that these variables are based on which could account for the discrepancy between the modelled and observed water levels. It must also be noted that groundwater is not accounted for in these simulations, however the deficit between modelled and observed water levels is not constant and therefore neglecting groundwater flow cannot be directly responsible for this deficit although it may play a part.

In Figure 3.10, the modelled water levels match the observed data until about 40 days into the simulation where the modelled water levels start to diverge away from the observed. This could be due to the significant amount of precipitation that the lake receives starting around that time but is not accurately represented in the model because the volume of water from precipitation and tributary data is dependant on surface area and it is not known if the surface area of the modelled lake and area of which the data is based from are the same. This could account for the difference in modelled and observed water levels.

The ELCOM simulated water levels compare relatively well to the observed data considering the size of the lake and its drainage basin as well as the of lack accurate forcing data for tributaries, overland flow and rain. In an effort to determine how much water is missing in the ELCOM simulated system, the tributary data was scaled. By trial and error, it was found that scaling the modelled tributary data by a factor of 1.2 gives optimal results as shown in Figure 3.13. Increasing the tributary data by a factor of 1.2 reduces the difference between observed and modelled peak water levels to 0.01 m.

3.4.3 Current Evaluation

North and east components of velocity comparisons are another common way of evaluating the effectiveness of a model at representing the hydrodynamics in a lake. Current meter data was available for two locations in the lake, at station 1266 offshore in the western side of the lake and station 1263 nearshore in the Kingston

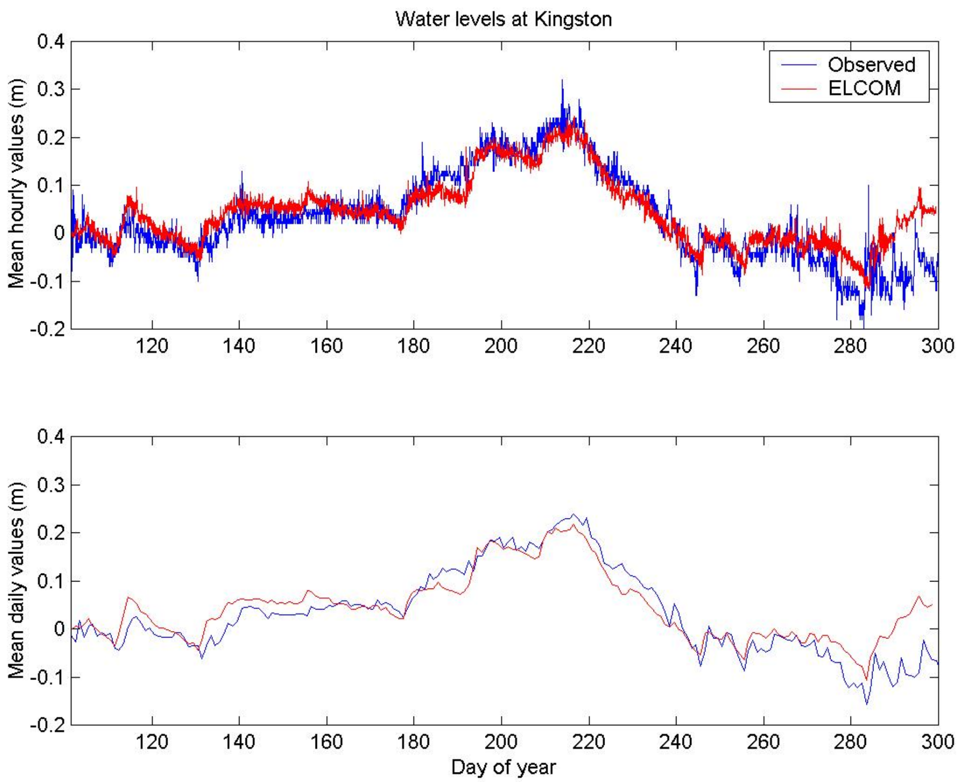

Figure 3.13: Modelled and observed hourly (top) and daily (bottom) water level fluctuations at station 1263. Simulation includes scaled tributary flow, precipitation, major inflows and outflow.

basin. The simulated currents at station 1266 compared better with observed data than current comparisons at station 1263. For the most part, the observed and simulated currents are not very strong, particularly below a 5-10 m depth, therefore small differences between observed data and simulated results are not of great significance. However, ELCOM does not capture the entire depth of the currents represented in the observed data. This may be attributed to numerical diffusion problems also seen in Laval *et al.* and Hodges *et al.* [11, 14, 19, 30] or, as mentioned above, the inability of the weather station at station 403 at capturing the extent of the storm event around day 150 in the vicinity of station 1266.

The the bathymetry of the nearshore region of station 1263 may have influenced poorer results compared to current profiles at station 1266 where the depth of the water column is almost 10 times deeper. In the nearshore region of station 1263, actual bathymetry is much more complicated than can be captured on a 2×2 km grid scale. Because of the shallow depth in this region, this could have a significant effect on simulated currents more so than in the deep water region of station 1266. Simulated currents for the bottom portion of the water column at station 1263 after day 160 are shown to be much smoother than observed. The extent of influence that bathymetry has on water movement in ELCOM is unknown but could still be a factor in contributing for the discrepancies between modelled and observed current profiles at this station. The direction of outflow in ELCOM could also play a role in contributing to the differences between modelled and observed current profiles at station 1263 because of the outflow's proximity to this station. The simulated outflow near this location is a straight east-west opening but in reality the flow curls north-east around Wolfe Island. The coarseness of the grid prevents an accurate representation of this outflow and the bathymetry around this nearshore region. This could have a negative effect on simulated currents and be another component leading to discrepancies between modelled and simulated currents. Because of the greater depth and simple bathymetry at station 1266, the current comparisons are much more satisfactory (Figure 3.14).

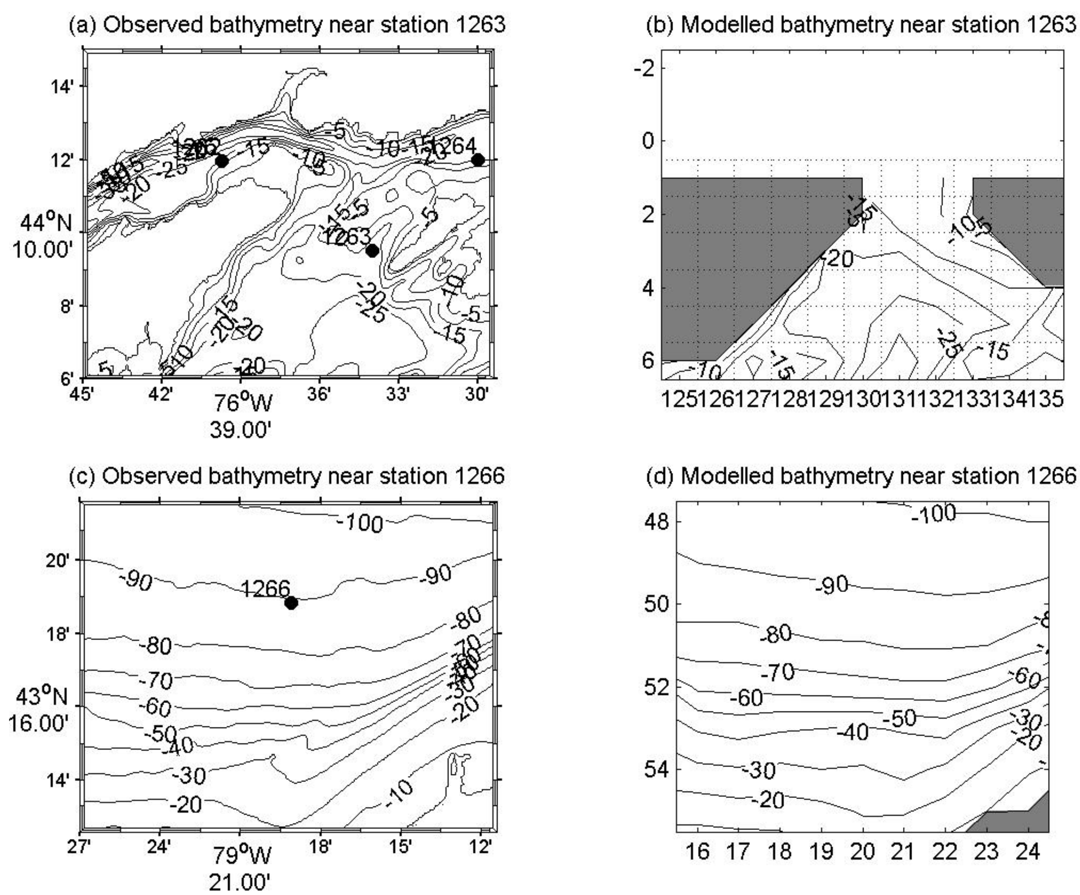

Figure 3.14: Observed bathymetry (a) compared to ELCOM 2 $\times$ 2 km grid (b) at nearshore station 1263 and observed bathymetry (c) compared to ELCOM 2 $\times$ 2 km grid (b) at offshore station 1266

Overall, current comparisons are much more variable than temperature profile comparisons. However, it is important to note that in order to provide forcing for an open boundary simulation in ELCOM only temperature profiles and water level fluctuations are required, current profiles are not needed. Also, simulating such an open boundary should be done in the mid-lake area away from any complicated bathymetry near the shoreline or outflows in order to be sure that the modelled data forcing the open boundary is accurate.

The ELCOM model was compared to observed 2006 summer season field data and for a holistic view of the circulation patterns it was compared with Beletsky *et al.*'s plot of summer circulation [8]. Beletsky *et al.*'s plot, shown in Figure 3.15, was constructed from an average of currents measured at depths of 15, 19, 30, 50 and 75 m therefore an output of averaged currents at these same depths are shown in Figure 3.16 for the 2006 summer simulation. Certain features of this figure compare well with Beletsky *et al.*'s plot of summer circulation. The cyclonic gyre which Beletsky *et al.* observed to be very stable is very well reproduced with the ELCOM simulation. The coastal current on the south shore of the lake also compares well. However, the ELCOM simulation portrays several small anticyclonic gyres as opposed to just one in the northwestern part of the lake as is shown by the Beletsky *et al.* plot. As well, a significant amount of water from the Niagara River seems to be circulating west which also is not shown on the Beletsky *et al.* plot. The differences between these two plots can be attributed to seasonal variations as the circulation in the western part of Lake Ontario has been previously shown to be different in different years [8]. Confidence is ensured that ELCOM is properly representing the currents in Lake Ontario because the stable features of summer circulation compare well to the ones mapped out by Beletsky *et al.* [8]. Averaged lake-wide currents at various depths were compared with other circulation maps of Lake Ontario from literature in Appendix C. It should be noted that interannual variability is not the focus of this study and has not been systematically studied in the past. However, past studies have indicated variations in summer circulation from year to year [8].

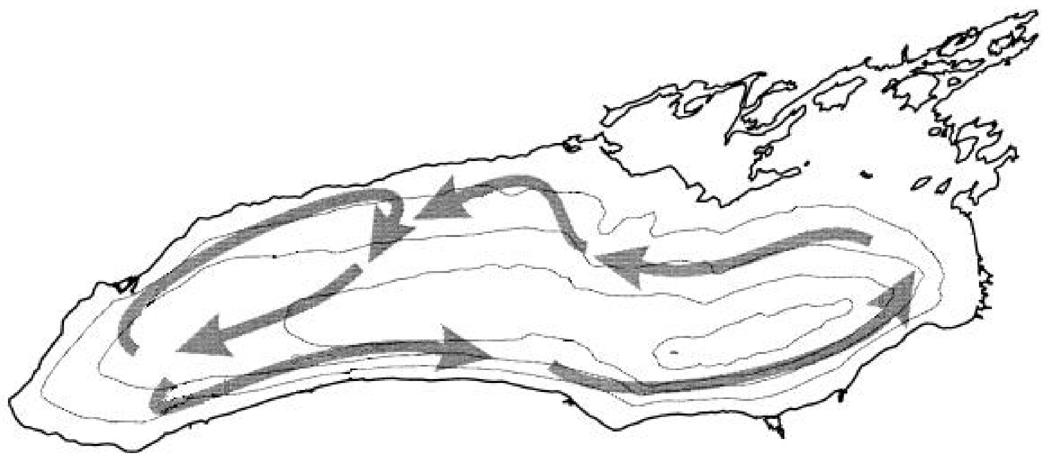

Figure 3.15: Beletsky *et al.*'s plot of summer circulation [8].

The focus of this study was to reproduce general lake circulation patterns in the nearshore and offshore regions and ELCOM's ability to reproduce high frequency waves was not the goal of this study. Therefore whether or not, ELCOM reproduces coastal jets, Poincaré and Kelvin waves is not examined as a horizontal grid scale of 2×2 km is to large to capture these basin-scale waves. A finer grid scale may be more appropriate in reproducing these higher frequency waves. Additional simulated temperature and current profile output at more locations throughout the lake and at lower time frequencies would be necessary to identify internal waves and their frequencies.

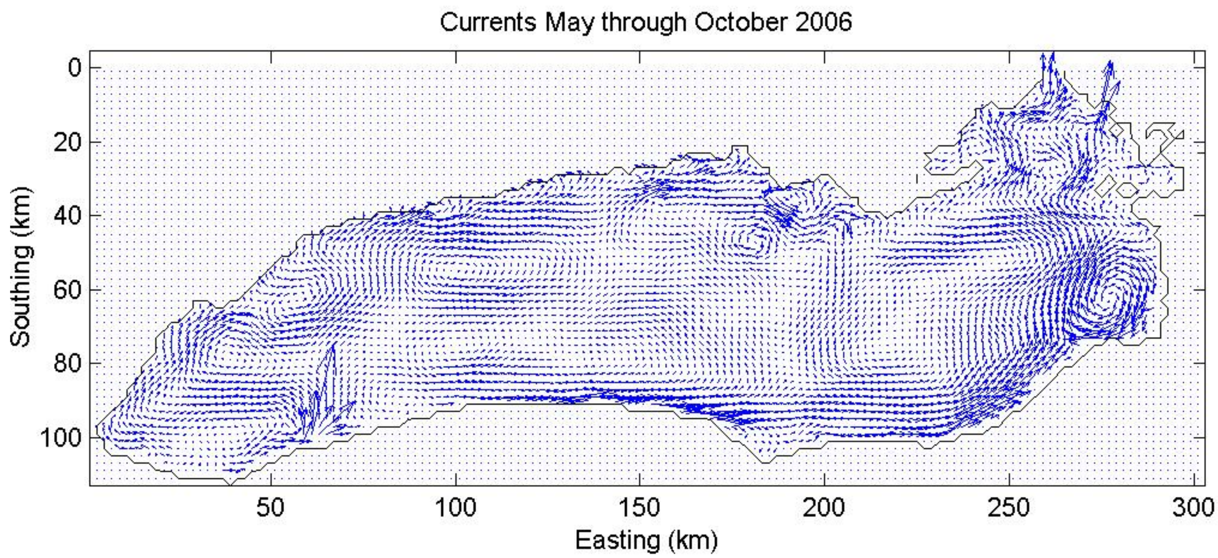

Figure 3.16: Lake-wide ELCOM mean circulation for May to October 2006 integrated at 15, 19, 30, 50 and 75 m depths.

3.5 Conclusion

The review and consideration of previous work relating to the circulation and modelling attempts also provided valuable information towards the successful completion of this project. To ensure that ELCOM properly simulates the hydrodynamics in Lake Ontario, modelled temperature profiles, water level fluctuations and current profiles were compared with available observational data. Agreement between modelled and observed temperature profiles was the most successful of the three as near- and offshore profiles compared equally well. The date at which stratification occurs, the depth of the thermocline as well as general temperatures were compared. Results were generally satisfactory for a coarse grid model except that even after scaling the long- and shortwave radiation, ELCOM's simulated temperatures were still slightly lower than observed.

It was of particular importance to evaluate ELCOM's performance with water levels as it has not previously been studied. Water level simulation results were also compared because they can be used to force an open boundary for a nearshore model of the Kingston basin and the upper portion of the St. Lawrence River. Water level simulation proved to be problematic because of the lake's size. Although major inflow and outflow data is easily acquired, rain as well as tributary and overland flows are provided as average values dependant on the lake surface area. More precise data is needed for better results. Tributary forcing data was increased by 20% to account for missing water volume.

Simulated to observed current profile agreement proved to be more variable than temperature profiles. Simulated currents in the offshore region at station 1266 had overall better agreement with observed data than at station 1263 in the nearshore. This can be attributed to the difference in depth between observation sites. In the shallow area where station 1263 is situated, the movement of water could be affected by bottom topography. Station 1263 is also near the outflow to the St. Lawrence River. The varied bathymetry and flow out of the lake is not properly captured by the coarse 2×2 km grid negatively effecting the current profiles at this location.

It was found that ELCOM does an equally good job at reproducing offshore and nearshore temperature profiles, however simulated to observed current profile comparisons agreed better in the offshore region then in the nearshore region on a coarse grid scale. The comparisons of temperature profiles, water level fluctuations and current profiles portrayed above give the confidence that, under the present forcing data, ELCOM does an overall good job at representing the general circulation patterns in the offshore regions of Lake Ontario on a coarse grid scale. It was found that the nearshore areas are not sufficiently resolved with a 2×2 km grid scale to properly simulate currents and that water level simulation requires more precise forcing data to obtain accurate results without scaling factors.

Considering all methods of evaluation, ELCOM does a good job at taking unaveraged, spatially varied meteorological forcing data as well as inflow and outflow data to accurately reproduce thermal stratification and general circulation patterns in Lake Ontario. It is also demonstrated that it is essential to model all inflows and outflows to properly simulate lake water level fluctuations. The occurrence of high frequency waves was not evaluated in this study. Temperature profiles and scaled water level results from this study are used in Chapter 4 to force an open boundary to better resolve nearshore hydrodynamics in the Kingston basin and the upper portion of the St. Lawrence River and provide scientific information to advance the CRCA study and the delineation of IPZs.

Chapter 4

Nearshore Hydrodynamic Model

4.1 Introduction

The Great Lakes have many functions including providing source drinking water and a sink for pollutants and runoff [1]. Serious water quality problems have been identified within the Great Lakes basin as a result of increased urbanization and industrial activity which is generally the cause of environmental degradation of many nearshore areas due to municipal and industrial discharge [32]. Although substantial advances have been made in the regulation of outfall location and permissible effluent quality, the ever increasing total volumes of wastewater heightens the need to understand coastal physical processes in greater detail [2].

Circulation in the Great Lakes has been of interest since the late 19th century for a variety of applications. Most recently, due to the Clean Water Act passed in October 2006 by the Ontario government, the responsibility of drinking water protection has been placed in the hands of each municipality. The Ontario Clean

Water Act is intended to ensure communities take the appropriate steps in protecting their drinking water supply through developing locally driven, science-based protection plans [33]. Hydrodynamic modelling provides the basis for simulating transport in response to meteorological forcing functions [6].

Computational requirements for lake-wide modelling is of concern. To avoid unmanageable computation times grid scale resolutions are coarse as in the case of the study by Hurdowar-Castro *et al.* who modelled the nearshore along the Toronto waterfront on a 500 m grid scale in order to evaluate the optimum position for a new drinking water intake. The results of this model alone were not conclusive due to the coarseness of the grid size. A smaller model with a 100 m grid scale was nested and validated with separate drogue experiments to improve study results which were then used to evaluate proposed locations of potential drinking water intakes [1].

Shen *et al.* nested a 500 m square grid of the Lake Ontario Toronto waterfront in a 2 km coarse grid model. The three-dimensional hydrodynamic/water quality model was successfully validated and results were used to simulate current and pollutant transport for a period of 5 days for both stratified and isothermal conditions [32].

A two-dimensional finite element model (FEM) of the entire lake with grid sizes varying between 80 m and 5 km have also been seen. Hayashida *et al.* modelled Lake Ontario using idealized meteorological forcing data with constant Niagara flows of 5000 m^3/s and 7000 m^3/s and concluded that models which do not include the whole lake may not be able to simulate the trajectory and dispersion of Niagara River water properly under all conditions [37].

A nested grid approach is also in progress using the Estuary, Lake and Coastal Ocean Model (ELCOM) for the Lake Ontario Toronto waterfront area [48]

The goal the Intake Protection Zone (IPZ) study initiated by the Cataraqui Region Conservation Authority (CRCA) is to first delineate drinking water intake protection zones and then produce an inventory and map of all threats and issues in those zones. Because the first stage in water quality tracking is understanding circulation, construction of an accurate flow model is necessary. Three dimensional hydrodynamic modelling is an appropriate tool for understanding the relevant processes in a source water body to simulate the changing conditions which may affect the quality of drinking water [6]. In Chapter 3, a coarse grid lake-wide model of Lake Ontario was evaluated. To properly model water circulation in the nearshore areas of the Kingston basin and the upper St. Lawrence River a 300 $\times$ 300 m grid model is evaluated. The objectives of this chapter is to test the sensitivity of the open boundary and the model's ability to reproduce temperature and current variations in the nearshore at this grid scale.

4.2 Model Description and Data

Three dimensional hydrodynamic model, ELCOM, is used as a tool for understanding general circulation and temperature patterns in the Kingston basin of Lake Ontario and the upper portion of the St. Lawrence River. A fine-grid model of 300 $\times$ 300 m is tested with three different forcing methods for the open boundary. Open boundary simulations require temperature and water level forcing data. The first case's open boundary (A) is forced by hourly historical Kingston water level data and temperature data at 10 min intervals originating from thermistor chain data from temporary mooring 1263[1] in the Kingston basin in close proximity to the location of the open boundary. The second simulation (B) was forced using hourly historical Kingston water level data and hourly surface temperature from Environment Canada permanent mooring C45135 located at 43.79°N and 76.87°W outside of the simulated area and the Kingston basin. The third and final open boundary simulation (C) is forced using hourly temperature and water level data output from the coarse grid model presented in Chapter 3. The run-time of simulations A and B was approximately 5 days whereas simulation C required over a week because of the large number of files required to force the horizontally varied open boundary condition.

ELCOM is driven by meteorological files comprised of wind speed (m/s), wind direction (degrees clockwise from north), air temperature (°C), relative humidity, measured shortwave radiation (W/m^2), incoming long-wave radiation (W/m^2) and atmospheric pressure (Pa) obtained from moored surface buoy 1263 (Figure 4.3) equipped with a weather station and provided by the National Water Research Institute (NWRI). Rainfall data[2] (m/day) is also included in the meteorological forcing files. The daily rainfall values were computed using a Thiessen polygon method which weights the observed data at every station according to its representative area [39]. All meteorological data, including rain were input into ELCOM at 10 min intervals (Figures 4.1 and 4.2). Realistic wind forcing has been shown to have a significant effect on resulting circulation patterns [16]. As only the Kingston basin and the upper portion of the St, Lawrence River are being modelled, spatially varied wind forcing was not determined to be necessary to force this model.

[1]Observed water temperature data for station 1263 was provided by C. H. Marvin, R. Yerubandi and B. Schertzer at NWRI

[2]Rainfall data was provided by Tim Hunter at NOAA

Bathymetry, as shown in Figure 4.4, was obtained from the National Oceanic and Atmospheric Administration (NOAA) - Great Lakes Environmental Research Laboratory (GLERL) [41]. The long and shortwave radiation was scaled by 1.15 and 0.9 respectively as seen in Laval *et al.* [28] to counteract ELCOM's tendency to underestimate temperatures. The inflow into the model from the lake was input using an open boundary, therefore temperature and water level data are required instead of flow data. Tributary flow was omitted for this model as it was assumed to be negligible.

ELCOM is incapable of simulating ice cover and instruments providing forcing and evaluation data were removed for the winter season. Therefore, the summer season is of interest. The ELCOM nearshore model was run from day 102.5 (noon on April 12, 2006) to 286.375 (9am on October 13, 2006). The simulation begins well before the onset of stratification allowing for the visualization of the entire onset of stratification. The simulation runs through to the deterioration of temperature stratification demonstrating the baroclinic nature of the Kingston basin and the upper St. Lawrence River. The simulation time-step is every 5 min, as used in a similar model of Lake Erie by León *et al.*, as it was shown to give the best results at an acceptable computational efficiency using a high performance desktop computer [6]. Modelled temperature profiles and current results were compared to thermistor chain, ADCP, and current meter data from stations 1262, 1263, 1264 and 1265 shown in Figure 4.3. In Chapter 3 and Appendix B, water levels were shown to be an important component of lake-wide model evaluation. However, due to insufficient water level data in the study area, simulated to observed water level comparisons are not addressed in this study.

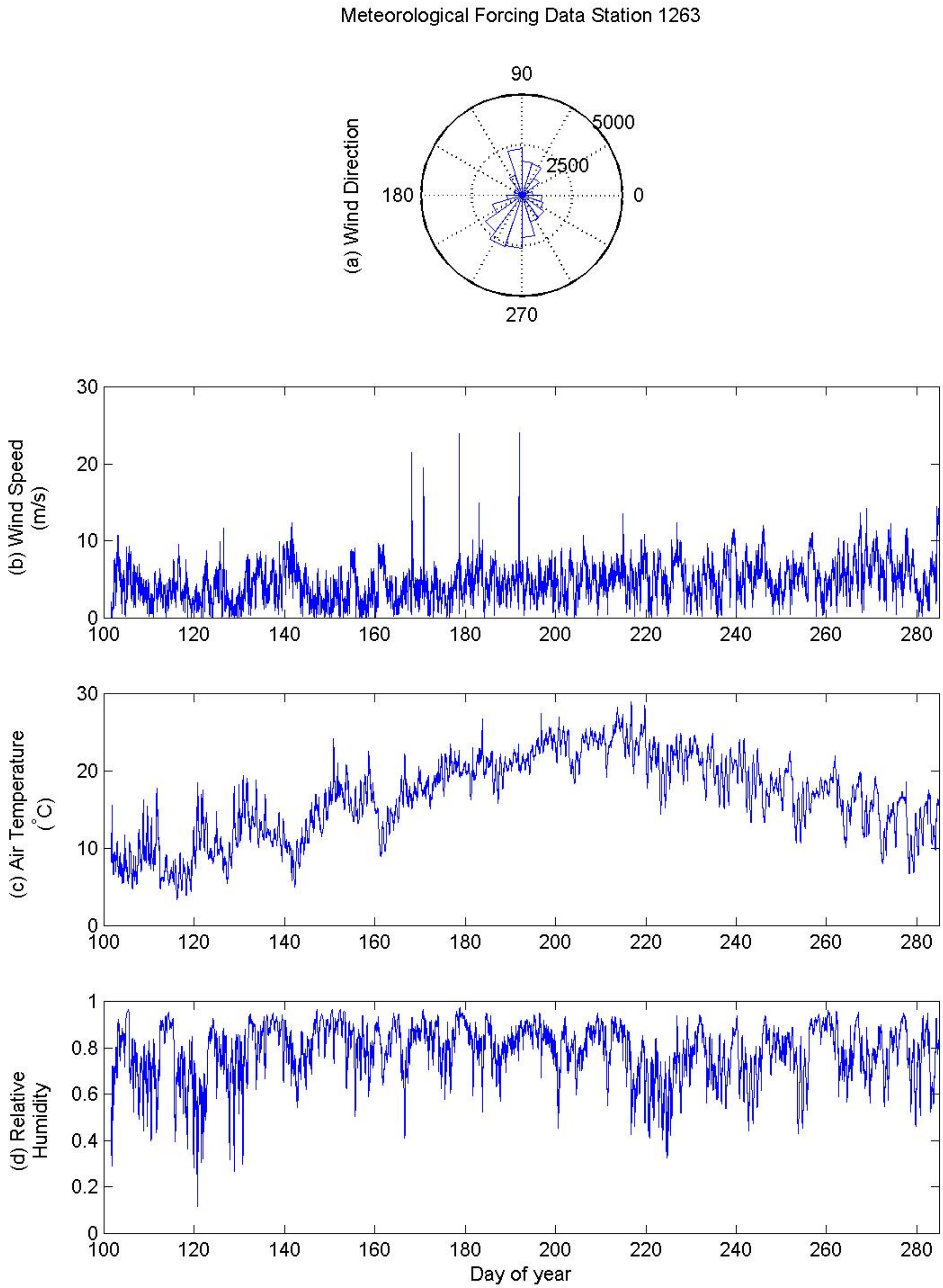

Figure 4.1: Meteorological forcing data used for simulations - (a) occurrence of wind direction in 18° bins, (b) wind speed in m/s, (c) air temperature in °C and (d) relative humidity at 10 min intervals.

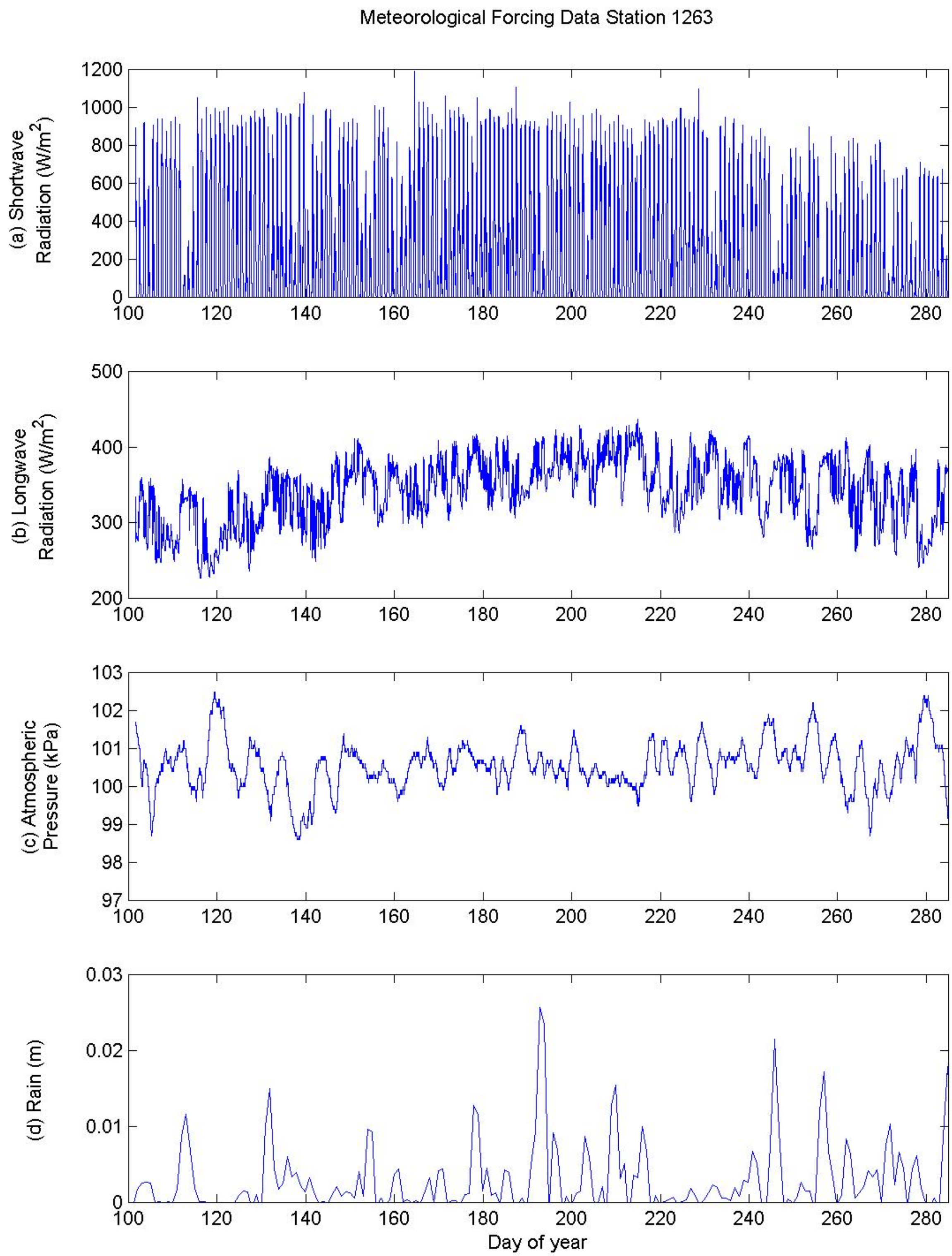

Figure 4.2: Meteorological forcing data used for simulations - (a) shortwave radiation in W/m^2, (b) long-wave radiation in W/m^2, (c) atmospheric pressure in kPa and (d) rain in m over the lake surface. All data is input at an interval of 10 min except for rain which is input daily.

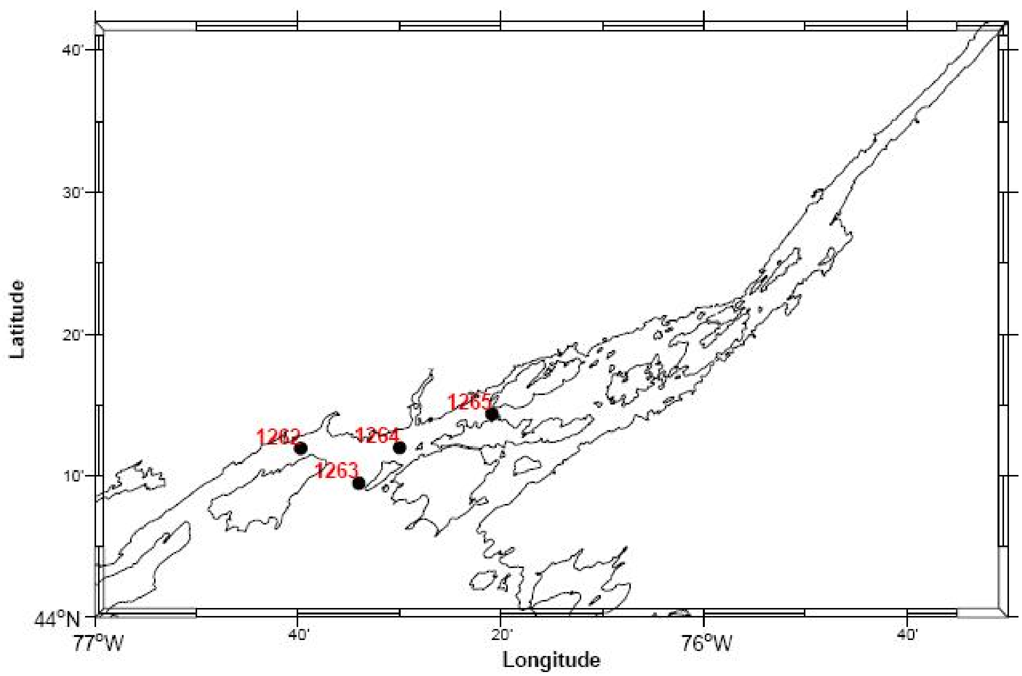

Figure 4.3: Map of the Kingston basin and the upper St. Lawrence River with the locations of stations 1262, 1263, 1264 and 1265

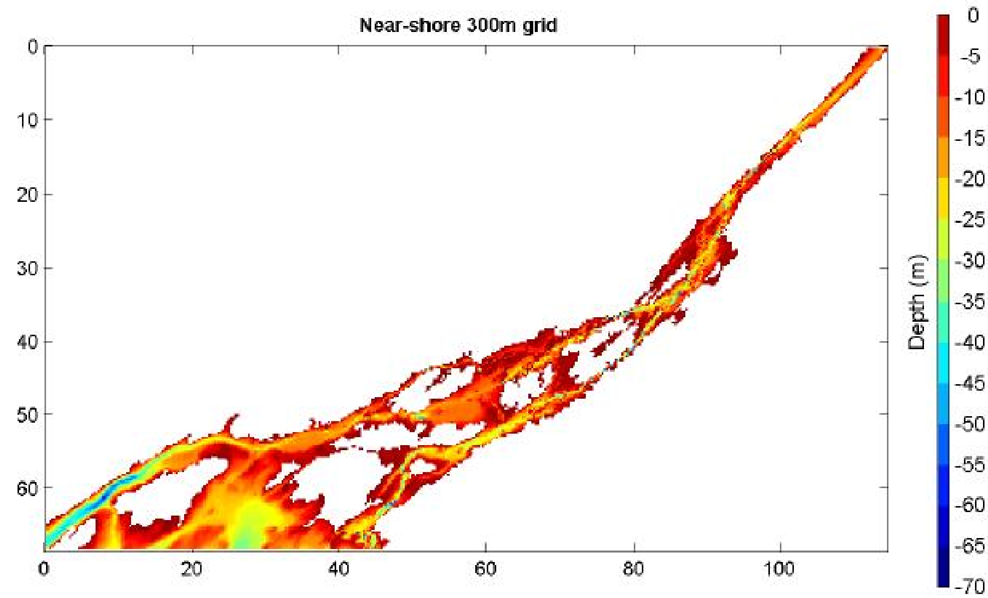

Figure 4.4: Gridded 300 × 300 m Kingston basin and upper St. Lawrence bathymetry

To force an open boundary in ELCOM, both water level and water temperature data is needed. The model outflow is simulated with water level and water temperature data measured at Cornwall and obtained from Environment Canada's Great Lakes St. Lawrence Regulation Office[3]. The inflow through the North Channel is simulated with a temperature profile obtained from station 1263 and Kingston historical water level data [45]. The water level and temperature forcing files for the open boundary connecting the Kingston basin to the main body of Lake Ontario were forced using three different combinations of water level and temperature data sets described above in order to determine which scenario provides the best modelled results and how sensitive the main inflowing open boundary is to

[3]Inflow and outflow data was obtained Len Falkiner at Environment Canada's Great Lakes St. Lawrence Regulation Office

spatially varied forcing data.

4.3 Results

4.3.1 Temperature Profiles

ELCOM results for all simulations were compared to observed temperature profiles recorded at 10 min intervals at stations 1262, 1263, 1264 and 1265 in Figures 4.5, 4.6, 4.7 and 4.8. Thermistor chain data at all observation stations were collected with Tidbit data loggers with 12-bit resolution and 0.2°C accuracy over a temperature range between -20 and 30°C [46].

At all stations, initially, simulation A temperature profiles are shown to warm the fastest. However, simulation C shows a warming event at station 1262 and 1263 which does not compare with observed data. Simulations B and C show equally warmer temperature profiles than simulation A at all stations locations. Results for simulation C at stations 1264 and 1265 along with results from simulation B at station 1265 portray warmer temperature values than is observed. All observed profiles are shown to have fairly uniform temperatures with depth starting between days 190 to 220. Simulations B and C compare well to observed temperature profiles at all stations. Cooling is slower in ELCOM simulations than in observed profiles at all stations. Observed temperature profile at station 1265 shows the formation of a thermocline at the bottom of the water column between days 180 and 200 which none of the ELCOM simulations at this station successfully reproduce. Therefore the thermocline is more diffuse in ELCOM simulations, probably due to numerical diffusion and the coarseness of the grid scale. It should also be noted

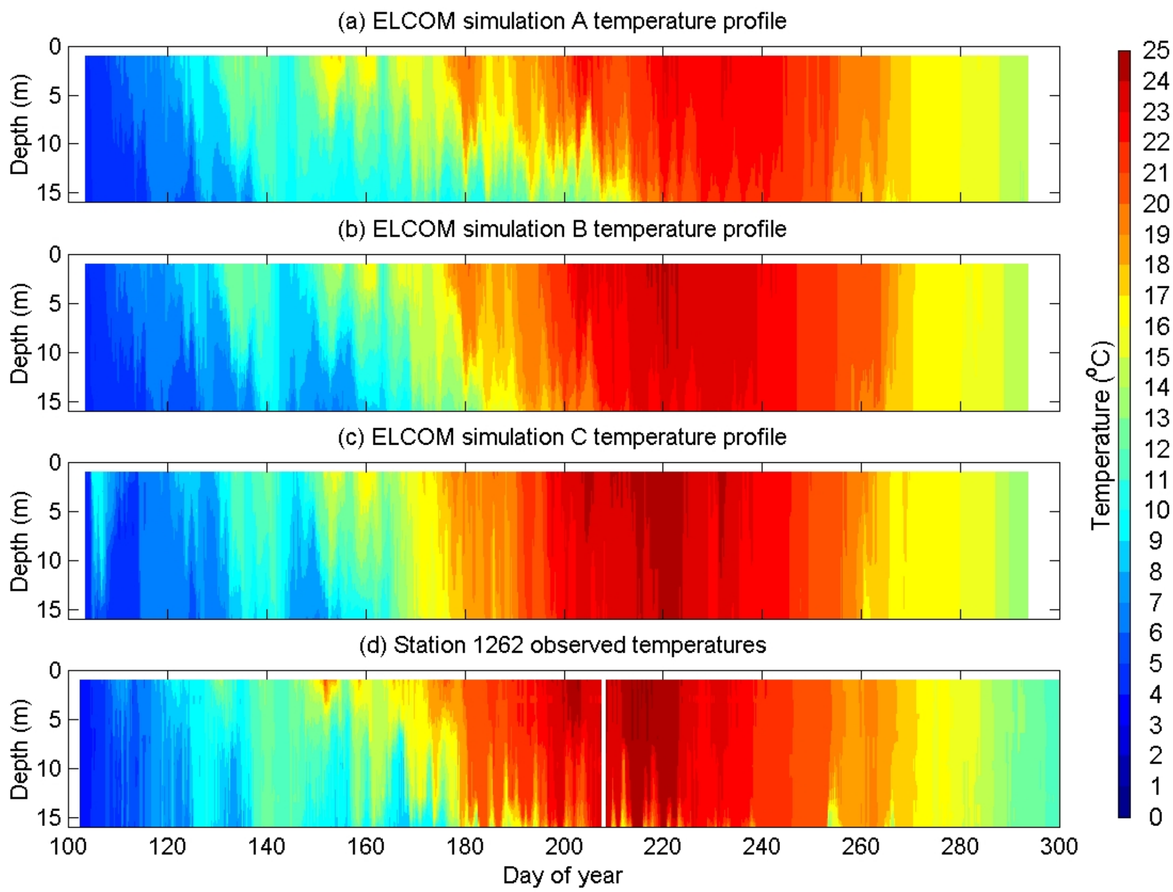

Figure 4.5: ELCOM simulations A (a), B (b) and C (c) temperature profiles are compared to observed (d) temperature profile at station 1262 at 10 min intervals. Modelled temperature output was interpolated at 1, 3, 5, 7, 9.5, 13, 15 and 16.5 m depths to match observed data.

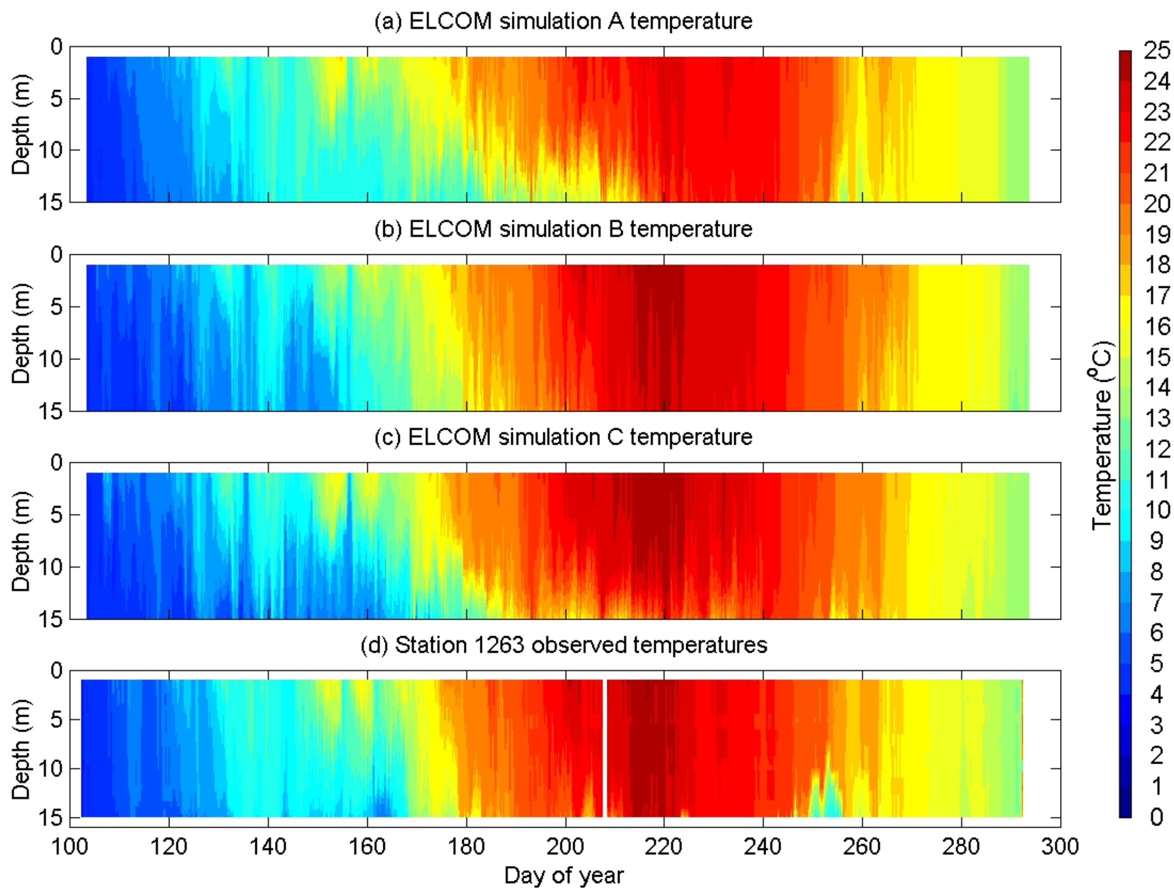

Figure 4.6: ELCOM simulations A (a), B (b) and C (c) temperature profiles are compared to observed (d) temperature profile at station 1263 at 10 min intervals. Modelled temperature output was interpolated at 1, 3, 5, 7, 10, 12, 14, 15 m depths to match observed data.

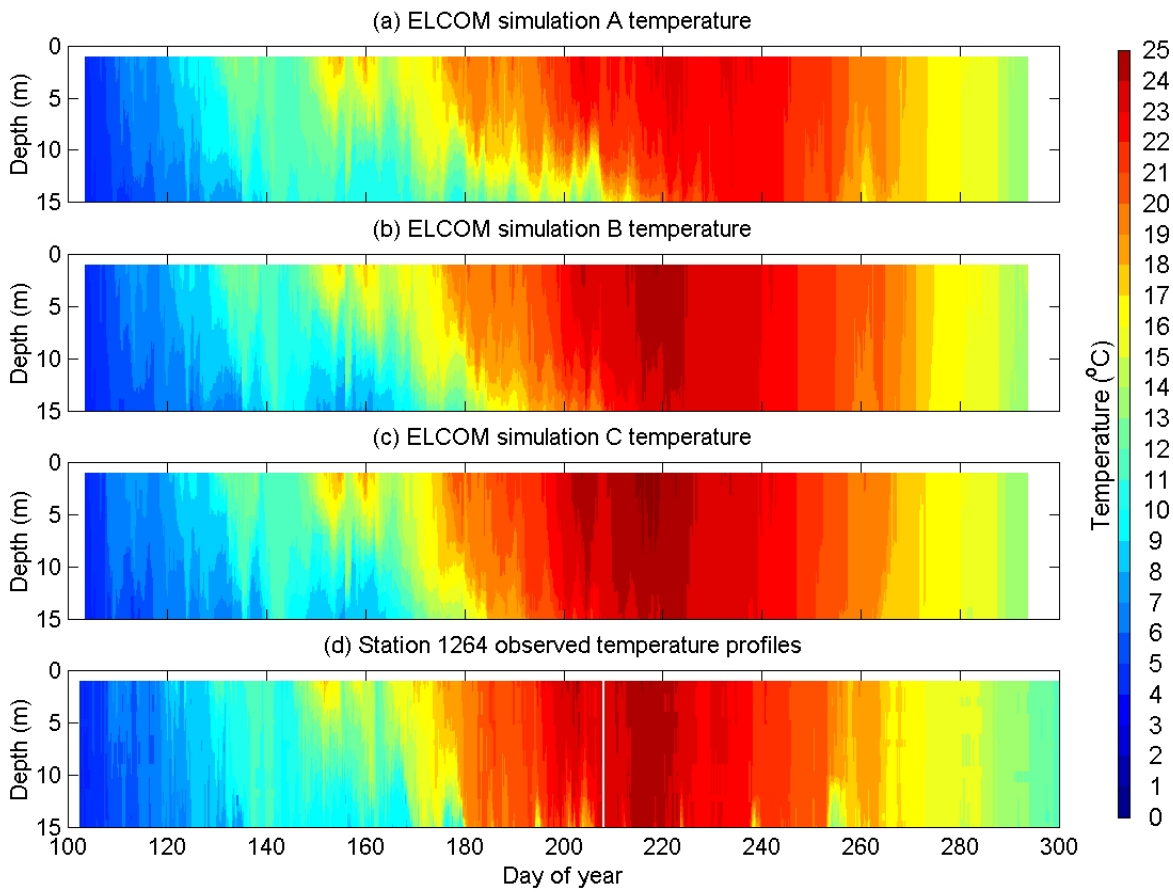

Figure 4.7: ELCOM simulations A (a), B (b) and C (c) temperature profiles are compared to observed (d) temperature profile at station 1264 at 10 min intervals. Modelled temperature output was interpolated at 1, 3, 5, 7, 10, 12, 14, 15 m depths to match observed data.

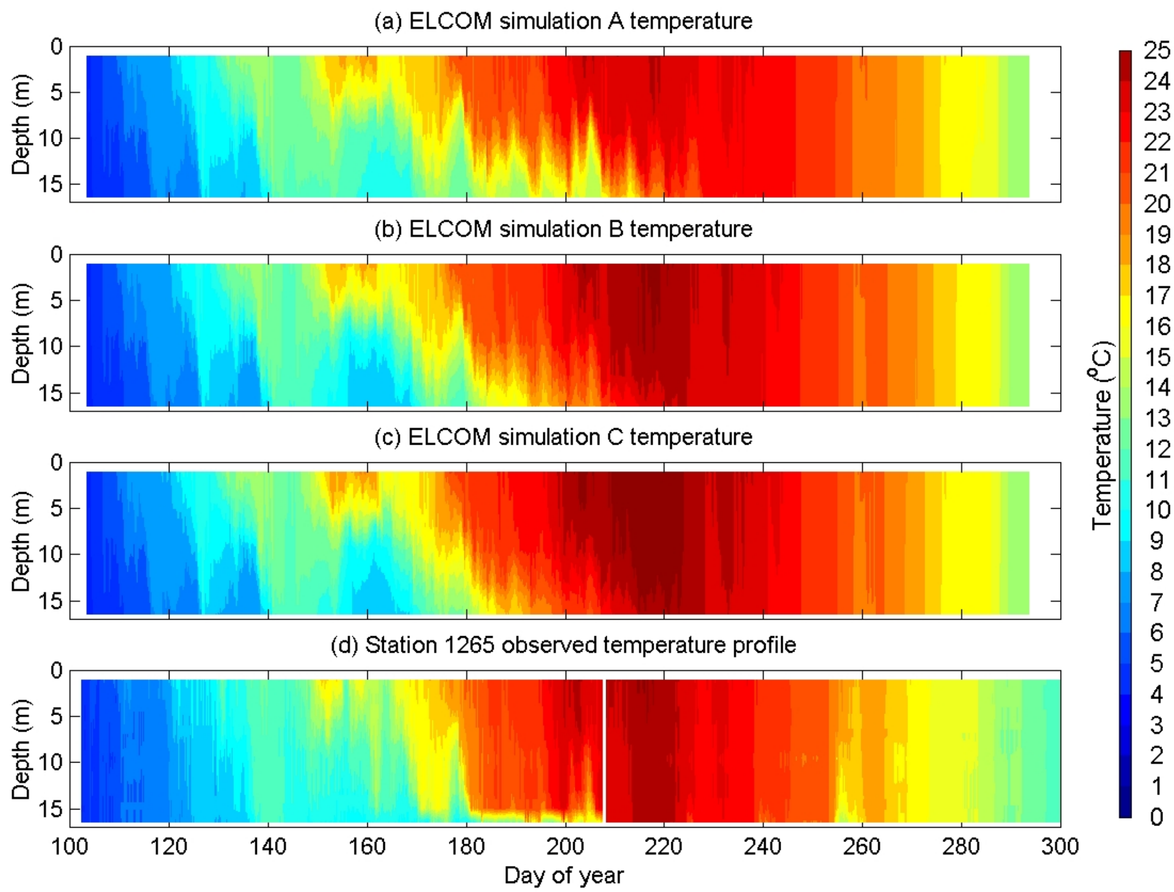

Figure 4.8: ELCOM simulations A (a), B (b) and C (c) temperature profiles are compared to observed (d) temperature profile at station 1265 at 10 min intervals. Modelled temperature output was interpolated at 1 3 5 7 9.5 13 15 16.5 m depths to match observed data.

Table 4.1: Depth averaged RMS analysis results for temperature profiles

Station	Simulation A	Simulation B	Simulation C
1262	2.35	1.87	1.81
1263	2.01	1.59	1.68
1264	1.99	1.51	1.32
1265	1.76	1.59	1.68

that temperature fluctuations are similar in all three simulations at station 1265.

For further comparison, a root mean squared (RMS) analysis was performed comparing the results from all three simulations to observed data. Figures 4.9, 4.10, 4.11 and 4.12 demonstrate the results of this analysis with depth. RMS graphical analysis shows that all simulated temperature profiles compare better with observed data for the top half of the water column and that simulations B and C show similar results which compare better to the observed data than the results for simulation A. Table 4.1 compares the overall RMS results at each station for each simulation.

The lower the RMS value the better simulated and observed temperature profiles agree. Temperature profile RMS results for each station vary slightly for each simulation. However, no one station has consistently better or worse RMS values which provides confidence that the model is performing equally well in terms of temperature over the entire simulated area. Both simulation B and C had the lowest RMS values at two stations, therefore simulations B and C performed equally well in terms of comparing temperature profiles.

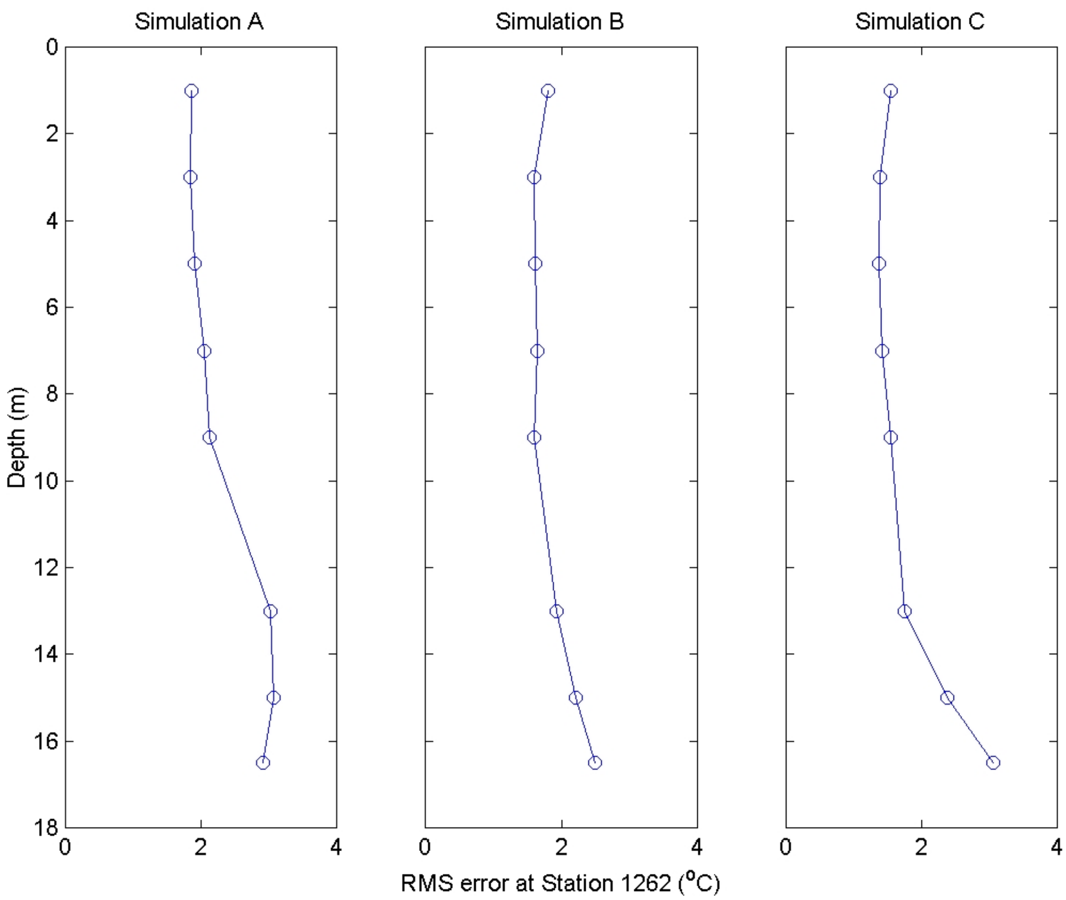

Figure 4.9: RMS analysis results for comparison of simulated temperature profiles and observed data for simulations A, B and C at station 1262.

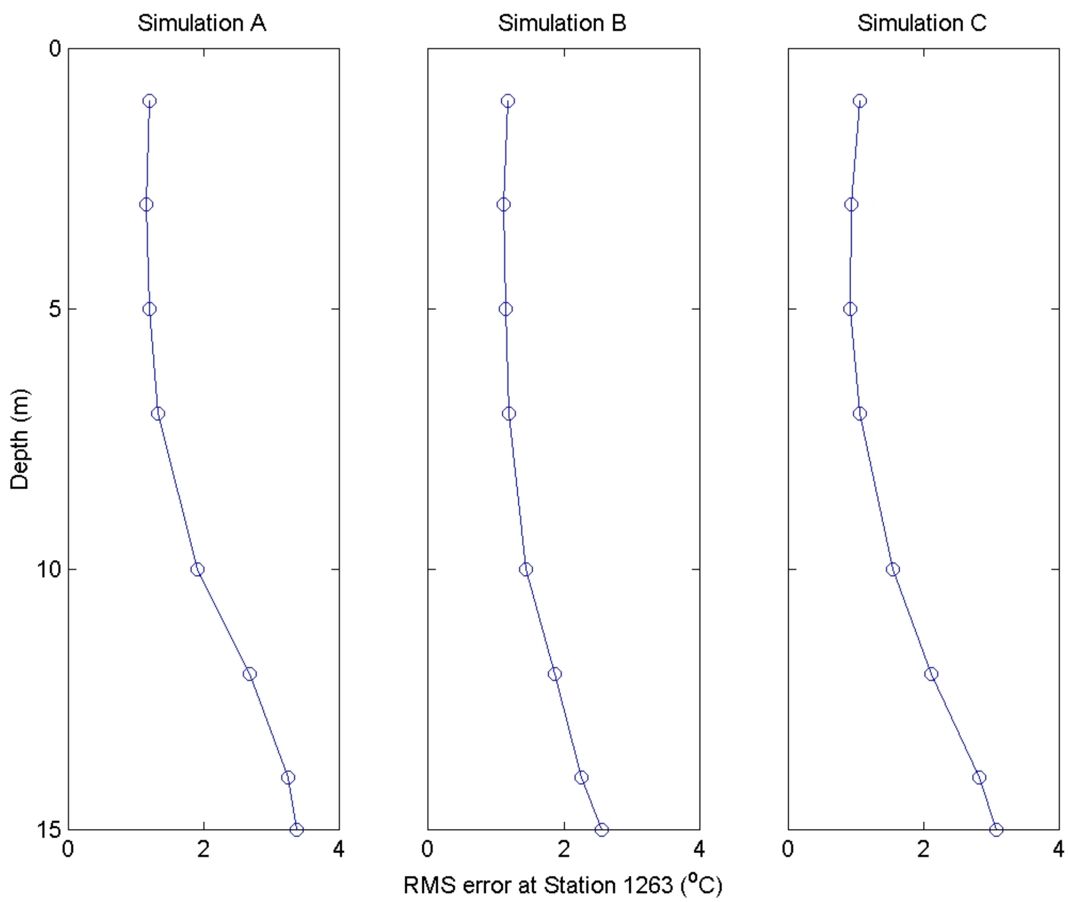

Figure 4.10: RMS analysis results for comparison of simulated temperature profiles and observed data for simulations A, B and C at station 1263.

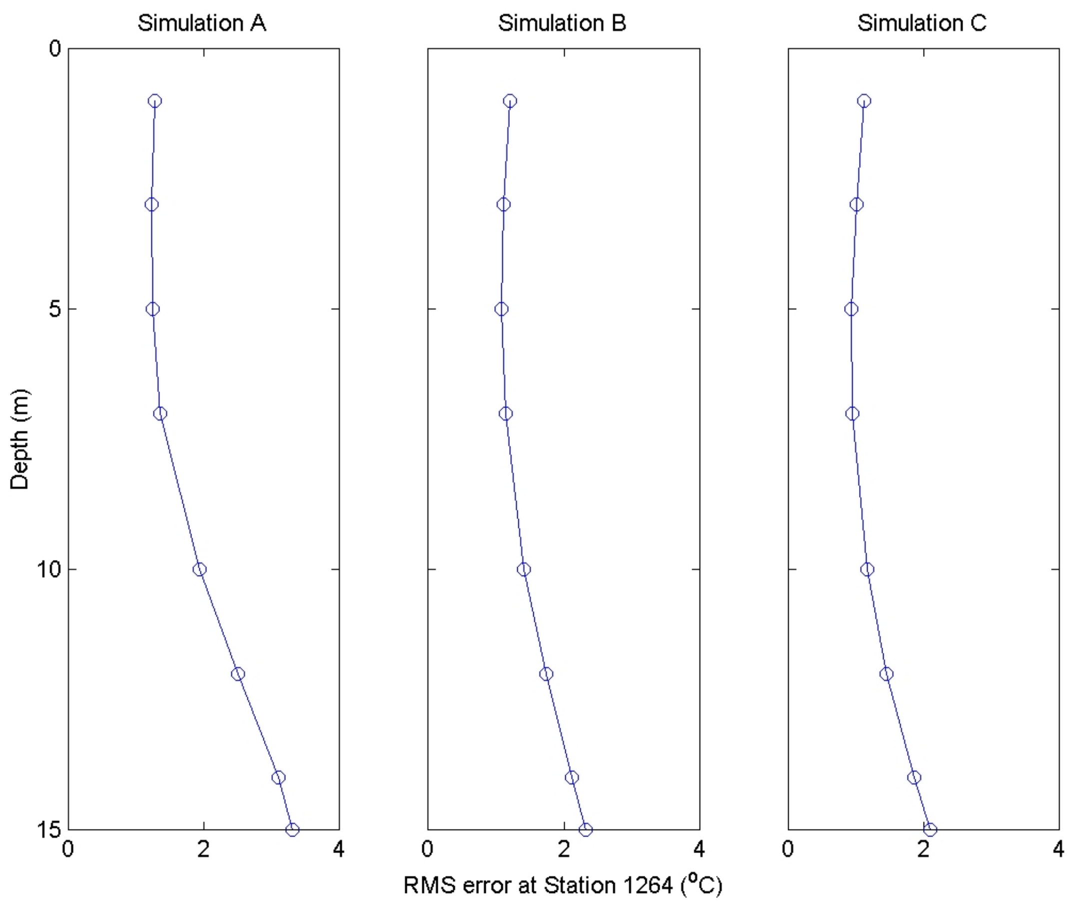

Figure 4.11: RMS analysis results for comparison of simulated temperature profiles and observed data for simulations A, B and C at station 1264.

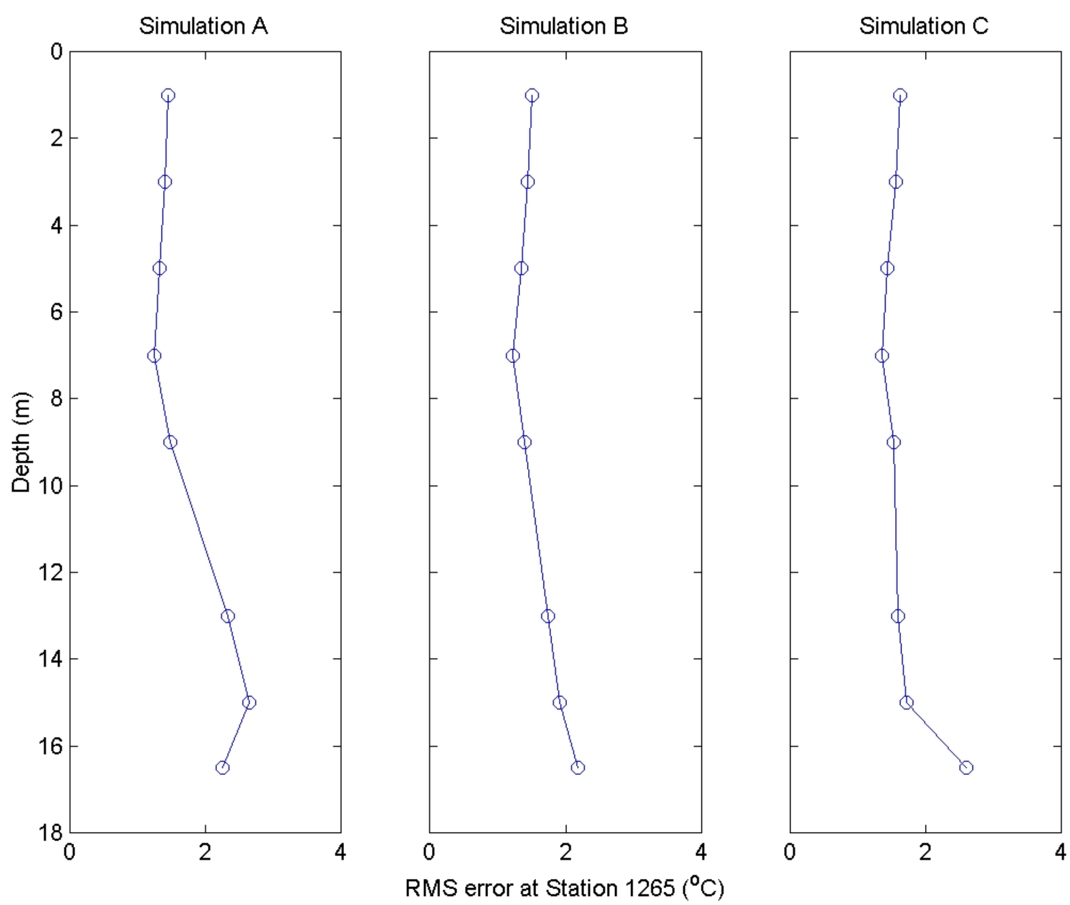

Figure 4.12: RMS analysis results for comparison of simulated temperature profiles and observed data for simulations A, B and C at station 1265.

4.3.2 Currents

Evaluating ELCOM's performance with reproducing currents in the nearshore was also of interest. Modelled current data was compared to observed data provided by NWRI at stations 1262 and 1263. Station 1262 was equipped with a Nobska MAVS-3SL current meter at a depth of 11 m with an speed and direction accuracy of 0.3 cm/s and 1 degree respectively, as well as a resolutions of 0.03 cm/s and +2 degrees. Station 1263 was equipped with an ADCP measuring currents at every meter throughout the water column with a velocity resolution of 0.125 to 0.25 cm/s and an accuracy of 0.5 cm/s [47]. Unfortunately current data was not available for the full lengths of the simulation time period. However, all data was available for sufficient periods of time in order to compare modelled and observed data and evaluate ELCOM's ability to reproduce mean circulation patterns in the nearshore area. Figure 4.13 portrays modelled to observed current meter data comparisons at stations 1262 and Figures 4.15 and 4.14 portray modelled to observed ADCP profiles at station 1263 for simulations A, B and C.

Modelled currents from simulations A and B are similar. At station 1262, modelled currents show greater speeds and more directional variation than is observed. Simulation C currents show larger south east velocities than observed velocities. Although all simulated currents vary more than observed in speed and direction, simulations A and B compare better than simulation C.

Observed currents at station 1263 were available for day 102 to 210. Modelled currents for simulations A and B are again shown to be similar at this station. The observed east component of velocity is weak, very seldom rising above a speed of 5 cm/s and only in the top few metres of the water column. However, the modelled

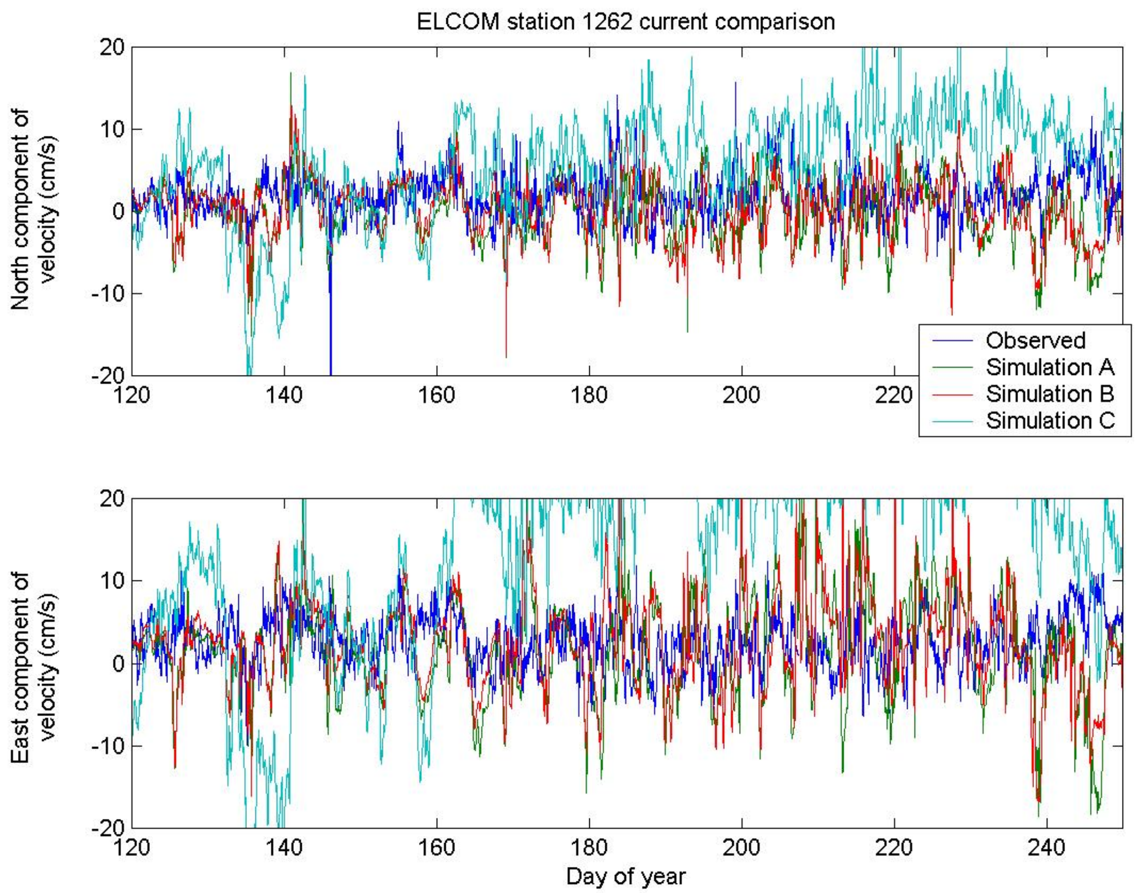

Figure 4.13: Simulation A, B and C north (top) and east (bottom) components of velocity compared to observed data at an 11 m depth at station 1262.

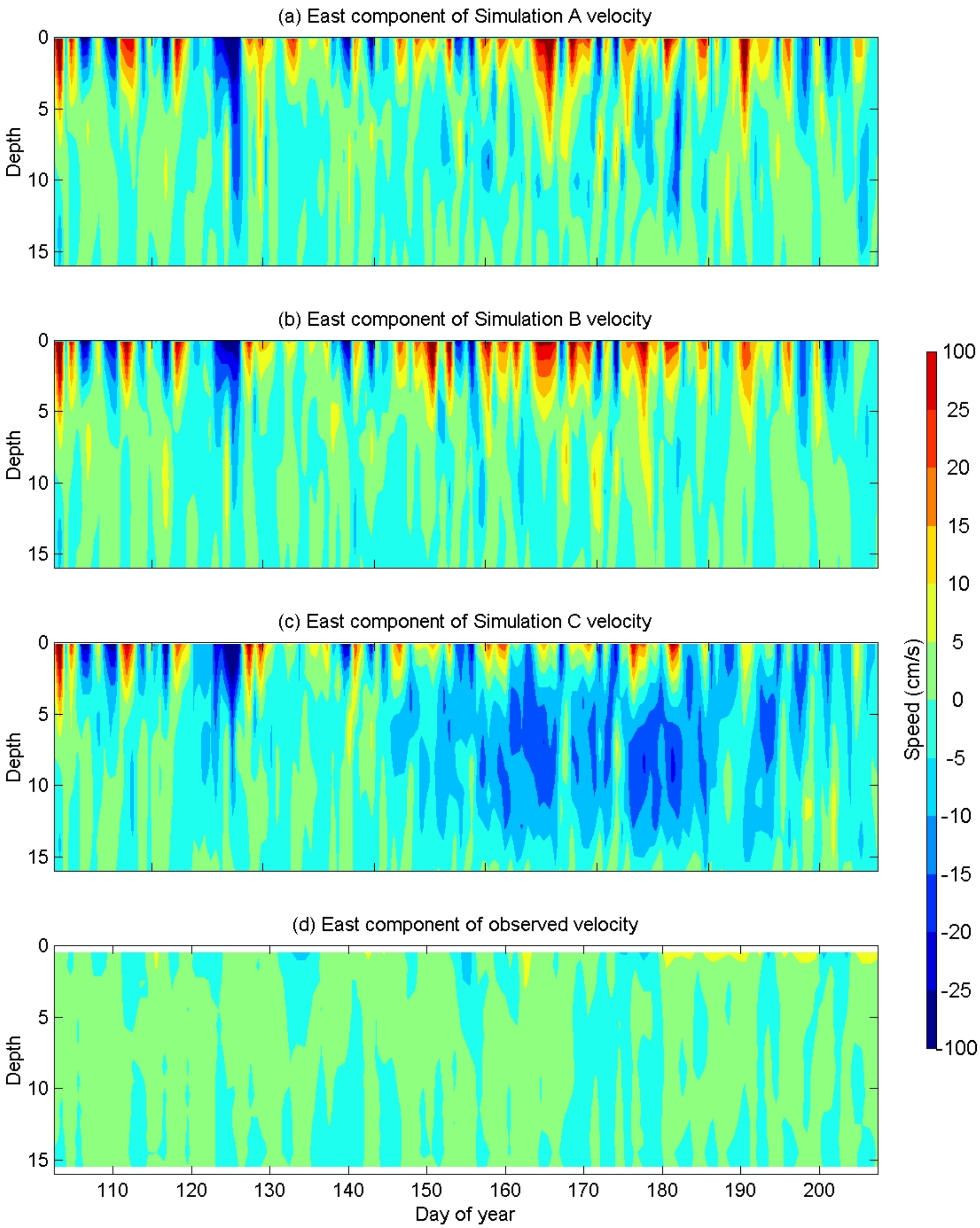

Figure 4.14: ELCOM east component of daily velocity comparison with observed data (d) for simulations A (a), B (b) and C (c) at station 1263.

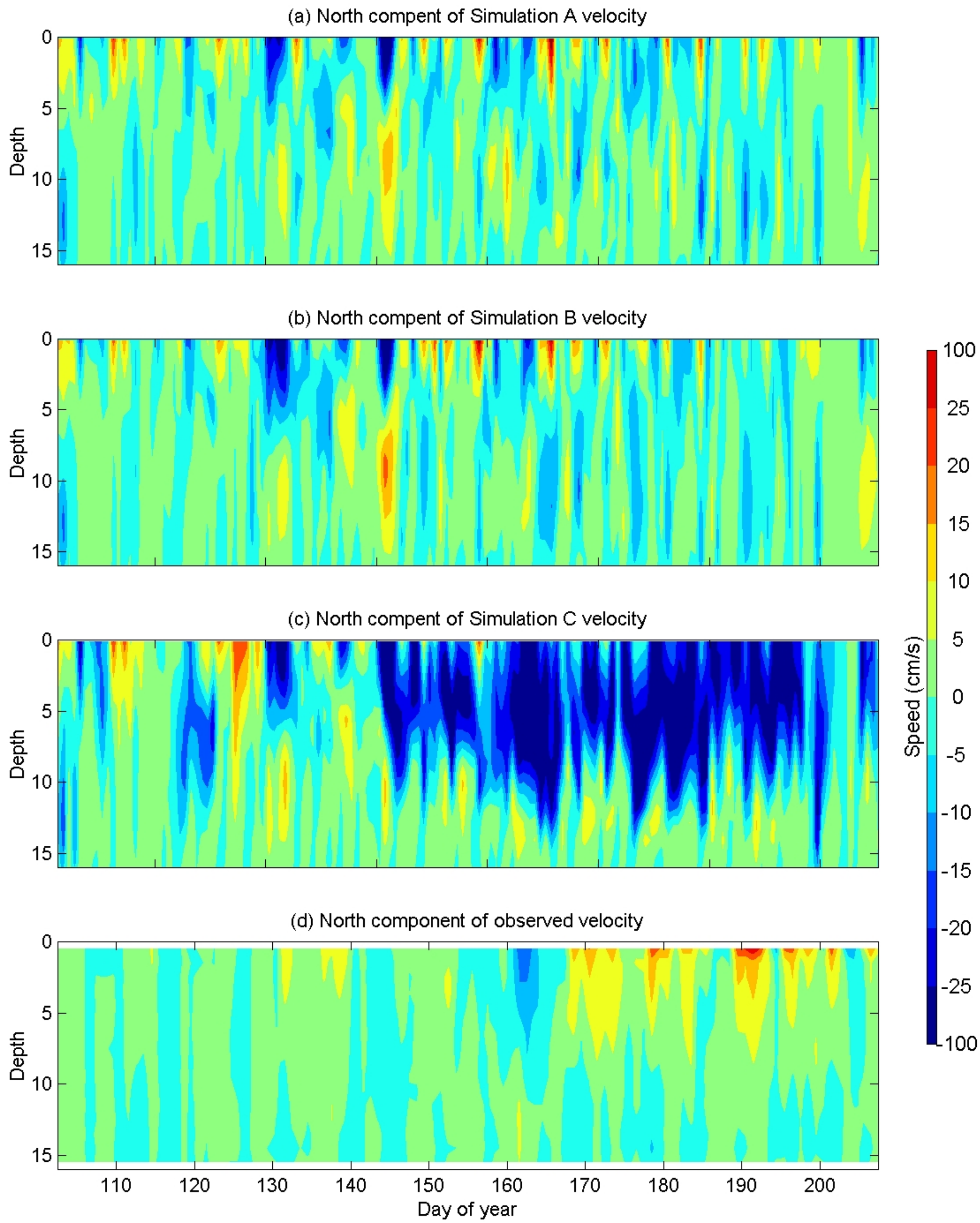

Figure 4.15: ELCOM north component of daily velocity comparison with observed data (d) for simulations A (a), B (b) and C (c) at station 1263.

east component of velocity for all simulations reaches speeds much higher than observed and direction is much more variable. The north component of observed velocity is shown to reach higher speeds than the observed east component and at a greater depth. The north component of observed data shows varied current direction with depth. These episodes portray the top half of the water column flowing north and the bottom half flowing south. These depth-varied currents are seen in ELCOM simulations A and B but do not compare well. Simulation C portrays the opposite with very strong south currents in the top three quarters of the water column and a weak north current direction in the bottom. The difference between modelled and observed velocity was plotted and is shown in Appendix E.

An RMS analysis was performed comparing modelled to observed current results for station 1263 (Figure 4.16). Simulations A and B show similar results but simulation C's analysis shows values about twice as large as those for simulations A and B. Therefore simulations A and B compare better to observed currents than simulation C. Modelled currents in the bottom half of the water column agree better with observed data for both north and east components. For the top half of the water column, the east component of simulated velocity agrees better with observed values than the north component. Mean RMS values were computed for the entire depth of the water column at station 1263 and at a depth of 11 m for station 1262 (Table 4.2). The simulated north component of velocity appears to compare better to observed values than the east component for all simulations at both stations 1262 and 1263.

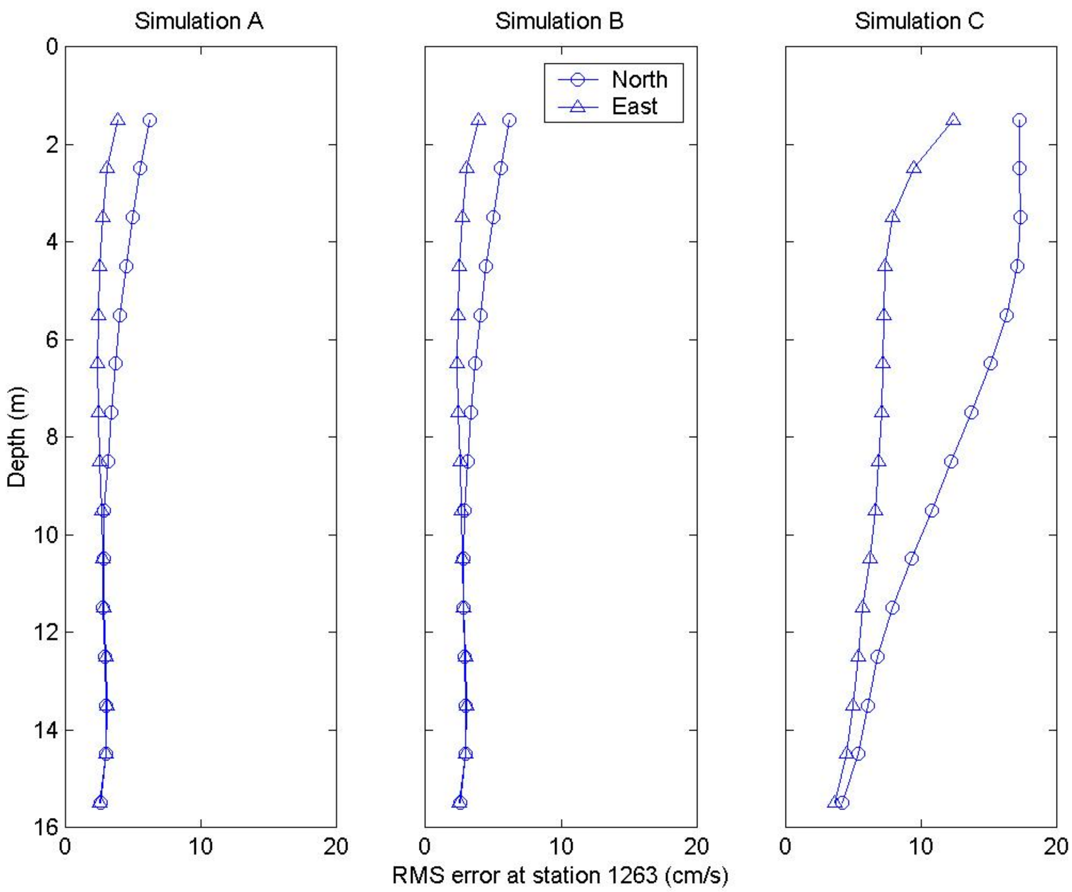

Figure 4.16: RMS analysis results for comparison of simulated currents profiles and observed data for simulations A, B and C at station 1263.

Table 4.2: RMS analysis results for current profiles

Station	Simulation A		Simulation B		Simulation C	
	North	East	North	East	North	East
1262	5.92	6.64	6.56	5.26	15.76	10.28
1263	3.69	2.79	3.69	2.79	11.78	6.81

4.4 Discussion

4.4.1 Temperature Profile Evaluation

Temperature profiles are an excellent means of visualizing lake-wide circulation [4, 10, 12, 20, 27] and have been a main component of numerical model evaluations as seen in literature [6, 14, 19, 30]. Therefore good agreement between modelled temperature and observed temperature is an indication of accurate model performance.

The onset of stratification occurs in the spring and carries through the summer months. Because of the shallow depth of the majority of the modelled area, the epilimnion extends practically the entire depth of the water column by mid summer. Observed temperature profiles at all stations show almost complete constant temperature with depth after around day 200. This means that vertical transport through the water column is not impeded by density barriers caused by temperature. Therefore, the circulation in the lake would be expected to act as it would under barotropic conditions as the thermocline depth is larger than the lake depth. Modelled and observed profiles show the cooling of the water as constant with depth at the end of the summer months as well. However, a brief period of stratification is observed at the bottom of the water column at station 1265 from day 180 to day 200 and was not captured by any of the ELCOM simulations. If persistant, a thermocline at the this depth can greatly affect circulation and therefore water quality which is often seen in Lake Erie [6] therefore it is important that ELCOM reproduce this thermodynamics feature.

The water in nearshore areas of the Kingston basin warms faster than the main body of the lake where mooring C45135 is situated. Because the water at station 1263 warms faster, simulation A's resulting temperature profile is initially warmer. However, once the water around mooring C45135 warms up, its surface temperature is warmer than the water below the surface at station 1263 and because simulation B is forced with uniform temperature with depth, simulation B's results are warmer overall than simulation A. The warmer surface water at C45135 is brought into the model throughout the water column at the open boundary. This results in warm water at surface temperatures being advected throughout the whole water column profile and resulting in warmer temperatures overall.

Simulation B and C resulted in the overall best modelled temperature profile to observed data comparison. Open boundary temperature forcing for simulation B originates from surface temperatures at buoy C45135 in the main body of Lake Ontario. Therefore, with temperature profile results from both simulations B and C being similar, it can be concluded that the open boundary forcing for this ELCOM model is not very sensitive to horizontal and vertical variability concerning temperature profiles.

The curtain from the Lake Ontario basin-scale model used to force simulation C is 19 2 $\times$ 2 km cells long. From each of these cells is computed an hourly temperature profile with depth as well as a water level forcing file. Each of these 19 temperature files and 19 water level files force 7 (8 for the first and last cells) of the nearshore open boundary cells which are 300 $\times$ 300 m in size, for a total open boundary length of 135 cells or 40.5 km. A total of 38 forcing files are required to force a vertically and horizontally varied open boundary. Because of the large amount of input files, simulation C requires over two times the amount of running time than simulation A or B without including the coarse grid model simulation required to create the forcing files. Therefore, simulation B provides equally acceptable temperature profiles at a fraction of the computational cost. Also, simulation B does not require the deployment of expensive temporary data acquisition equipment and is therefore the least expensive of the simulations.

4.4.2 Current Evaluation

Current comparisons are also a means of assessing the model's performance in terms of general circulation patterns. However, it has been seen in Chapter 3 that modelled and observed current agreement varies significantly more than temperature profile agreement and that ELCOM modelled currents in the nearshore do not agree well with observed data because of the coarse grid resolution. This is also the case in the current comparisons for stations 1262 and 1263 as shown graphically and though an RMS analysis.

Graphical and RMS analysis showed that simulations A and B provided better modelled to observed current comparisons. Open boundaries for simulations A and B were forced with the same water level data therefore results were almost identical. Simulation C was forced with horizontally varied water level profiles from results of the lake-wide model presented in Chapter 3. This resulted in much more varied and stronger currents which agreed less with observed currents at stations 1262 and 1263. It seems that ELCOM is not doing a good job at modelling currents at the open boundary. Excessive velocities are likely propagating from the open boundary to station 1263. Excessive velocities are shown in current profiles at both stations 1262 and 1263 for simulation C. Modelled to observed current profile comparisons for simulations A and B are more agreeable than those for simulation C particularly when looking at the deeper water currents at both station 1262 and 1263 probably because the current velocities at depth are smaller and less variable. ELCOM was developed with the intent to reproduce temperature stratification and variations in a water body. Simulated to observed currents have not been widely reported on to date.

Further research beyond the scope of this study is needed to understand why ELCOM currents do not perform well in the nearshore. Three dimensional nested grid and coupled models are fairly recent developments, therefore much documentation is not yet available. However, Hurdowar-Castro *et al.* and Shen *et al.* presented models of the Toronto waterfront featuring nested grids. Both stated that the model compares well with field observations but did not present comparisons or comment on the open boundary condition requirements for the model [1, 32]. The lack of agreement between modelled and observed currents could be due to grid size. A previous FEM model of Lake Ontario by Hayashida *et al.* found that a grid size of less than 100 m is required for modelling smaller-scale flow structures in the nearshore area [37].

4.5 Conclusion

ELCOM appears to represent temperature variations in the study area very well at all four observation stations. Overall, temperature profile and RMS results from simulations B and C were equally successful at reproducing observed temperatures. Simulation B which is forced with surface temperature data uniform with depth from NWRI mooring C45135 and observed historic water levels at Kingston is monetarily and computationally much less expensive and performs much better in terms of currents than simulation C which is forced with a horizontally and vertically varied temperature and water level profiles from the coarse grid model from Chapter 3. This reveals that an ELCOM open boundary is not as sensitive to temporal variability in water temperature as it is to the overall water temperature.

Temperature profile results show that the summer temperature profile in the Kingston basin of Lake Ontario and the upper portion of the St. Lawrence River is uniform with depth. This has significant impact on the vertical circulation throughout the water column as there is no density barrier caused by stratification. Modelled and observed profiles show the cooling of the water as constant with depth at the end of the summer months. However, a brief period of stratification is observed at the bottom of the water column at station 1265 which is not captured by any of the ELCOM simulations.

Current results were similar for simulations A and B because the open boundary water level input file was the same. Simulation C current results were much stronger and varied. They also graphically compared least with observed data. Modelled current results are more variable than temperature profile results. Overall, ELCOM simulated currents compared poorly to observed data throughout the entire depth of the water column. However, deeper current comparisons agreed better than shallower water currents. With the results of this study and from a current modelling perspective, the coarse grid lake-wide model should not be coupled with the nearshore model as error from the coarse grid model is propagated to the neashore model current results. Further investigation such as ELCOM tracer simulations verified with drogue releases to understand why ELCOM does not properly reproduce currents at a fine grid scale would be beneficial.

Overall, the open boundary was found to perform best with spatially non-varied forcing files and uniform with depth temperature profiles. Modelled temperature results compared well with observed data. However further simulations and analysis is needed for confidence in the model's ability to reproduce currents at this grid scale before IPZs can be delineated.

Chapter 5

Conclusions

5.1 Lake-Wide ELCOM Results

A 2 × 2 km coarse grid lake-wide model of Lake Ontario was used to simulate temperature, water levels and currents in the offshore and nearshore regions. The model results were evaluated with observed data and literature with the objective of evaluating the Estuary Lake and Coastal Ocean Model's (ELCOM) ability to reproduce general circulation patterns in the near- and offshore regions.

Simulated to observed temperature profiles compared better than water level and current comparisons. ELCOM adequately reproduces the setup and deterioration of stratification at offshore observation stations 403, 586 and 1266. Both observed and simulated temperature profiles in the nearshore area of station 1263 showed uniform temperature with depth for most of the simulation time period. However, ELCOM was found to slightly underestimate temperatures for all profile comparisons.

ELCOM's ability to reproduce water levels has not been previously discussed in literature. Water level comparisons at station 1263 were compared with observed water level data at Kingston. It is important to include precise inflow, outflow and precipitation forcing data to accurately model water levels in ELCOM. Modelling the water levels proved to be problematic because of the large size of the lake and its drainage basin. Both minor tributary flow and precipitation data are spatially averaged data entered as uniform values over the lake surface. If the surface area of the modelled lake is different than the surface area for which tributary inflow and precipitation data are calculated, the modelled water balance of the lake is misguided and resulting simulated water levels will not compare well with observed data.

ELCOM water level fluctuations matched observed lake levels for the first 40 days of the simulation. However, because of the size of the lake basin and the coarseness of the modelled grid scale, simulated water level values began to diverge steadily from the observed values after that as the lake begins to receive significant amounts of precipitation. It was therefore inferred that there was insufficient water volumes from rain and tributary flow probably because of differences between actual and modelled lake surface areas. Results for a 20% increase in tributary flow data compared much better to observed data.

ELCOM has been previously shown to properly reproduce basin-wide general circulation patterns in several lakes and reservoir [38]. Comparison of modelled and observed offshore currents at station 1266 compared better than the nearshore current comparisons at station 1263. However, ELCOM does not reproduce the stronger currents at the surface to the same depth at which they are observed at station 1266. The nearshore area of station 1263 is much shallower than the offshore area of station 1266. The actual bathymetry at station 1263 is much more complicated than is represented in ELCOM because of the coarseness of the model grid scale. Station 1263 is also in close proximity to the outflow to the St. Lawrence River. Both of these factors make it more difficult for ELCOM to properly reproduce currents in the nearshore area. ELCOM currents at station 1263 are shown to be stronger and more variable than those observed. General, lake-wide ELCOM circulation patterns compare well to previously measured and modelled lake-wide currents presented in literature by reproducing some of the consistent lake-wide circulation patterns documented.

A storm event shown in the observed current and temperature profiles at station 1266 is not properly captured by ELCOM. This is attributed to the lack of proximal meteorological data available to force the model in the immediate vicinity of that station. Because of the distance between station 403 and 1266, the meteorological equipment at station 403 did not capture the full extent of the storm, therefore emphasizing the need for spatially varied meteorological forcing at more than the current three locations. Observed temperature profiles at stations 403 and 586 show evidence of this storm event which also is not reproduced by the ELCOM simulation.

Overall, ELCOM does a satisfactory job at taking unaveraged spatially varied meteorological forcing data as well as inflow and outflow data to model thermal stratification and general circulation patterns for Lake Ontario. Offshore circulation was shown to be better reproduced than nearshore circulation.

5.2 Nearshore ELCOM Results

Three different open boundary forcing methods are compared in an ELCOM nearshore model of the Kingston basin in Lake Ontario and the upper St. Lawrence River with the objectives of evaluating the sensitivity of an open boundary and how well the ELCOM performs at a fine grid scale in the nearshore areas. The open boundary for simulation A was forced with a temperature file varied with depth from the nearby thermistor chain at station 1263 and historical Kingston water level data. Simulation B's open boundary was forced with a temperature file constant with depth from the permanent Environment Canada mooring C45135 in the main body of the lake and historical Kingston water level data. Lastly, the open boundary for simulation C was forced using varied temperature with depth files and water level files computed from the coarse grid model presented in Chapter 3 which were spatially varied over the length of the open boundary.

Nearshore ELCOM temperature profiles and root mean squared (RMS) analysis results shows good agreement with observed data for all three simulations. Both modelled and observed temperature profiles at all four stations show summer water temperatures to be constant with depth except for a brief period of 20 days at station 1265 where a thermocline near the very bottom of the water column is shown. Neither of the three ELCOM simulations were able to reproduce a thermocline at this time and location.

Modelled currents were compared to observed data at stations 1262 and 1263. Graphical and RMS current results showed that current comparisons are much more variable than temperature comparisons and that the east component of velocity compared better to observed data than the north component. Simulations A and B were forced with the same spatially non-varied water level data and therefore showed almost identical results which were better than current results for simulation C. Further studies should be conducted with the release of tracers in ELCOM and verified with drogue experiments. Currently, ELCOM currents appear to have significant discrepancies in speed and direction when compared to observed data.

When considering temperature evaluations, the overall best results were produced by simulations B and C, which shows that an ELCOM open boundary is not sensitive to horizontal and vertical temperature variability in terms of temperature profile results. Simulation C is particularly computationally and monetarily expensive to run. Whereas, simulation B produces equally satisfactory temperature profile results with a non-horizontally and non-depth-varied temperature and water level forcing. It also requires a fraction of the computational time required for simulation C and runs with free and easily available temperature and water level data for open boundary forcing. Simulation B current results are also much more agreeable with observed data than results from simulation C. Simulating the open boundary with constant temperature with depth and hourly water level data produces the best current and temperature results.

5.3 Future Work

Future work for both the coarse grid lake-wide and fine grid nearshore models presented in Chapters 3 and 4 is recommended. The current lake-wide model uses a 2×2 km grid scale which should be reduced in order to test the model's ability to reproduce lake-wide circulation patterns such as the Kelvin wave, as the current resolution is too large. Much work is still needed until the nearshore model can confidently be used as a tool to delineate IPZs. Further sensitivity analysis is recommended testing open boundary conditions. ELCOM tracer simulations should be compared to drogue experiments carried out in the Kingston basin and the St. Lawrence River. Lastly, a finer grid scale should be tested with the nearshore model as well to determine if this improves ELCOM nearshore current results.

Bibliography

[1] D. Hurdowar-Castro, I. Tsanis, and I. Simanovskis. Application of a Three-dimensional Wind Driven Circulation Model to Assess the Locations of New Drinking Water Intakes in Lake Ontario. *Journal of Great Lakes Research*, 33:232–252, 2007.

[2] Y. R. Rao and C. R. Murthy. Nearshore Currents and Turbulent Exchange Processes during Upwelling and Downwelling Events in Lake Ontario. *Journal of Geophysical Research*, 106:2667–2678, 2001.

[3] Y. R. Rao and C. R. Murthy. Coastal Boundary Layer Characteristics during Summer Stratification in Lake Ontario. *Journal of Physical Oceanography*, 31:1088–1104, 2001.

[4] G. T. Csanady. The Coastal Boundary Layer in Lake Ontario: Part I. The Spring Regime. *Journal of Physical Oceanography*, pages 41–53, 1972.

[5] S. Prakash, J. F. Atkinson, and M. L. Green. A Semi-Lagrangian Study of Circulation and Transport in Lake Ontario. *Journal of Great Lakes Research*, 33:774–790, 2007.

[6] L. F. León, J. Imberger, R. E. H. Smith, R. E. Hecky, D. C. L. Lam, and W. M. Schertzer. Modelling as a Tool for Nutrient Mnagement in Lake Erie: a Hydrodynamics Study. *Journal of Great Lakes Research*, 31(suppl.2):309–318, 2005.

[7] L. Boegman, J. Imberger, G. N. Ivey, and J. P. Antenucci. High-Frequency Internal Waves in Large Stratified Lakes. *Limnolology and Oceanography*, 48:895–919, 2003.

[8] D. Beletsky, J. H. Saylor, and D. J. Schwab. Mean Circulation in the Great Lakes. *Journal of Great Lakes Research*, 25(1):78–93, 1999.

[9] D. B. Rao and T. S. Murty. Calculations of the Steady State Wind-Driven Circulations in Lake Ontario. *Journal of Applied Meteorology*, pages 195–210, 1970.

[10] D. Beletsky, W. P. O'Connor, D. J. Schwab, and D. E. Dietrich. Numerical Simulation of the Internal Kelvin Waves and Coastal Upwelling Fronts. *Journal of Physical Oceanography*, pages 1197–1215, July 1997.

[11] B. R. Hodges, B. Laval, and B. M. Wadzuk. Numerical Error Assessment and a Temporal Horizon for Internal Waves in a Hydrostatic Model. *Ocean Modelling*, 13:44–64, 2006.

[12] J. P. Antenucci, J. Imberger, and A. Saggio. Seasonal Evolution of the Basin-Scale Internal Wave Field in a Large Stratified Lake. *Limnology and Oceanography*, 45:1621–1638, 2000.

[13] A. Wuest and A. Lorke. Small-Scale Hydrodynamics in Lakes. *Annual Review Fluid Mechanics*, 35:373–412, 2003.

[14] B. R. Hodges, J. Imberger, A. Saggio, and K. B. Winters. Modelling Basin-Scale Internal Waves in a Stratified Lake. *Limnolology and Oceanography*, 45(7):1603–1620, 2000.

[15] A. Saggio and J. Imberger. Internal Wave Weather in a Stratified Lake. *Limnolology and Oceanography*, 43(8):1780–1795, 1998.

[16] D. J. Schwab and D. Beletsky. Relative Effects of Wind Stress Curl, Topography, and Stratification on Large-Scale Circulation in Lake Michigan. *Journal of Geophysical Research*, 108:1–10, 2003.

[17] G. T. Csanady. Hydrodynamics of Large Lakes. Technical Report 3340, Woods Hole Oceanographic Institution, 1975.

[18] Robert G. Wetzel. *Limnology: Lake and River Ecosystems*. London: Academic, SanDiego, California, third edition, 2001.

[19] B. Laval, J. Imberger, B. R. Hodges, and R. Stocker. Modelling Circulation in Lakes: Spatial and Temporal Variations. *Limnolology and Oceanography*, 48(3):983–994, 2003.

[20] J. R. Bennett. A Three-Dimensional Model of Lake Ontario's Summer Circulation I. Comparison with Observations. *Journal of Physical Oceanography*, 7:591–601, 1977.

[21] R. H. Spigel and J. Imberger. The Classification of Mixed-Layer Dynamics in Lakes of Small to Medium Size. *Journal of Physical Oceanography*, 10:1104–1121, 1980.

[22] C. H. Mortimer. Lake hydrodynamics. *Mitteilugen der internaltionale Vereinigung für theoretische und angewandte Limnologie*, 20:124–197, 1974.

[23] T. J. Simons, C. R. Murthy, and J. E. Campbell. Winter Circulation in Lake Ontario. *Journal of Great Lakes Research*, 11:423–433, 1985.

[24] R. L. Pickett. The Observed Winter Circulation of Lake Ontario. *Journal of Physical Oceanography*, 7:152–156, 1977.

[25] A. E. Gill. *Atmosphere-Ocean Dynamics*, volume 30 of *International Geophysics Series*. Academic Press, New York, 1982.

[26] D. J. Schwab. Internal Free Oscillations in Lake Ontario. *Limnology and Oceanography*, 22(4):700–708, July 1977.

[27] G. T. Csanady. The Coastal Boundary Layer in Lake Ontario: Part II. The Summer-Fall Regime. *Journal of Physical Oceanography*, pages 168–176, 1972.

[28] B. Laval, B. R. Hodges, and J. Imberger. Reducing Numerical Diffusion Effect with Pycnocline Filter. *Journal of Hydraulic Engineering*, pages 215–224, 2003.

[29] B. Hodges and C. Dallimore. *Estuary, Lake and Coastal Ocean Model: ELCOM v2.2 Science Manual*, June 2006.

[30] B. R. Hodges, J. Imberger, B. Laval, and J. Appt. Modelling the Hydrodynamics of Stratified Lakes. July 2000.

[31] R. Gilbert. Physical Limnology Class Notes, 2005.

[32] H. Shen, I. K. Tsanis, and M. D'Andrea. A Three-Dimensional Nested Hydrodynamic/Pollutant Transport Simulation Model for the Nearshore Areas of Lake Ontario. *Journal of Great Lakes Research*, 21(2):161–177, 1995.

[33] Clean Water Act. *http://www.ene.gov.on.ca/en/water/cleanwater/index.php*, Government of Ontario, October 2007. Cited Jan 22, 2008.

[34] T. J. Simons. Verification of Numerical Models of Lake Ontario: Part I. Circulation in Spring and Early Summer. *Journal of Physical Oceanography*, 4:507–523, 1974.

[35] R. L. Pickett and F. P. Richards. Lake Ontario Mean Temperatures and Currents in July 1972. *Journal of Physical Oceanography*, 5:775–781, 1975.

[36] T. J. Simons. Verification of Numerical Models of Lake Ontario: Part II. Stratified Circulations and Temperature Changes. *Journal of Physical Oceanography*, 5:98–110, 1975.

[37] T. Hayashida, J. A. Atkinson, J. V. DePinto, and R. R. Rumer. A Numerical Study of the Niagara River Dsicharge Near-Shore Flow Field in Lake Ontario. *Journal of Great Lakes Research*, 25(4):897–909, 1999.

[38] Centre for Water Research, University of Western Australia : ELCOM. *http://www.cwr.uwa.edu.au/research/publications.php?title=&keywords=ELCOM&author=&ED_Number=&type=Journal&publication_status=Published&year_from=&year_to=&search=Search*.

[39] R. S. Gupta. *Hydrology and Hydraulic Systems*. Waveland Press, Inc., Long Grove, Illinois, second edition, 2001.

[40] L. F. León, D. Lam, W. Schertzer, and D. Swayne. Lake and Climate Models Linkage: a 3-D Hydrodynamic Contribution. *Advances in Geosciences*, 4:57–62, 2005.

[41] D. J. Schwab and D. L. Sellers. Great Lakes Bathymetry and Shoreline Data. *http://www.glerl.noaa.gov/data/bathy/bathy.html*, Great LakesEnvironmental Reseach Laboratory, National Atmospheric Administration.

[42] B. Hodges and C. Dallimore. *Estuary, Lake and Coastal Ocean Model: ELCOM v2.2 User Manual*, February 2007.

[43] I. K. Tsanis and C. R. Murthy. Flow Distribution in the St. Lawrence River System at Wolf Island, Kingston Basin, Lake Ontario. *Journal of Great Lakes Research*, 16(3):352–365, 1990.

[44] Lake Ontario, Physical and Environmental Features of the Lake Ontario Basin. *http://epa.gov/greatlakes/ontario.html*, U.S. Environmental Protection Agency, November 2007. Cited March 21, 2008.

[45] Historic Great Lakes Water Level Data - Station Selection. *http://tidesandcurrents.noaa.gov/station_retrieve.shtml?type=Historic+Great+Lakes+Water+Level+Data*, National Oceananic and Atmospheric Association, 2006.

[46] TidbiT Data Logger. *http://www.microdaq.com/occ/other/tidbit_data_logger.php*, TheDataLoggerStore.com, 2008.

[47] *SC-ADCP Technical Manual - Appendix S: Spcifications and Dimentions*. Burlington, ON, 1991.

[48] L. F. León. Lake Ontario 3D Modelling. *http://www.science.uwaterloo.ca/ lfleonvi/ontmodel/ lakemodel_main.html*, University of Waterloo, 2008.

[49] B. K. Pal, R. Murthy, and R. E. Thomson. Lagrangian Measurements in Lake Ontario. *Journal of Great Lakes Research*, 24(3):681–697, 1998.

[50] B. Hodges. *Numerical Techniques in CWR-ELCOM (code release v.1)*, March 2000.

Appendix A

Scaled vs Non-Scaled Temperature Profiles

Over course of several ELCOM simulations, it was found that both long and shortwave radiation as well as air temperature, are the most important factors influencing the temperature of the modelled water body. Because ELCOM has a tendency to underestimate water temperatures, both the long and shortwave radiation values were scaled by 1.15 and 0.9 respectively as was done by Laval *et al.* for Lake Kinneret simulations to improve modelled results [28]. Figures A.1, A.2, A.3 and A.4 compare unscaled and scaled radiation ELCOM results with observed temperatures. Scaled temperature profile results portray overall warmer water than unscaled data. Although scaled results are still cooler than observed, they compare better than unscaled results.

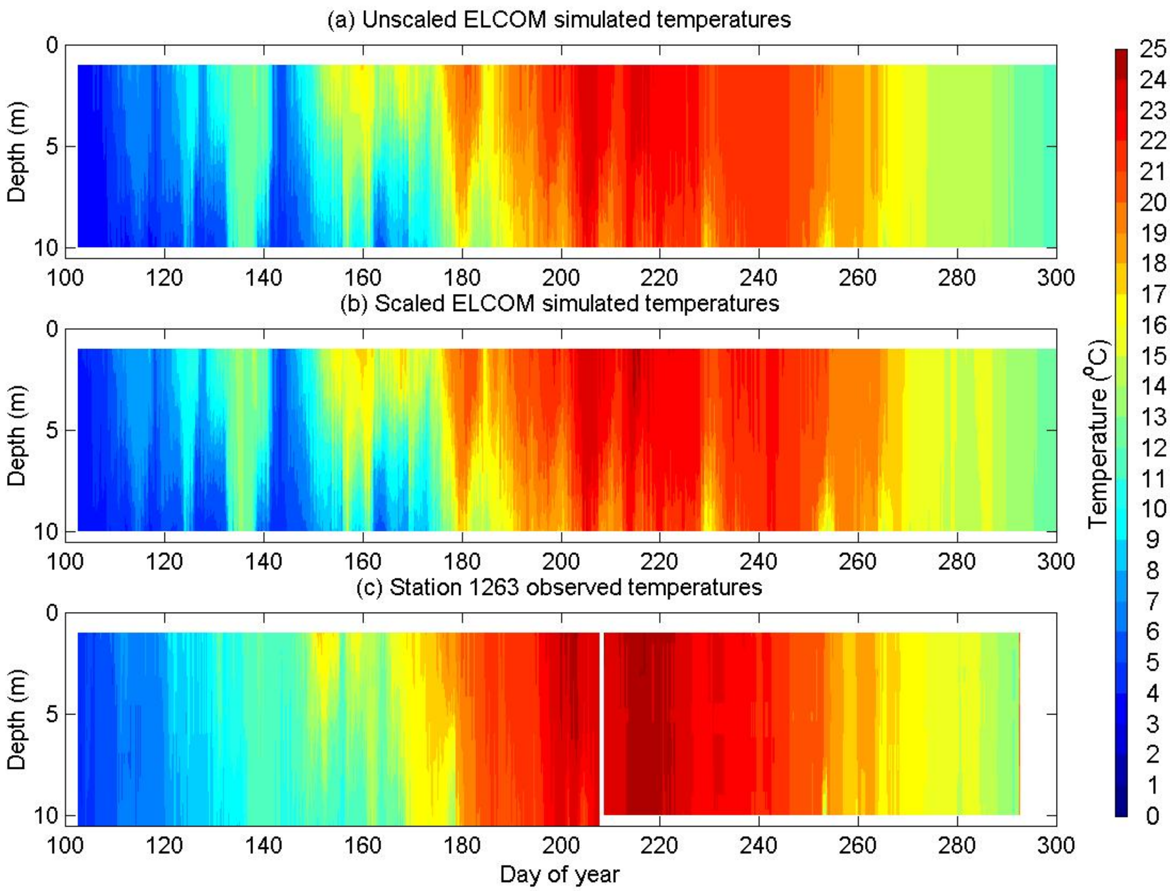

Figure A.1: Unscaled (a) versus scaled (b) ELCOM simulated temperature profiles compared with observed data (c) at station 1263.

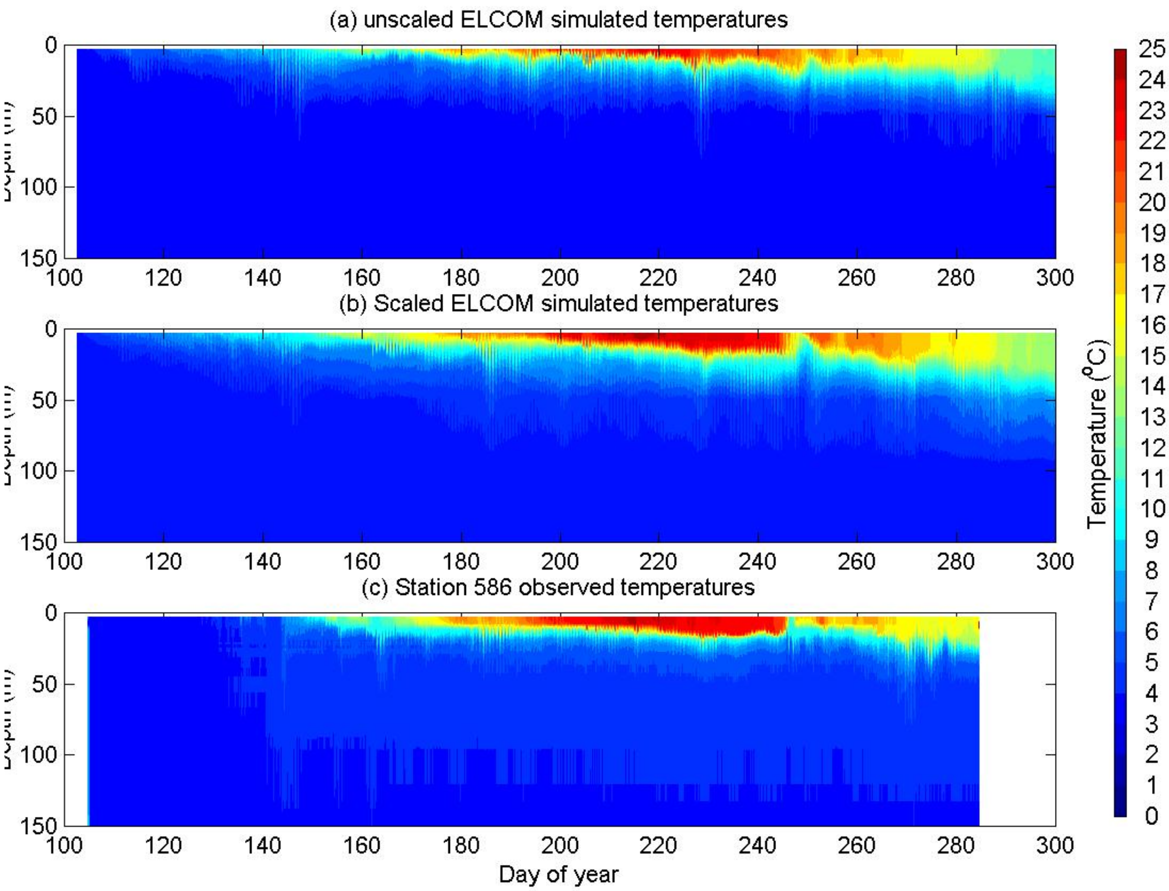

Figure A.2: Unscaled (a) versus scaled (b) ELCOM simulated temperature profiles compared with observed data (c) at station 586.

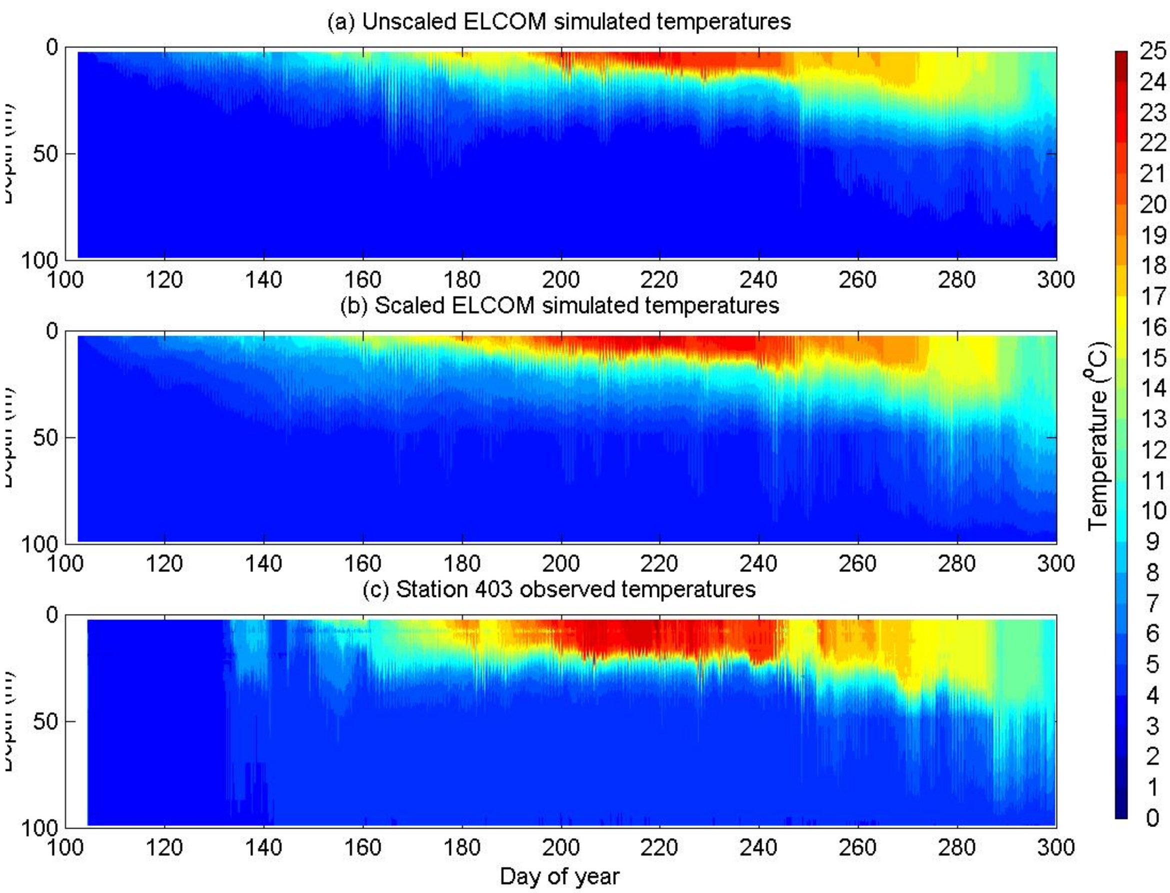

Figure A.3: Unscaled (a) versus scaled (b) ELCOM simulated temperature profiles compared with observed data (c) at station 403.

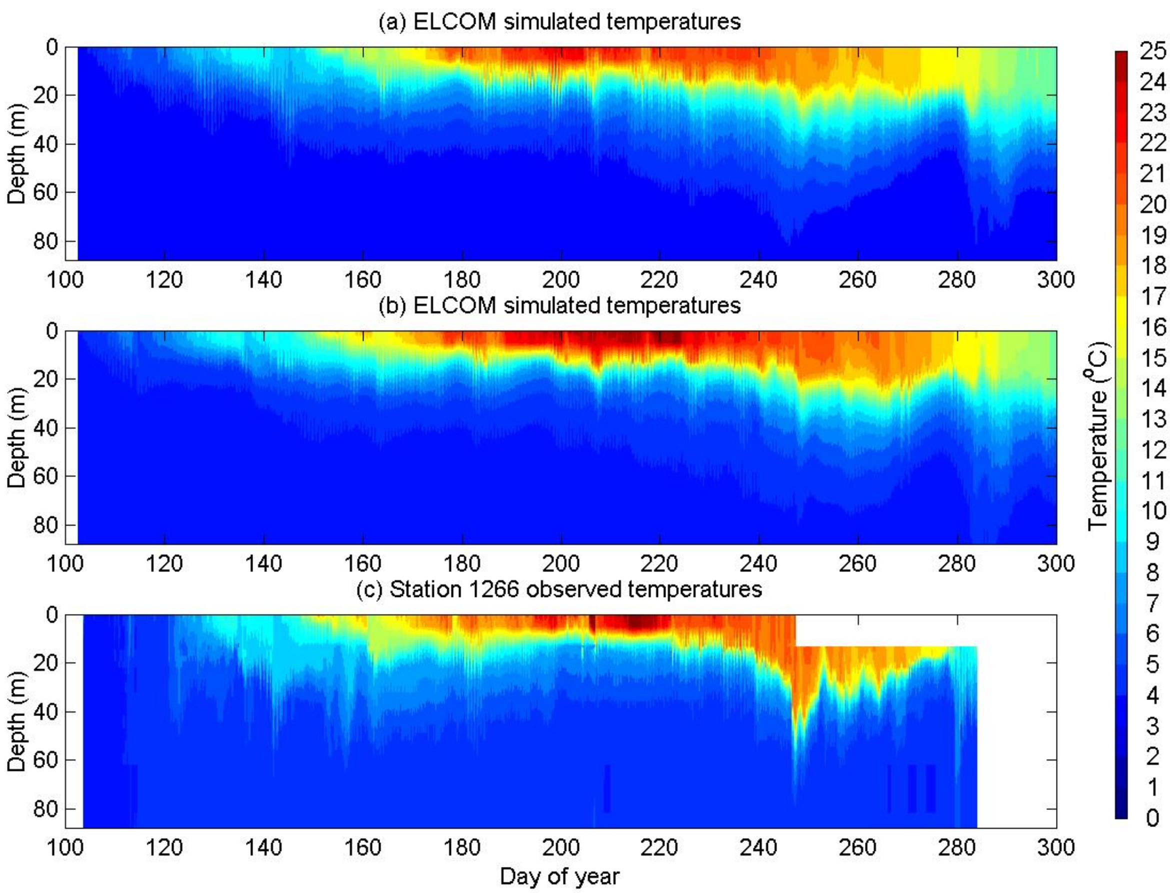

Figure A.4: Unscaled (a) versus scaled (b) ELCOM simulated temperature profiles compared with observed data (c) at station 1266.

Appendix B

Water Levels

The first lake-wide numerical models were closed basin models, not accounting for water flow in and out of the lake, or models having constant inflow and outflow effectively canceling out this term in the water balance equation [5, 34, 36]. At such coarse grid scales it was thought that inflows and outflows would not significantly impact the model results. However, with the large volume of water in lakes the size of the Great Lakes, inflows and outflows can significantly impact water volumes in ELCOM simulations. Newer models such as the ELCOM model of Lake Erie includes major inflows and outflows [6]. Using as many available data sources as possible when evaluating the performance of a lake-wide model is preferred to be certain that simulations are properly reproducing observed lake hydrodynamics. ELCOM was compared to observed thermistor chain data, current meter data and historic water level data. Both simulated temperatures and currents compared well for ELCOM models of Lake Erie and Lake Kinneret [6, 14]. When evaluating ELCOM water levels for Lake Ontario, it became obvious that the lake's water balance was very important in order to be sure that the model properly represented all the lake's hydrodynamic processes. The model was first run as a closed basin as seen in Figure B.1. The difference between simulated and observed hourly water level fluctuations in Figure B.1 exemplifies

Table B.1: Modelled monthly tributary flow data obtained from NOAA

Monthly Tributary Flow Data (m)						
April	May	June	July	August	September	October
0.14318	0.09484	0.06701	0.08679	0.03662	0.10766	0.23729

the need for lake simulations which include inflows and outflows as shown in Figure B.2. In this figure, observed lake water levels are much higher than is simulated by ELCOM. Because precipitation is not accounted for in the model, simulated water levels steadily decrease over the course of the simulation. Figure B.3 portrays an ELCOM simulation which includes major inflows, outflows and precipitation. Figure B.3 shows better agreement between simulated and observed water levels than Figure B.2. However, simulated water levels in Figure B.3 are still decreasing over the course of the simulation compared to observed data. Chapter 3 discusses the need to include tributary and overland flow data in ELCOM. Groundwater inflow and outflow is not accounted for in this model due to lack of forcing data. Groundwater is not included in ELCOM simulations but should be examined in future modelling attempts in which the simulation of water levels is of interest. Minor tributary and overland flow is usually considered to be of little significance to the overall lake water balance. In the case of Lake Ontario, which has a large drainage basin, about 14% of all inflowing water is accounted for by minor tributaries and overland flow [44]. Modelled monthly tributary data as included in Chapter 3 was available and is shown in Table B.1. This data is divided into daily values corresponding to daily precipitation and was then added to simulations (Figure 3.10). Simulated water levels are also important because, coupled with temperature profiles, they can be used to simulate the open boundaries of finer grid models such as the nearshore model of the Kingston basin presented in Chapter 4.

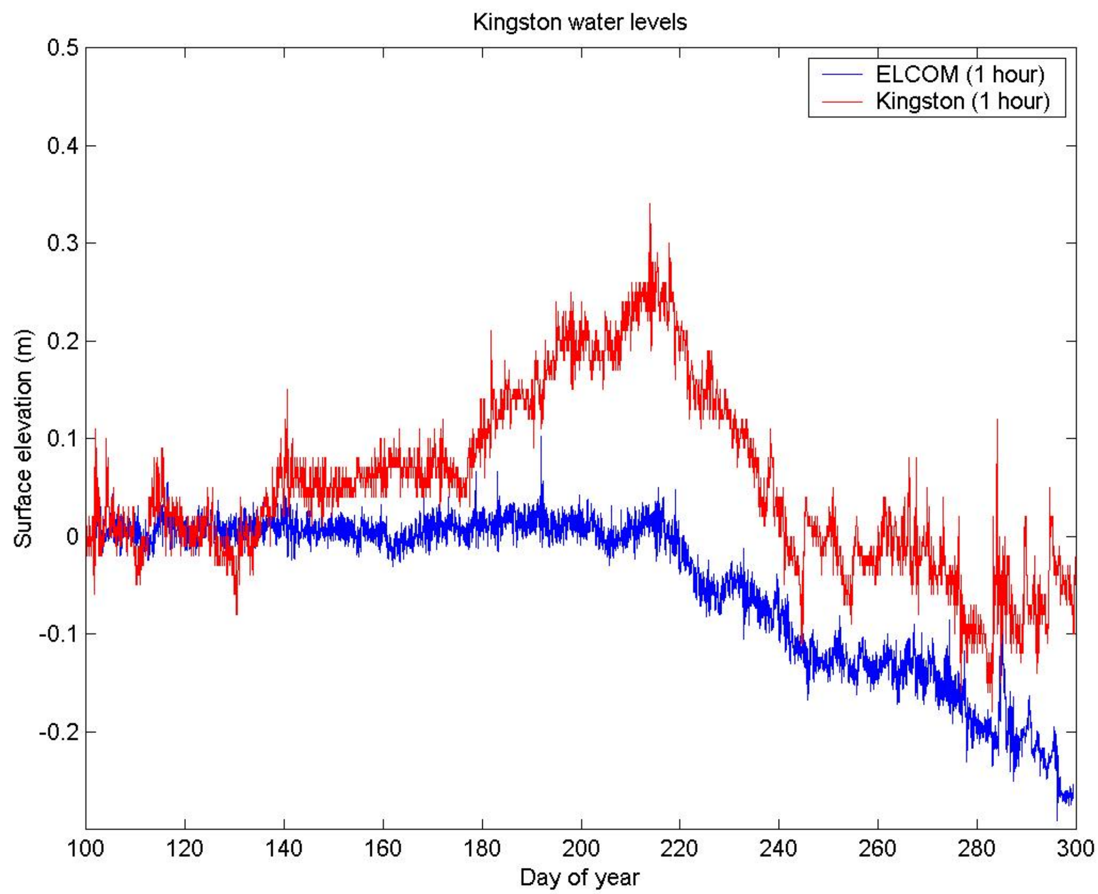

Figure B.1: Observed and simulated hourly water level fluctuations for a closed basin simulation.

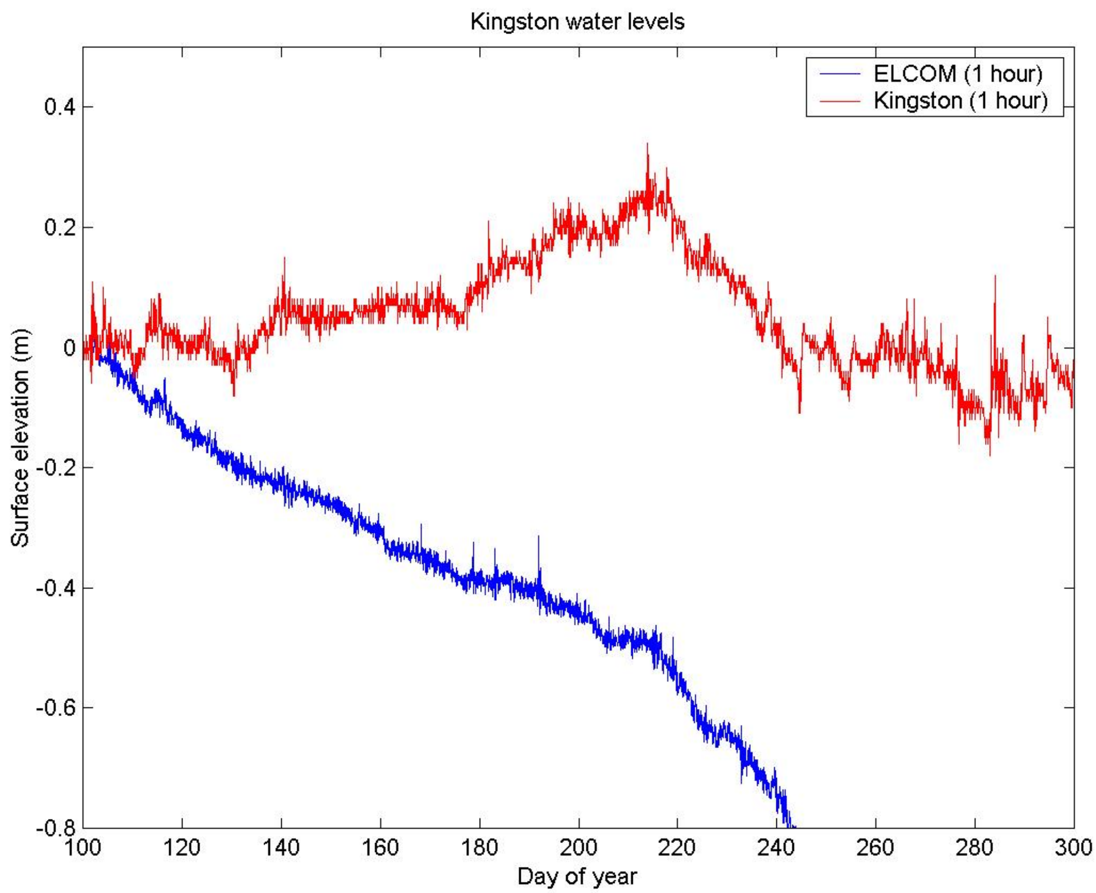

Figure B.2: Observed and simulated hourly water level fluctuations. Simulation includes major inflows from the Niagara River and Welland canal as well as outflow from the St. Lawrence River.

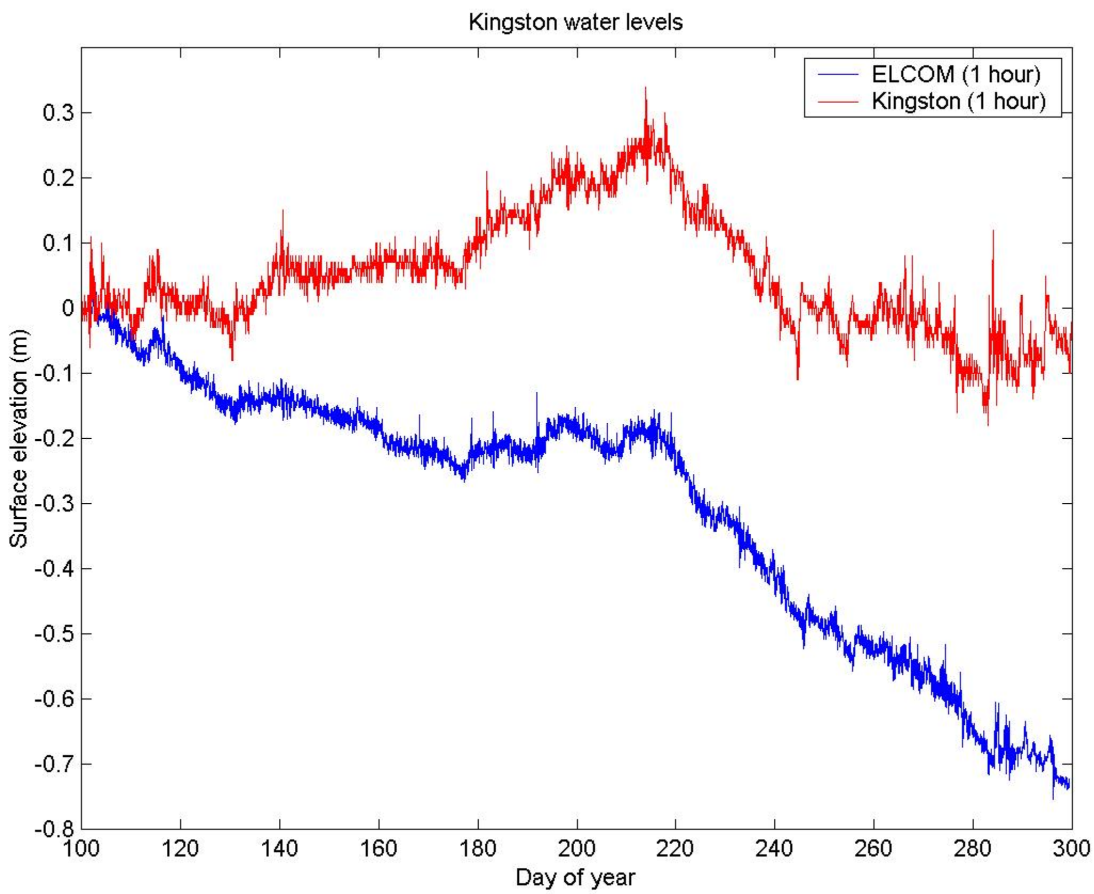

Figure B.3: Observed and simulated hourly water level fluctuations. Simulation includes major inflows, outflows and precipitation.

Appendix C

Lake-Wide Current Comparisons

A lake-wide current plot is presented in Chapter 3 in comparison to Beletsky *et al.*'s plot of general summer circulation. This plot was computed using ELCOM current results at depths of 15, 19, 30, 50 and 75 m. Figure C.1 demonstrates the depth averaged ELCOM simulated circulation in all of Lake Ontario for the entire length of the 2006 simulation. This figure is the best representation of the model's performance. Further current comparisons with literature are discussed below.

Prakash *et al.* used a PTM to study surface circulation and noted a coastal current along the southern shore east of the Niagara River and a clockwise gyre in the Rochester basin in August [5]. Surface simulated summer coastal currents are reproduced throughout the ELCOM simulation shown in Figure C.2.

The gyre in the Rochester basin seen in the August simulation of surface currents in Prakash *et al.* is not as pronounced in the ELCOM 2006 August simulation results (Figure C.3), instead there is a small clockwise gyre coupled with a another small anticlockwise gyre directly to the north. This discrepancy can be attributed to interannual variability.

ELCOM May 2006 surface circulation in Figure C.4 generally compares well to May circulation patterns seen in Prakash *et al.* with the exception of the coastal current along

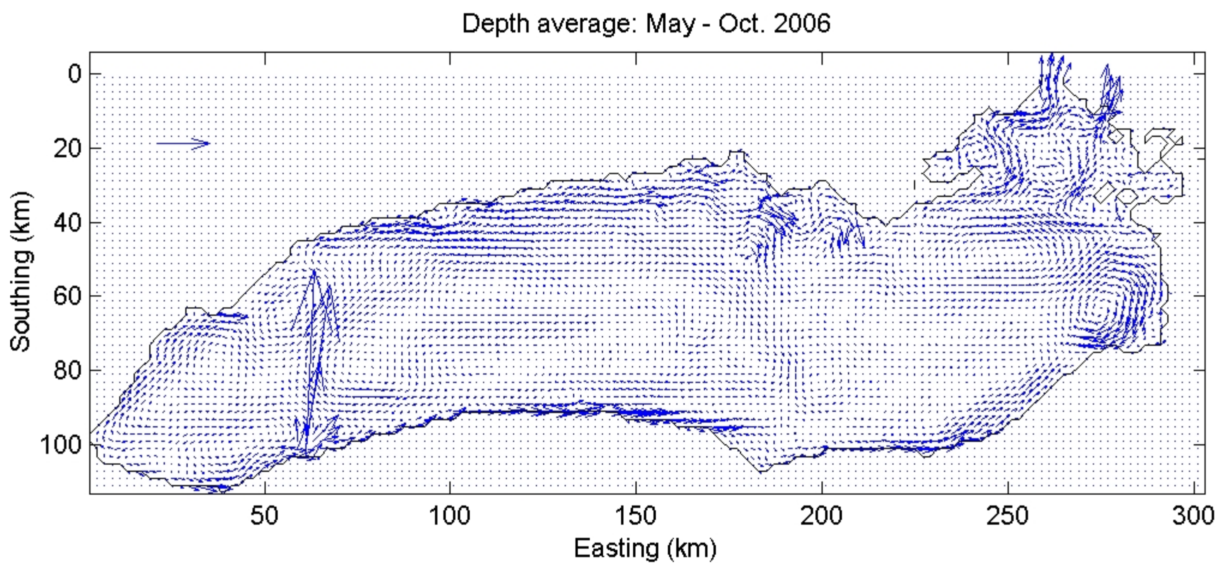

Figure C.1: Lake-wide ELCOM simulated summer depth averaged currents in Lake Ontario.

the south shore which is less evident in the ELCOM simulation.

For comparison to Pal *et al.* [49], ELCOM mean summer currents at a depth of 3.5 m were plotted in Figure C.5. The counterclockwise gyre in the south-western part of the lake as seen in Pal *et al.* is well reproduced by ELCOM along with the south coastal current. The gyre portrayed in Pal *et al.* in the north part of the lake [49] is not reproduced by the ELCOM simulation. This could be due to seasonal variations or insufficient drifter data. However, more analysis would be required to further comment on this but is beyond the scope to this project. ELCOM can be used to model the release of drifters to simulate the studies described in Pal *et al.* which would give a more comprehensive comparison.

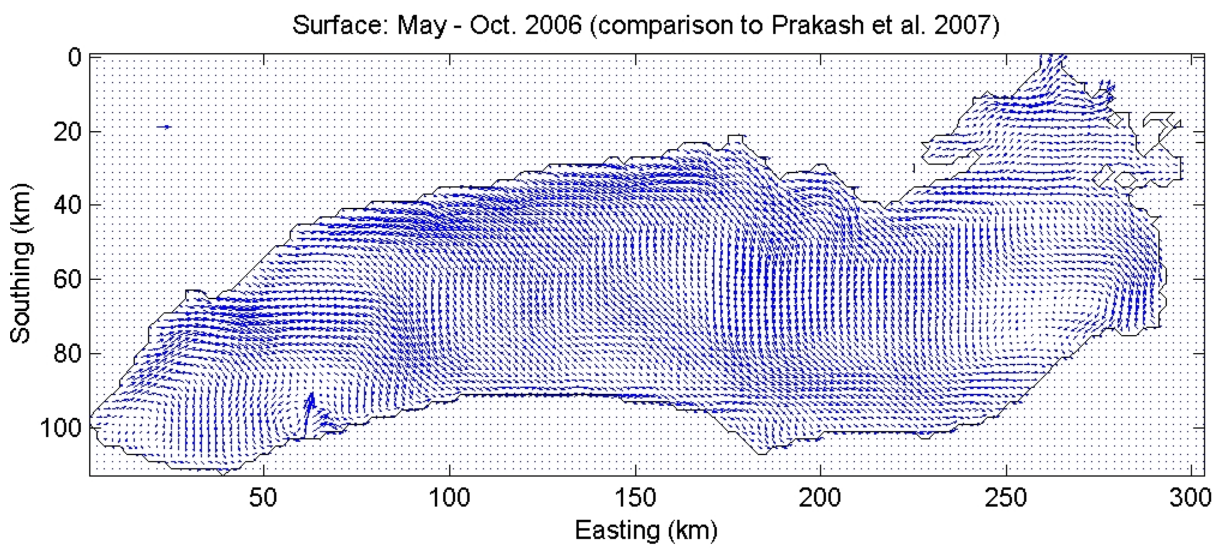

Figure C.2: Lake-wide ELCOM simulated summer surface circulation in Lake Ontario.

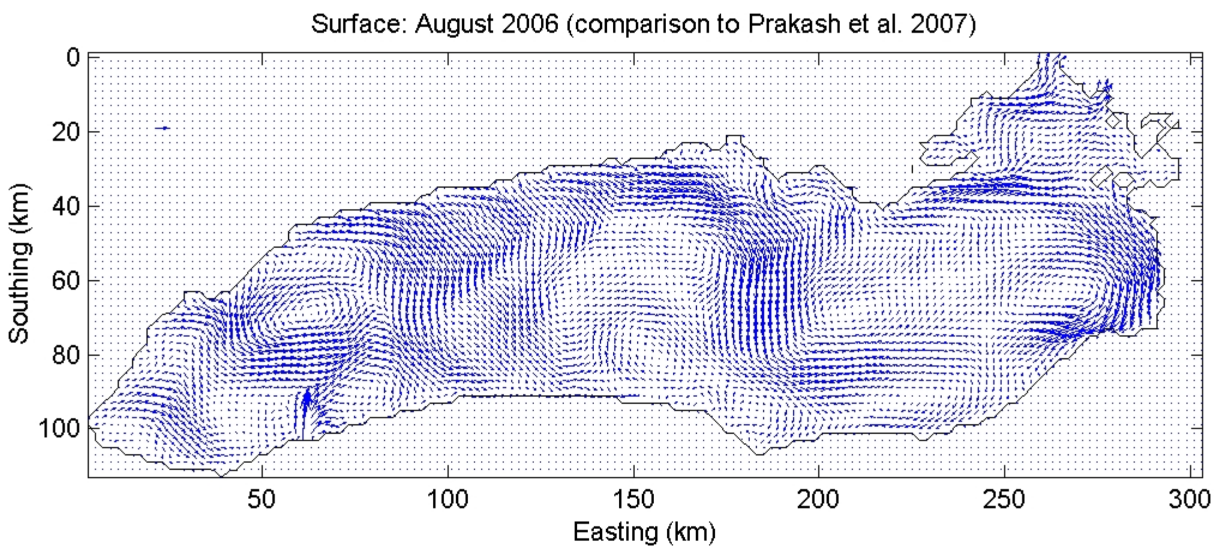

Figure C.3: Lake-wide ELCOM simulated surface currents for August 2006 in Lake Ontario.

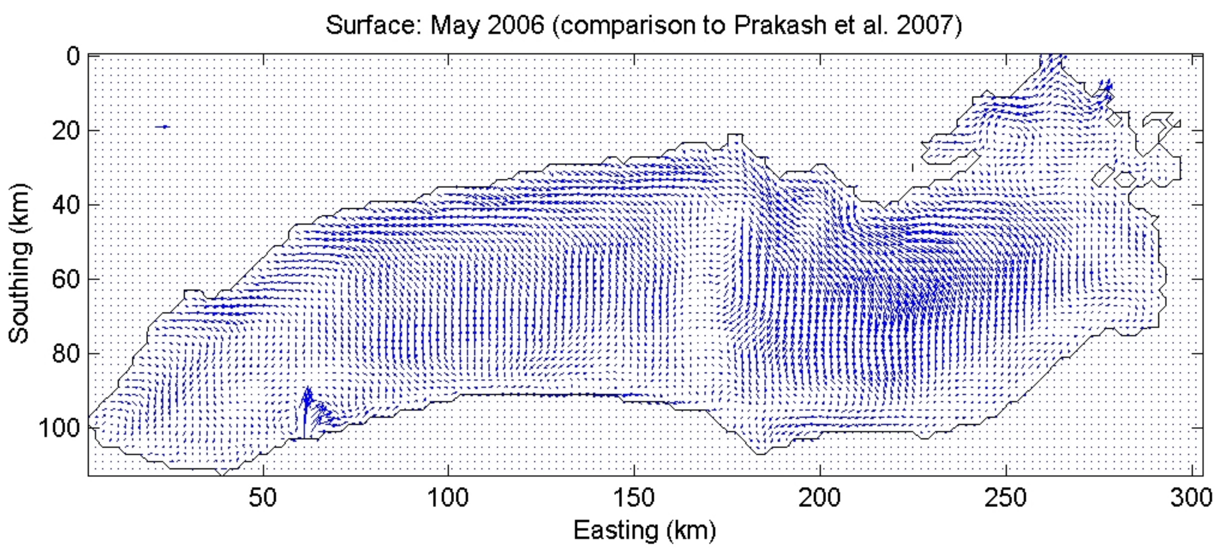

Figure C.4: Lake-wide ELCOM simulated surface currents for May 2006 in Lake Ontario.

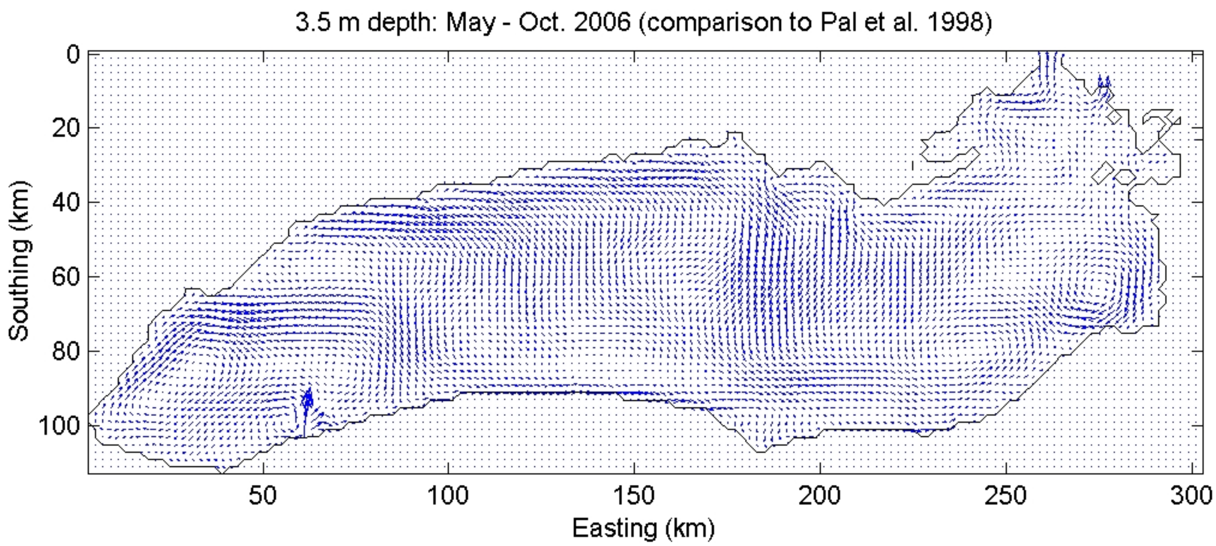

Figure C.5: Lake-wide ELCOM simulated currents at a depth of 3.5 m in Lake Ontario.

Appendix D

ELCOM Transport Equations

ELCOM transport equations (Figure D.1) and nomenclature (Figure D.2) are shown below as found in literature.

Hydrodynamic equations

Transport of momentum:

$$\frac{\partial U_\alpha}{\partial t} + U_j \frac{\partial U_\alpha}{\partial x_j} = -g\left\{\frac{\partial \eta}{\partial x_\alpha} + \frac{1}{\rho_0}\frac{\partial}{\partial x_\alpha}\int_{z'}^{\eta} \rho' dz\right\} \tag{2.1}$$

$$+ \frac{\partial}{\partial x_1}\left\{\nu_1 \frac{\partial U_\alpha}{\partial x_1}\right\} + \frac{\partial}{\partial x_2}\left\{\nu_2 \frac{\partial U_\alpha}{\partial x_2}\right\} + \frac{\partial}{\partial x_3}\left\{\nu_3 \frac{\partial U_\alpha}{\partial x_3}\right\} - \epsilon_{\alpha\beta} f U_\beta$$

Continuity

$$\frac{\partial U_j}{\partial x_j} = 0 \tag{2.2}$$

Boundary conditions on momentum

free surface:

$$\frac{\partial U_\alpha}{\partial x_3} = 0 \tag{2.3}$$

bottom and sides:

$$U_i = 0 \tag{2.4}$$

Transport of scalars:

$$\frac{\partial C}{\partial t} + \frac{\partial}{\partial x_j}(C U_j) = \frac{\partial}{\partial x_1}\left\{\kappa_1 \frac{\partial C}{\partial x_1}\right\} + \frac{\partial}{\partial x_2}\left\{\kappa_2 \frac{\partial C}{\partial x_2}\right\} = \frac{\partial}{\partial x_3}\left\{\kappa_3 \frac{\partial C}{\partial x_3}\right\} + S \tag{2.5}$$

Boundary conditions on scalars

$$\frac{\partial C}{\partial x_j} = 0 \tag{2.6}$$

Free-surface evolution

$$\frac{\partial \eta}{\partial t} = -\frac{\partial}{\partial x_\alpha}\int_b^{\eta} U_\alpha dz \tag{2.7}$$

Free-surface wind shear

$$(u_*)_\alpha^2 = C_{10}\frac{\rho_{(air)}}{\rho_{(water)}}(W_\beta W_\beta)^{\frac{1}{2}} W_\alpha \tag{2.8}$$

Momentum input by wind

$$\frac{dU_\alpha}{dt} = \frac{(u_*)_\alpha^2}{h} \tag{2.9}$$

Figure D.1: ELCOM equations as found in literature [50]

Nomeclature in hydrodynamic equations

i, j, k, m	three component space (*e.g.* $i = 1, 2, 3$)
α, β	horizontal two component space (*e.g.* $\alpha = 1, 2$)
U	Reynolds-averaged velocity
η	Reynolds-averaged free surface height
ρ_0	reference density
ρ'	density anomaly (*i.e.* the difference between the *in situ* density and the reference density)
g	gravitational constant
f	Coriolis constant
h	height of wind-mixed layer
δ_{ij}	Kronecker delta (0 for $i \neq j$, 1 for $i = j$)
$\epsilon_{\alpha\beta}$	two-component permutation tensor
ν	molecular viscosity
ν_{km}	eddy-viscosity tensor
Q	scalar source term
S_c	turbulent Schmidt number (or Prandtl number for temperature)
c	scalar concentration
b	x_3 value at bottom of domain
W_β	vector wind speed in β direction
C_{10}	bulk wind stress coefficient for wind values at 10 meters
$(u_*)_\alpha$	wind shear velocity in α direction

Figure D.2: ELCOM nomenclature as found in literature [50]

Appendix E

Velocity Difference

The absolute difference between ELCOM and observed north-south and east-west components of velocity was plotted for the coarse grid lake-wide model presented in Chapter 3 at station 1263 (Figure E.1) and station 1266 (Figure E.2). Figure E.1 shows both components of velocities to compare similarly. Both components of velocity show discrepancies between modelled and observed data mostly between 0 and 10 cm/s. Larger deficiencies occur periodically and are shown in both components of velocity. Figure E.2 first portrays the north-south component of velocity to agree well with observed values as discrepancies are between 0 and 4 cm/s for water in the hypolimnion. The water in the top portion of the profile shows slightly larger discrepancies in velocity especially around day 250 at the time of the storm event discussed in Chapter 3. The simulated east-west component of velocity at this location agrees less with with observed values than the north-south component and around the time of the storm event (day 250) where discrepancies between the modelled and observed velocities is very high.

The absolute difference between ELCOM and observed north-south and east-west components of velocity was plotted for the nearshore model of the Kingston basin and the upper portion of the St. Lawrence River presented in Chapter 4 at station 1263 (Figures

E.3 and E.4). Figure E.3 shows similar velocity discrepancies in the north-south direction for simulations A and B. Larger discrepancies are shown to occur in the top half portion of these two profiles. Discrepancies in the comparison of modelled and observed north-south components of velocity for simulation C are shown to be much larger throughout most of the water column especially in the second half of the simulation. Figure E.4 portrays again similar discrepancies in the east-west component of velocity for simulations A and B. The first half of the these two profiles show smaller discrepancies than is seen in the north-south component of velocity. However the second half of the simulation shows larger discrepancies in than is seen with the east-west component. The east-west component of velocity for simulation C again shows much larger velocity discrepancies than simulations A or B, but smaller discrepancies than is seen in the north-south component of velocity for simulation C.

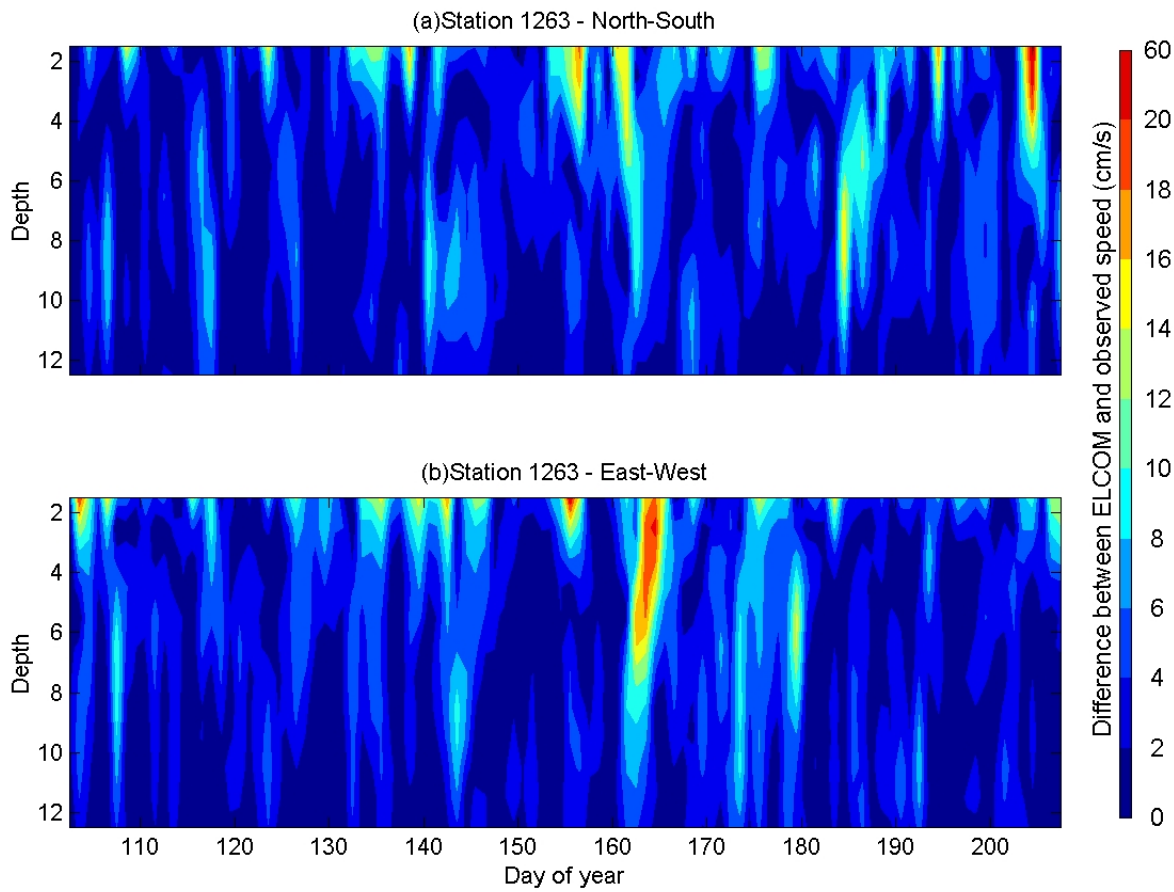

Figure E.1: Coarse grid model velocity difference. Absolute difference between ELCOM daily velocities and observed daily velocities in cm/s at 1 m depth intervals. North-south component of velocity difference (a) and the east-west component of velocity (b).

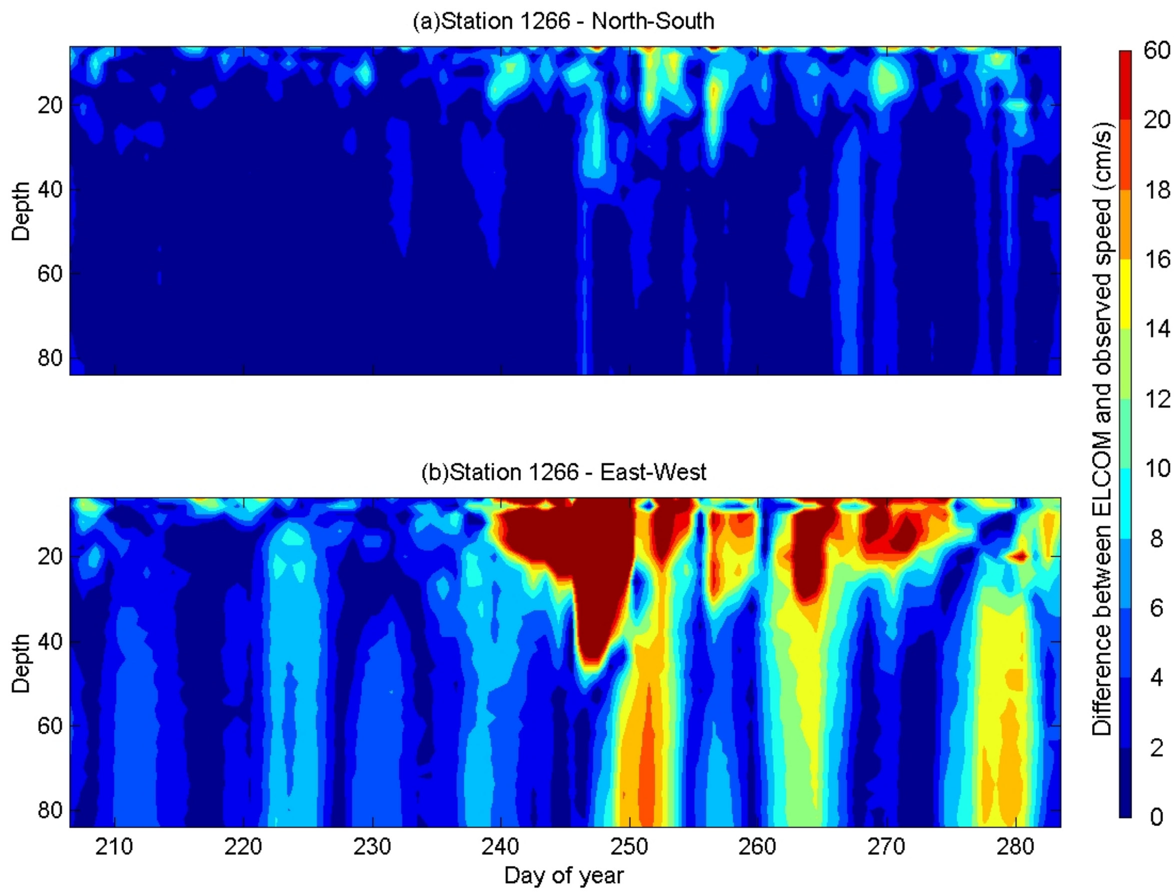

Figure E.2: Coarse grid model velocity difference. Absolute difference between ELCOM daily velocities and observed daily velocities in cm/s at 2 m depth intervals. North-south component of velocity difference (a) and the east-west component of velocity (b).

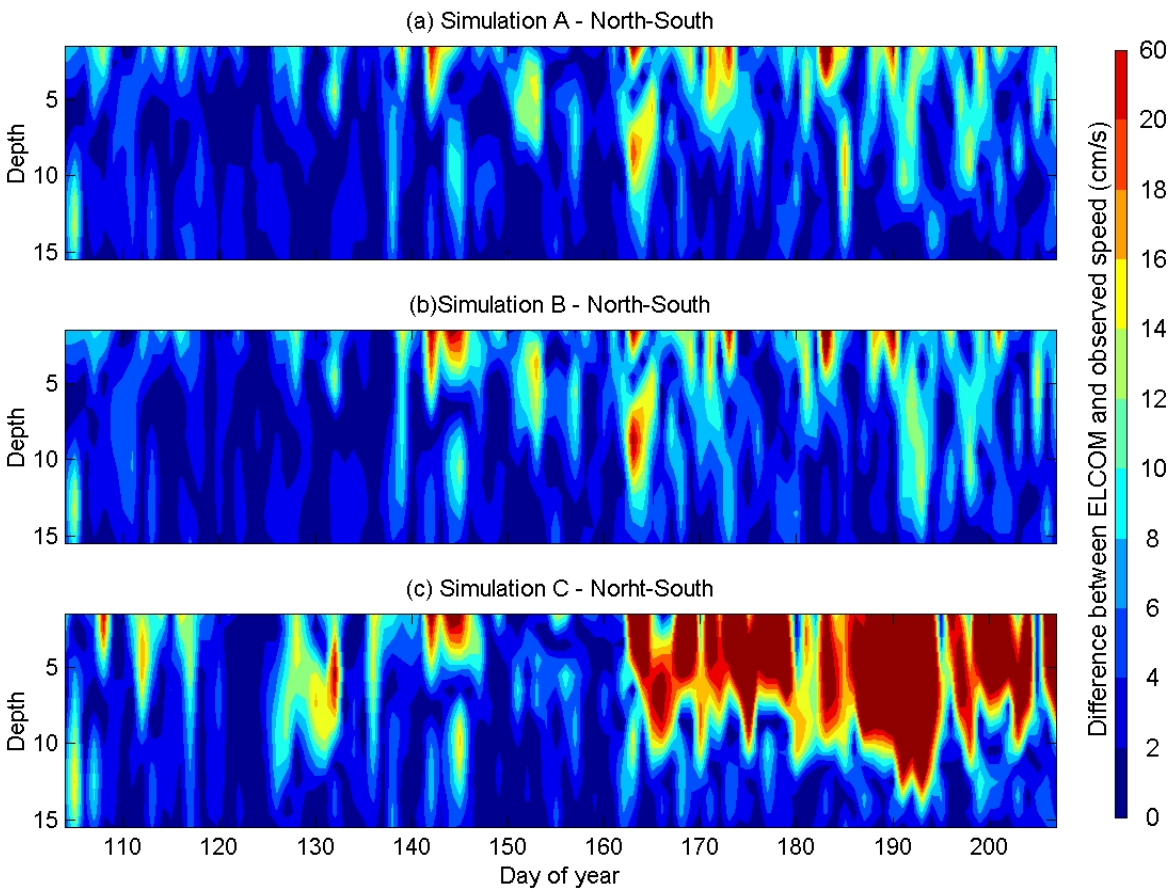

Figure E.3: Nearshore model north component of velocity difference at station 1263. Absolute difference between ELCOM daily velocities and observed daily velocities in cm/s at 1 m depth intervals. North-south component of velocity difference for simulation A (a), simulation B (b) and simulation C (c).

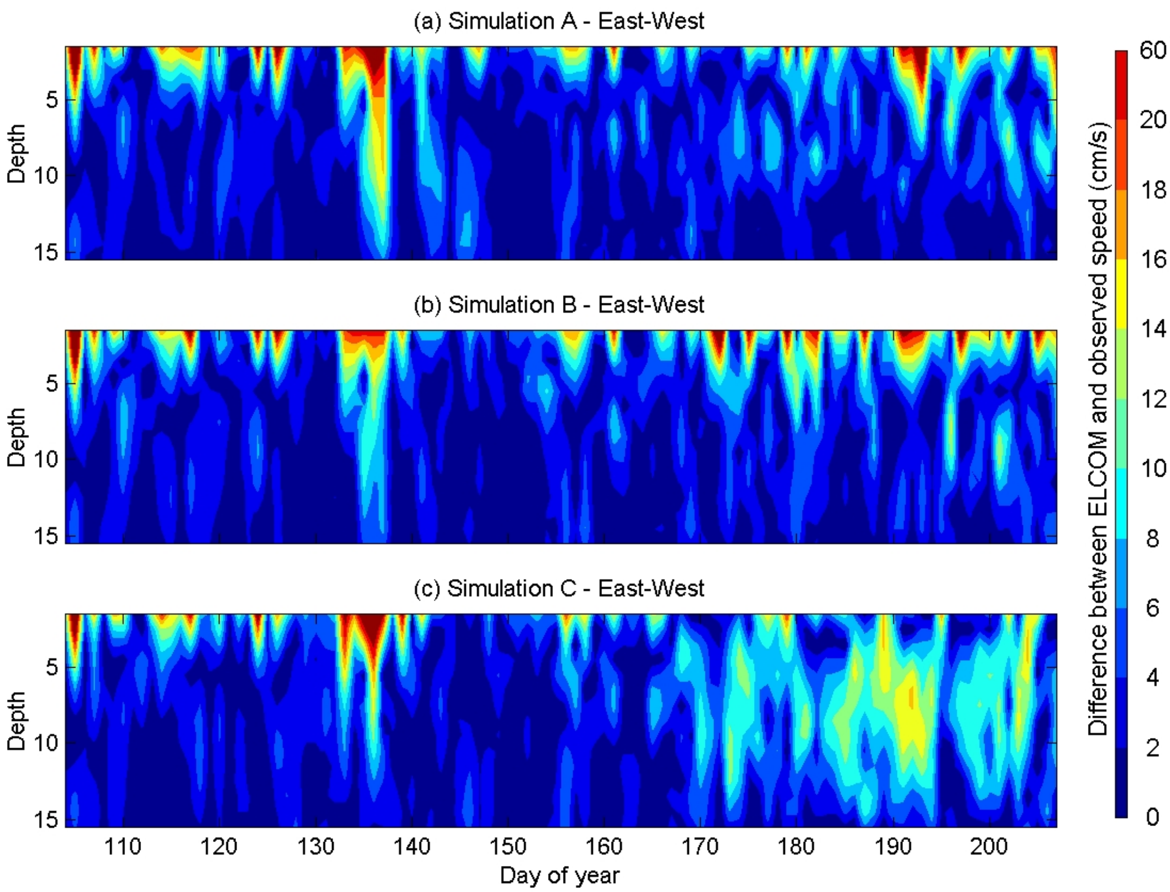

Figure E.4: Nearshore model east component of velocity difference at station 1263. Absolute difference between ELCOM daily velocities and observed daily velocities in cm/s at 1 m depth intervals. East-west component of velocity difference for simulation A (a), simulation B (b) and simulation C (c).